# Nonlinear Thermoviscoelastic Behavior of Polymers

Thesis by
Giancarlo Umberto Maria Losi

In Partial Fulfillment
of the Requirements for the Degree of
Doctor of Philosophy

California Institute of Technology
Pasadena, California

1990
(submitted September 26, 1989)

*To my mother*

*and to the memory of my father*

## Acknowledgments

It is difficult to summarize in a few lines the help and encouragement I have received while pursuing my doctoral degree. The principal subject of my thanks is the Caltech scientific community in general which is, in several ways, unique to my limited experience of the scientific world. Among the several people, a few names need to be extracted though, in a random sequence. I have to thank my advisor, Dr. Wolfgang G. Knauss, for guidance and for his down-to-earth intuitive reasoning which has sometimes helped restrain my youthful scientific drives, which were not always in the right direction. Dr. Paul Dimotakis was able to communicate to me part of his insatiable scientific curiosity; the late Dr. Eli Sternberg showed me that scientific rigor is not a void concept but a powerful tool instead. Dr. Joel Franklin is responsible for my introduction to the realm of stochastic analysis, and Dr. G. Ravichandran helped me shape the necessary tools of numerical analysis. Jean Anderson and Pat Gladson, from the Aeronautics Library, showed unbelievable kindness every time I asked them for a particular reference. I also want to thank my fellow students, senior and junior, for the scientific discussions, praise and criticism without which this work would not have been put together, the Office of Naval Research, in particular Dr. Larry Peebles, for the support under grant N00014-84-K-0424, and the National Science Foundation and San Diego Supercomputer Center for providing access to the computational facilities.

Above all, I would like to thank my mother for her love and for the time she had to spend on her own, away from her only child, on the other side of the Atlantic. This thesis is dedicated to her.

## Abstract

The rheological behavior of polymers in the neighborhood of the glass transition has been investigated in the framework of the free volume theory of nonlinear viscoelastic behavior. Free volume theory as normally applied above the glass transition was modified to account for the effect of the residual volume of vacancies below the glass transition; this modification was accomplished by modelling the changes in the state of the polymer as the sum of viscoelastic changes and a random disturbance deriving from the thermal collisions between molecules. The changes in mechanical properties going across the glass transition follow from the freezing-in of relaxation mechanisms and of free volume. The pressure dependence of the glass transition was found to be in qualitative agreement with measurements on PVAc, while the ratio of the glassy and rubbery heat capacities was found to coincide with the ratio of the equilibrium bulk compliances in the glassy and rubbery domains. The predictions of the model for the problem of transient and residual thermal stresses were compared with those of two simpler models.

The second part of the thesis studies the consequences of the nonlinear viscoelastic behavior on the decohesion zone in front of a crack propagating through an adhesive layer. The softening of the material response in the cohesive zone is taken to be effected by free volume induced change in relaxation times of the cohesive material and by void growth; the latter is assumed to depend on a critical value of strain at the beginning of the cohesive zone. The stress intensity factor for steady crack propagation is obtained by imposing the finiteness of strains at the crack tip. For the case where the properties of the adherends are the same as the linearized properties of the adhesive, the predictions show three regimes of crack propagation: a low speed regime where the adherends behave elastically with the rubbery prop-

erties, an intermediate range where their response becomes increasingly stiffer, and a high speed regime characterized by glassy behavior of the adherends and control of the crack growth process exclusively by the nonlinearly viscoelastic behavior of the failing material.

## Table of contents

## List of Symbols for Chapter 1

$a_t$ ..... time shift factor

$A$ ..... amplitude of the white noise affecting the free volume changes

$B$ ..... parameter of the Doolittle equation

$c$ ..... parameter of the hole potential energy U

$C_p$ ..... heat capacity at constant pressure, per unit volume

$C_{pg}$ ..... isobaric heat capacity below the glass transition

$C_{pl}$ ..... isobaric heat capacity above the glass transition

$d\underline{b}$ ..... white noise (derivative of the Wiener process)

$D$ ..... material fluidity

$E(x)$ ..... expected value of the random variable $x$

$f = \frac{V_f}{V}$ ..... fractional free volume

$f_0$ ..... reference fractional free volume

$G(t)$ ..... shear modulus

$G_i$ ..... element of the Prony series representation for $G(t)$

$G_\infty$ ..... asymptotic value of $G(t)$

$J(t)$ ..... shear compliance

$J_i$ ..... element of the Prony series representation for $J(t)$

$J_0$ ..... instantaneous value of $J(t)$

$K(t)$ ..... bulk modulus

$K_\infty$ ..... asymptotic value of $K(t)$

$K_i$ ..... element of the Prony series representation for $K(t)$

$M(t)$ ..... bulk compliance

$M_i$ .....element of the Prony series representation for $M(t)$

$M_0$ ..... instantaneous value of $M(t)$

$N$ ..... number of molecules

$p$ ..... pressure

$p(v)$ ..... probability distribution of free volume size

$t$ ..... time

$T$ ..... temperature

$T_g$ ..... glass transition temperature

$U$ ..... internal energy

$U$ ..... elastic energy of medium surrounding a hole

$v_f = \frac{V_f}{N}$ ..... average free volume per molecule

$v_{min}$ ..... minimum free volume for molecular mobility

$V = V_f + V_{occ}$ ..... total volume

$V_f$ ..... total free volume

$V_{occ}$ ..... occupied volume

$W$ ..... number of ways of redistributing free volume

$\alpha_g = \frac{\partial V}{\partial T}$ ..... isobaric coefficient of thermal expansion below $T_g$

$\alpha_l = \frac{\partial V}{\partial T}$ ..... isobaric coefficient of thermal expansion above $T_g$

$\beta_{fo} = \frac{\delta}{1-\delta}$ ..... ratio between free and occupied volume changes above $T_g$

$\Gamma$ ..... geometric parameter of the Doolittle equation

$\delta = \frac{\beta_{fo}}{1+\beta_{fo}}$ ..... ratio $\frac{\partial V_f}{\partial (V_f + V_{occ})}$

$\eta$ ..... material viscosity

$\kappa$ ..... heat conductivity

$\rho$ ..... material density

$\sigma$ ..... variance of a random variable

$\tau_i$ ..... relaxation times of a Prony series representation

$\xi$ ..... internal time

## List of Symbols for Chapter 2

$a_t$ ..... time shift factor

$B$ ..... parameter of the Doolittle equation

$c$ ..... position of the crack tip in a reference system moving with the crack

$\dot{c}$ ..... crack speed

$E(t)$ ..... Young's modulus

$E_i$ ..... element of the Prony series representation for $E(t)$

$E_0$ ..... asymptotic value of $J(t)$

$f$ ..... fractional free volume

$f_0$ ..... reference fractional free volume

$J(t)$ ..... shear compliance

$J_i$ ..... element of the Prony series representation for $J(t)$

$J_0$ ..... instantaneous value of $J(t)$

$K$ ..... stress intensity factor

$M(t)$ ..... bulk compliance

$M_i$ .....element of the Prony series representation for $M(t)$

$M_0$ ..... instantaneous value of $M(t)$

$t$ ..... time

$v$ ..... crack opening displacement

$x, y$ ..... coordinates in a reference system moving with the crack

$X, Y$ ..... coordinates in a material reference system

$z = x + iy$ ..... complex coordinate in the moving reference system

$\Gamma$ ..... cohesive fracture energy

$\delta$ ..... ratio between free and total volume changes

$\epsilon_{ij}$ ..... $i - j^{th}$ component of the Cauchy-Green strain tensor

$\epsilon_{crit}$ ..... critical strain for the onset of void growth

$\epsilon_{max}$ ..... normalizing strain for void growth

$\nu$ ..... Poisson's ratio

$\xi$ ..... internal time

$\sigma_{ij}$ ..... $i-j^{th}$ component of the Cauchy stress tensor

$\tau_i$ ..... relaxation times of a Prony series representation

$\phi$ ..... complex potential

$\Psi$ ..... void growth function

# Preface

This thesis is devoted to the study of the rheological behavior of amorphous polymers and to its consequences on the macroscopic properties, durability and fracture toughness. It is comprised of two parts.

The first part focuses attention on the constitutive properties of polymers above and below the glass transition and on the interrelations between glassy and rubbery behavior. The observations on the rheological behavior lead to the definition of a nonlinear constitutive model which takes into account nonequilibrium effects on the mechanical response. The model is then used in a finite element code for the prediction of the transient and residual thermal stresses in a particular kind of amorphous polymer, PVAc; the model predictions are also compared with those of simpler material descriptions.

In part two the consequences of nonlinearly viscoelastic behavior on the failure of polymeric adhesives is investigated. The steady propagation of a crack in an adhesive layer is studied under the assumption of the existence of a cohesive zone at the crack tip which prevents the build-up of singular stress and strain fields in the polymer. The cohesive zone is taken to be characterized by material softening due to nonlinearly viscoelastic behavior and by void growth, the onset of which is set to depend on a critical value of strain. For the case where the properties of the adherends are the same as the linearized properties of the adhesive, the results of the analysis are compared with those of simpler fracture criteria.

CHAPTER 1

# Free volume theory and nonlinear thermoviscoelasticity

## Introduction

Today's technology often relies on the use of polymers whenever lightweight, easily formable and tough structural components are needed. The best known advanced application of this class of materials is found in the field of composites, where different kinds of polymers can be arranged together to form a macroscopically isotropic solid (*e.g.,* rubber-toughened plastics) or when they are used to support a network of stiff fibers of different composition (*e.g.,* fiberglass, carbon-fiber composites). Polymers are also increasingly replacing rivets and welds for the connection of structural members through the use of polymeric adhesives.

These materials, as any other material on Earth, can fail. The failure of an adhesive joint or a composite panel can be just a nuisance or a disaster, depending on the application, and the failure can occur in different ways, such as, among others, decohesion between the fiber and the matrix in composites, cracks propagating through adhesives, degradation of the polymer due to solvents or radiation. What is common to all these types of failure is the predominant role played by the temperature and possibly rate dependent constitutive properties of the polymer, and the large differences in the ultimate strength that can arise from different manufacturing processes. As a consequence, the accurate prediction of the final conditions of a

polymer subject to a given stress, strain and temperature history is of tremendous importance for the assessment of the durability and reliability of a structure or its parts. There are two main areas in which these investigations are performed: on the one hand, there is a continuous effort by the physics and chemistry community to construct models of constitutive behavior based on the analysis of phenomena occurring at the molecular level; on the other hand, the mechanics and engineering community tries to reconcile these molecular models with macroscopically measurable behavior through the use of more phenomenological theories, and also addresses the effect of inhomogeneities in the material history, such as those which result from thermal transients or localized softening. The work presented here tries to narrow the gap between these two points of view and devotes particular attention to the problem of residual stresses which can arise in a polymer during a manufacturing process or because of environmental changes in temperature.

The constitutive properties of general amorphous materials, of which polymers are a particular class, have been the object of extensive investigations; for example, researchers have studied the problem of the temperature dependence of the viscosity of glass-forming liquids (Eyring and Hirschfelder, 1937; Leaderman, 1943; Tobolsky and Eyring, 1943; Williams, Landel and Ferry, 1955; Cohen and Turnbull, 1959; Adam and Gibbs, 1965) and the nature and rate dependence of the glass transition in polymers or general amorphous materials (Gibbs and DiMarzio, 1958; Turnbull and Cohen, 1961; Cohen and Grest, 1979). Because most of the theoretical studies concentrate on the description of the rheological behavior of amorphous materials through equilibrium thermodynamics theory (*e.g.,* the hole theory of liquids), notable discrepancies have been found to occur between their predictions and the experimental evidence below the glass transition, particularly when the constitutive properties of long-chain polymers are of interest (McKinney and Goldstein, 1974).

For polymers, the problem is complicated further by the presence of a continuous spectrum of relaxation times, as opposed to a single viscosity for monomeric glasses, and a constitutive response which is in great part effected by the rubbery-elastic behavior of the chain network. Given the difficulty of the problem, polymeric behavior has therefore often been approached within the framework of semi-empirical or phenomenological descriptions, relying to a large extent on modifications of the linear laws of small strain viscoelasticity. The common feature to all these theories is an attempt to bridge the gap existing between the straightforward predictions of equilibrium thermodynamics or molecular dynamics applied to simple systems and the macroscopically measurable properties, as the time-dependent constitutive material response characterizing the complex behavior of a network of polymer chains with a very complicated geometry. Some of the areas which have been addressed include the time-dependent thermal expansion/contraction of polymers (Kovacs, 1958), the effect of stress and strain histories on the material properties (Ferry and Stratton, 1960; Knauss and Emri, 1981; Shay and Caruthers, 1986), and the effects of physical aging on the material response (Struik, 1978; Cizmecioglu *et al.*, 1980; Curro, Lagasse and Simha, 1981).

This chapter on constitutive behavior is divided into two major parts. The construction of a consistent phenomenological theory for the constitutive behavior of amorphous and homogeneous polymers is addressed in section 1.1; in section 1.2 the constitutive assumptions are incorporated into a numerical study of the residual stresses arising in a polymer subjected to temperature changes.

The first part begins with a brief exposition of free volume theory in its simplest form. Section 1.1.1 gives a short history of the origin of such theory starting from observations on the temperature dependence of the relaxation behavior of polymeric

and monomeric liquids. Section 1.1.2 discusses in greater detail how the free volume changes are affected by the mechanical history and gives an elementary model visualizing the time-dependent response. The following sections 1.1.3 through 1.1.7 address some limitations of free volume theory as it is currently used in its simplest form; section 1.1.3 deals with the first extension of such theory to consider the problem of residual free volume, *i.e.,* residual disorder in the glass below $T_g$ which can affect the relaxation behavior of the polymer. The following section 1.1.4 considers the effects of disequilibrium below the glass transition on the mechanical response, and discusses inferences of the model parameters from experimental data. Section 1.1.5 addresses the dependence of the glass transition on the rate of cooling, while section 1.1.6 investigates the approximations involved in relating the macroscopic dilatation to the free volume induced shift in the time scale of the relaxation behavior. Some additional topics regarding the thermodynamic nature of the glass transition, its pressure dependence and the role of viscosity are discussed in section 1.1.7.

The second part addresses the application of the constitutive assumptions to the problem of residual stresses. Section 1.2 presents the predicted transient and residual thermal stress fields for three different constitutive assumptions: an elementary model, often used in the literature, by which the effect of temperature is computed by subtracting the thermal strains from the dilatational history, the current model and a simplification of the latter in which the time scale of the relaxation behavior is temperature controlled. The differences in the predictions of the three models are found to increase as the time scale of the thermal transients approaches or becomes smaller than the time scale of viscoelastic relaxation.

## 1.1 Constitutive modelling

### 1.1.1 Elementary free volume theory

The common denominator of the studies of monomeric and polymeric glasses is the effort to quantify the dependence of the molecular mobility on the instantaneous state, and possibly history, of the material. Molecular mobility is the main factor governing the evolution of a glass from one nonequilibrium state to another one in which the free energy reaches a minimum for given values of temperature and pressure, and in which further changes in the thermodynamic state of the material do not arise unless the environmental conditions are again modified. Following the work of Eyring (1937), who suggested a connection between the viscosity of liquids and their lattice structure, a useful theoretical contribution to describe the rheological behavior of monomeric glasses was offered by Cohen and Turnbull (1959), who derived an expression for the dependence of the viscosity on the density of vacancies in the solid (after a semi-empirical expression had been proposed by Doolittle in 1951). Cohen and Turnbull considered the phenomenon of molecular transport in a liquid composed of hard spheres, schematically represented in Fig. 1.1, in which diffusive motion occurs when density fluctuations open up spaces sufficiently large for a molecule to slip in and for a second molecule to replace the first one in its original position. In that work, free volume was defined as the region accessible to the center of a molecule through a drifting motion that does not require interaction with its neighbors. In contrast, the remaining, occupied volume was defined as that space in which a diffusing molecule would overlap partially with another one; these definitions will be adopted throughout this work. If one denotes with $R_0$ the radius at which molecular interaction becomes significant, then the free volume accessible

to each particle is the space delimited by spheres of radii $2R_0$ centered at neighboring molecules. Such a volume model is shown in Fig. 1.2 for molecules $A$ and $B$.

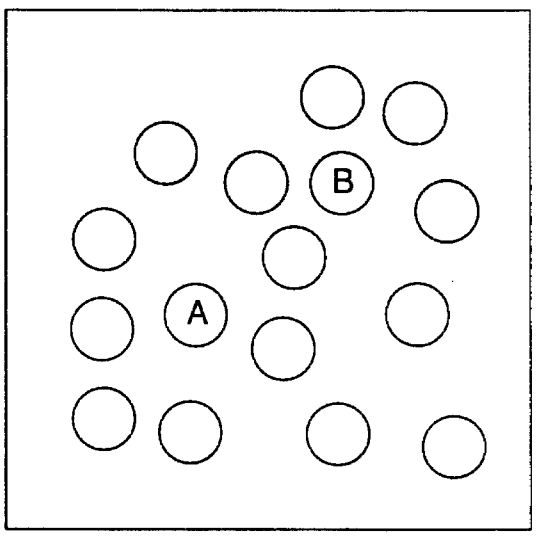


FIGURE 1.1 Schematic representation of a liquid of hard spheres.

Under these conditions, Cohen and Turnbull suggested that the fluidity $D$ of the material be proportional to the probability of a molecule finding a sufficiently large hole, *i.e.*, a hole greater than a critical value, $v_{min}$, so that such molecule could step into the vacancy and another one take its original position; they assumed therefore

$$D = \frac{1}{\eta} \propto \int_{v_{min}}^{\infty} p(v)\, dv \quad , \tag{1.1.1}$$

$\eta$ being the intrinsic material viscosity and $p(v)$ the probability distribution of the size of free volume sites. Cohen and Turnbull next considered the distribution of free volume sites for a liquid of hard spheres in which no energy change was required for a redistribution of hole volumes. If $N$ is the total number of monomeric molecules,

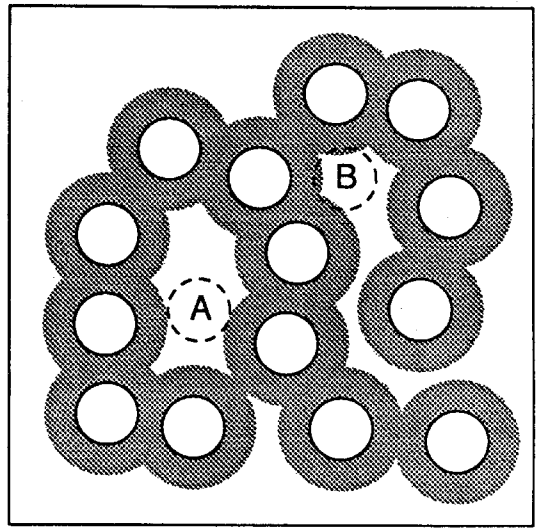


FIGURE 1.2 Free volume.

and $V_f$ the total free volume, then the average free volume $v_f$ per molecule is

$$v_f = \frac{V_f}{N} . \tag{1.1.2}$$

A discretized model of the free volume distribution was used, in which the total range of free volume was divided into small regions having average value $v_i$, such that

$$\sum_i N_i v_i = V_f , \tag{1.1.3}$$

and

$$\sum_i N_i = N. \tag{1.1.4}$$

The number of ways of redistributing the free volume without changing $N_i$ is

$$W = \frac{N!}{\Pi_i N_i!}. \tag{1.1.5}$$

By maximizing $W$ and passing to the continuum limit with the constraints 1.1.3 and 1.1.4, Cohen and Turnbull obtained for $p(v)$

$$p(v) = \frac{1}{v_f} \exp(-\frac{v}{v_f}) . \tag{1.1.6}$$

The material viscosity is then predicted from Eq. 1.1.1 as

$$\eta \propto exp\left(\frac{\Gamma\, v_{min}}{v_f}\right) , \tag{1.1.7}$$

where $\Gamma$ is a material parameter which accounts for possible overlapping of free volume. The same Eq. 1.1.7 can be cast in terms of the fractional free volume $f$, *i.e.*, the ratio $\frac{V_f}{V}$, instead of using the average free volume per molecule, yielding

$$\eta \propto exp\left(\frac{B}{f}\right) , \tag{1.1.8}$$

where $B$ is given by the expression

$$B = \frac{\Gamma v_{min} N}{V} . \tag{1.1.9}$$

The material viscosity is the governing factor in the relaxation behavior of a glass, *i.e.*, higher viscosities imply longer times needed to reach equilibrium or, alternatively, the evolution of the glass towards equilibrium needs to be scaled in time by the instantaneous value of $\eta$. This idea leads to the concept of internal time, denoted here by $\xi(t)$, a material time scale which is related to the experimental one through a factor, usually called the time shift*, which is the ratio of the instantaneous viscosity to the one measurable in some reference condition

$$\xi(t) = \int_0^t \frac{d\tau}{a_t} = \int_0^t \frac{d\tau}{\frac{\eta}{\eta_0}} . \tag{1.1.10}$$

If one takes the ratio of viscosities given by the Cohen-Turnbull result, Eq. 1.1.8, corresponding to different values of free volume, one obtains

$$\log(a_t) = log\left(\frac{\eta}{\eta_0}\right) = B\left(\frac{1}{f} - \frac{1}{f_0}\right) , \tag{1.1.11}$$

---

* Historically, the reason for this terminology is that a multiplying factor is equivalent to a shift on a logarithmic plot, which is the form in which viscoelastic relaxation or creep data are usually presented.

where $f_0$ is the reference fractional free volume, *i.e.*, the fractional free volume of the state in which the time-dependent (linear) material properties are measured. The above equation is commonly designated as the Doolittle equation (Doolittle, 1951), following his experimental studies on the temperature dependence of the viscosity of glass-forming liquids.

Let us consider a different and more straightforward way of deriving the Cohen-Turnbull results; the following method also has a simple connection to the basic principles of statistical mechanics. Consider the existence of an entropy associated with the free volume probability distribution which, in a Boltzmann sense, can be written as

$$S_v \;=\; -k \int_0^\infty p(v)\, log(p(v))\, dv \;, \qquad (1.1.12)$$

where $k$ is Boltzmann's constant. Eq. 1.1.12 differs from the usual definition of Boltzmann entropy since the distribution being considered is not a distribution in phase space, which is composed of physical coordinates and their conjugate momenta, but rather refers to a probability of existence of holes of a certain size in the lattice. On the other hand, if one assumes that a particle can migrate freely within a vacancy, then the integral over the physical spatial coordinate can be translated into one over the free volume, provided that its distribution is homogeneous throughout the material. The above Eq. 1.1.12 can therefore be interpreted as the entropy of migration associated with a particle that can freely wander within the holes of the molecular network. If one furthermore imposes the restraints

$$\int_0^\infty p(v)\, dv \;=\; 1 \;, \qquad (1.1.13)$$

and

$$\int_0^\infty v\, p(v)\, dv \;=\; f \;, \qquad (1.1.14)$$

by maximizing the entropy with the above constraints, one recovers the expression 1.1.6: the method of Lagrange multipliers requires the maximization of the integral

$$I = \int_0^\infty [-k\, p(v)\, log(p(v)) + \lambda_1 p(v) + \lambda_2 v p(v)] dv \ . \qquad (1.1.15)$$

The Euler equation applied to this integral then reads

$$-k\, log(p(v)) = \lambda_1 + \lambda_2 v - k \ , \qquad (1.1.16)$$

or

$$p(v) = exp(-\frac{\lambda_2}{k} v + 1 - \frac{\lambda_1}{k}) \ . \qquad (1.1.17)$$

It is then easy to see that the constraints 1.1.13 and 1.1.14 require $\lambda_1 = k(1 - log(f))$ and $\lambda_2 = \frac{k}{f}$, from which expression 1.1.6 is recovered.

Eq. 1.1.11 is also the basis of the time-temperature superposition principle, which originates from the observation that the time-dependent properties of viscoelastic materials at different temperatures can be collapsed onto a single master curve via a shift on the logarithmic time scale, a shift which varies with temperature. Again, this indicates the possibility of scaling the time-dependent material properties so that they are expressed in terms of the reference conditions and the current internal time scale of the material, given by

$$\xi(t) = \int_0^t \frac{d\tau}{a_t(T)} \ , \qquad (1.1.18)$$

in which $a_t(T)$ is the time shift at the temperature $T$; $a_t$ is equal to unity if the temperature is the same as that at which the time-dependent material properties are measured. A linear dependence of the free volume on temperature and Eq. 1.1.11 predict amazingly well the time-temperature shift $a_t(T)$ of polymeric materials above the glass transition, as it was first noted by Williams, Landel and Ferry (1955). In particular, if one takes $B = 1$ and

$$f = f_0 + (\alpha_l - \alpha_g)(T - T_0) \ , \qquad (1.1.19)$$

where $\alpha_l$ and $\alpha_g$ are the coefficients of thermal expansion in the rubbery and glassy state and the reference condition is taken to coincide with the status of the material at its glass transition temperature, then one obtains the so-called WLF equation, derived from the initials of Williams, Landel and Ferry who also proposed a universal value of 2.5 percent for the fractional free volume at the glass transition.

An extension of the free volume model to include solvent concentration and pressure histories was first proposed by Ferry and Stratton (1960) and later refined by Knauss and Emri (1981). In the Ferry-Stratton model, free volume is set to depend on several parameters

$$f = f_0 + \alpha_f \Delta T + \beta_f \Delta p + \gamma_f \Delta c \ , \tag{1.1.20}$$

where $\Delta T$, $\Delta p$, $\Delta c$ represent the changes in temperature, pressure and solvent concentration with respect to the condition in which the reference free volume, $f_0$, is measured, and $\alpha_f, \beta_f, \gamma_f$ are material parameters. Knauss and Emri (1981) extended the Ferry-Stratton model to the case where the material properties, such as $\alpha_f, \beta_f, \gamma_f$, are time-dependent, in which case the relation 1.1.20 needs to be expressed in terms of convolution integrals over the time histories of temperature, pressure and solvent concentration, *i.e.*, for the case of temperature variations only

$$f = f_0 + \int_0^t \alpha_f(\xi(t) - \xi(\tau)) \frac{\partial T}{\partial \tau} d\tau \ , \tag{1.1.21}$$

where the material internal time $\xi(t)$ is now expressed as

$$\xi(t) = \int_0^t \frac{d\tau}{a_t(f(t))} \ , \tag{1.1.22}$$

and $a_t(f)$ is computed through Eq. 1.1.18 and the instantaneous value of free volume as given by Eq. 1.1.21. The Knauss-Emri model has interesting consequences on the predicted material behavior since the molecular mobility is made to depend on

the instantaneous fractional free volume, the changes of which in turn depend on the molecular mobility. Such interconnection effects a strong coupling between the material relaxation and the stress state, coupling which effects softening behavior when polymers are subject to high tensile stresses, as experimental evidence shows (Knauss and Emri, 1981).

There are some relevant questions which need to be addressed in full detail in order to establish a consistent nonlinear theory for the constitutive behavior of polymers. These questions, presenting themselves quite naturally, can be summarized as follows:

1. How does the free volume change depend upon macroscopic deformations?
2. Is there an instantaneous change in free volume when a polymer is taken through a sudden volume deformation?
3. Is there an equilibrium value of the free volume corresponding to macroscopic values of temperature and pressure below the glass transition, as there is above it?
4. Can free volume attain zero values, or is there always a residual amount that remains in the polymer and, if so, what is the mechanism which prevents the total annihilation of the voids between molecules?

In order to address these questions, and in particular questions 1 and 2, it is useful to first look at simple representations of phenomena at the molecular level, *e.g.,* the liquid of hard spheres, and then try to extend the related results to the situation of more complex polymeric chains. Within such simple representations of glass-forming materials, the physical phenomena underlying the Knauss-Emri

constitutive model and the implications of the model will be discussed in the next section, and a simple mechanical analogy for the description of the material behavior will be given. The end of the next section 1.1.2 will conclude that part of this thesis which is dedicated to the exposition of the free volume theory of nonlinear viscoelasticity as it is currently known; the limitations of the basic theory and the refinements needed to overcome such limitations will then be addressed in the following sections 1.1.3 trough 1.1.7.

### 1.1.2 A simple constitutive model

In order to construct a model for the constitutive response, one has to consider the different aspects of the behavior of polymers. It is well known that these materials react to sudden changes in the environmental conditions, such as pressure or temperature, with an instantaneous response and a time-dependent evolution which can last, depending on the values of pressure and temperature, from the microsecond scale up to several years. The time-dependent response can be of linearly viscoelastic nature or it can also affect the time scale of material relaxation, in the case of the process denoted as physical aging. If one defines an equilibrium state as a state in which there are no changes in the internal variables** of the polymer, it is evident that the instantaneous response by itself is unable to bring the material to equilibrium and that the macroscopic time-dependent response, such as the one represented by the viscoelastic moduli, is a manifestation of the evolution of the material towards such a state. These considerations can apply to macroscopic deformations, such as the time-dependent thermal expansion (Kovacs, 1958), to the

** Internal variables are quantities such as the distribution of holes in the solid, the local stress state or the orientation of the polymer chains, quantities which are difficult to measure experimentally.

stress state in a relaxation experiment, or also to the distribution of free volume in the polymer. The rate at which equilibrium is achieved has been shown to be dependent not only on temperature, but also on the amount of disorder in the polymer network, which is ideally quantified through the free volume content† (Kovacs, *ibid.*; Knauss and Emri, 1981; Shay and Caruthers, 1986). Since the reaction rate of the material is governed by molecular mobility, and the molecular mobility is in turn dependent on free volume, it is of great importance to assess how the free volume changes are connected to the macroscopic deformation, in particular how they are related to the instantaneous and asymptotic response.

The first step in addressing the equilibrium and nonequilibrium aspects of the free volume is to define an equilibrium state. There are several kinds of equilibria, and the one which is addressed in this section is intended as a state in which no changes occur in the status of the material, a condition which can also be present in what we define as a metastable equilibrium. A metastable equilibrium occurs when the thermodynamic equilibrium is not attainable, such as is the case when crystallization of the polymer is prevented by the nature of its complex geometry. The distinction between metastable and thermodynamic equilibrium is only meaningful below the glass transition, since only under those conditions can a metastable equilibrium exist. The considerations in this section apply only to thermodynamic equilibrium, *i.e.*, for temperatures above the glass transition. The incorporation of a metastable equilibrium in the model and the extension of the nonlinear viscoelastic model to this regime will be addressed in Section 1.1.3.

It is commonly assumed that the equilibrium free volume of the material is a

---

† This is, apart from considerations about the distribution of free volume which are addressed in Section 1.1.6, a good approximation in the case of small strains; for large strains, additional factors, such as a preferred molecular orientation, need to be taken into account.

function of temperature, for which the direct temperature dependence is removed and replaced by an indirect one (for a discussion of this assumption, see Fox and Flory, 1950). Sufficiently far above the glass transition temperature $T_g$, changes in the equilibrium free volume can be assumed to be some fraction of the total deformation; current molecular theories predict (*e.g.,* Simha and Somcynsky, 1969) that such fraction is a constant above $T_g$. In addition, the nonequilibrium free volume fraction, *i.e.,* the difference between the current amount and the asymptotic one, has been shown to affect the mechanical relaxation, as in the experiments by Cizmecioglu *et al.* (1980), who measured the effects of physical aging on the material properties. Similar conclusions derive from the dilatometric experiments by Kovacs (1958) where, after thermal transients had settled down, the evolution towards equilibrium at a given temperature was found to be dependent on the direction of approach, *i.e.,* whether the material underwent a heating or cooling process, a phenomenon which can readily be explained through the concept of nonequilibrium free volume.

Previous theoretical attempts to include nonequilibrium aspects in the treatment of free-volume induced time shift include the work of Curro, Lagasse and Simha (1981), who used the fraction of unoccupied sites in the Simha-Somcynsky equation of state to allow for nonequilibrium behavior; time dependence was accommodated through the use of the volume recovery data by Cizmecioglu *et al.* to quantify the dilatational aging ‡ of PMMA. Shay and Caruthers (1986) followed the approach of Curro *et al.* and used the equilibrium Simha-Somcynsky theory to compute the free volume fraction as a function of the instantaneous values of volume, temperature and pressure. Within the framework of an equilibrium, time-

‡ *i.e.,*the change in the time scale of material relaxation effected by variations in the molecular disorder.

independent theory, an extension of the Simha-Somcynsky equation of state was also suggested by Peng *et al.* in order to accommodate a more general state of stress, other than the uniform pressure which solely could be addressed within such a formulation.

The mentioned studies, as others in the literature, have the common feature of starting from an equilibrium equation of state, often derived under idealized conditions such as the assumption of a regular molecular lattice, and allowing for some substitutional time dependence in its variables. While this is certainly a possible approach, it is sometimes difficult to precisely reconcile the predictions of a "simple" theory with the behavior of a complex system of polymeric chains characterized by a complicated and random geometry. One can raise the question whether another point of view, namely a phenomenological model based on the experimentally measurable nonequilibrium behavior such as the one shown by the time-dependent bulk and shear moduli, would give different results or simply arrive at the same conclusions (in terms of constitutive behavior) but in a more straightforward manner. Such considerations motivate the approach presented here, which is basically phenomenological and tries to abstain, for as long as possible, from the use of equilibrium equations of state for the time-dependent material response. In the context of a phenomenological theory such as the Knauss-Emri model, some aspects of the dependence of the time scale of material relaxation on the density of vacancies will be discussed and the first subject to be considered will be the issue of instantaneous free volume change upon sudden deformation.

The question of existence of an instantaneous free volume change, as implied by Eq. 1.1.20 or Eq. 1.1.21, will be addressed now in the context of a simple molecular model, similar to the liquid of hard spheres considered by Cohen and Turnbull.

Such a simple model does not take into account the chain-like nature of polymer molecules, which is the main factor governing the constitutive response, but is helpful in understanding how the time scale of such response is affected by the morphological features of the polymer, in particular the amount of space not occupied by the molecules. Instead of assigning rigid behavior to the particles of this idealized model, a better representation would consider the boundaries of the molecules to be deformable and as regions in which molecule-molecule interaction becomes significant. The regions surrounding two particles can overlap in this simple schematization, but this overlapping would require some energy storage or expenditure through their interaction. Assume that the situation at equilibrium is initially the same as the one depicted in Fig. 1.2, with $R_0$ being the initial radius of the molecules. Suppose next that $R_0$ is subjected to a change or, equivalently, remains constant while the whole system shrinks or expands in a self-similar fashion changing the distances between the centers of the molecules through a common proportionality factor (*e.g.*, a sudden expansion or contraction of the polymer). Such a situation, depicted in Fig. 1.3, where the radius of the shaded area surrounding each molecule has been increased, keeping the positions of the centers unchanged, shows that there is a change in free volume which depends on the local geometry of the network; the new free volume accessible to molecules A and B* is clearly smaller. The local variation is difficult to quantify unless one has a detailed knowledge of the geometry on such a very small scale, but one can reasonably assert that, upon sudden deformation involving the total volume of the material, an instantaneous change in free volume takes place, and this change immediately affects the relaxation behavior.

Subsequent to this instantaneous free volume change, which is the first step

---

* these two molecules are not entirely shown for purpose of clarity.

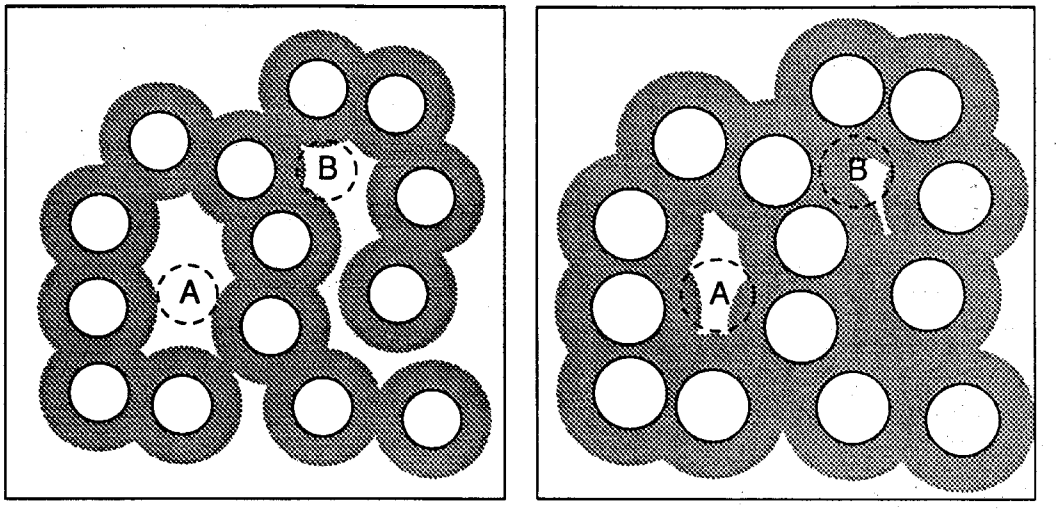


FIGURE 1.3 Free volume (left) and new free volume (right) after sudden deformation for molecules A and B.

of the evolution towards equilibrium, a time-dependent one takes place. A question arises about the connection between the two and their relation with the total macroscopic dilatation or contraction. It is conceivable to depict a situation in which the nonequilibrium changes in occupied and free volume do not obey the simple law of proportionality in relation to the total deformation, *i.e.*, during this time-dependent process the fraction of the volume change that contributes to one or the other is not a constant. In addition, molecular rearrangements could modify the chain topology in such a way that a "trading" between free and occupied volume occurs, as would be the case when the regions where molecules partially overlap change in size without a macroscopic change in volume. A major simplification will be made here, partly because of ignorance of the molecular details and partly to simplify the implementation of the model for purpose of analysis: the nonequilibrium fractional free volume changes will be assumed to be a (constant) fraction of the time-dependent dilatation, *i.e.*, they will be written as

$$f = f_{init} + \delta \cdot \epsilon_{kk} , \qquad (1.1.23)$$

where $\delta$ is a constant** parameter and $f_{init}$ is the initial fractional free volume of the material. The initial fractional free volume is representative of the amount of vacancies in the equilibrium initial condition†, before the latter is perturbed by a temperature or pressure change. Eq. 1.1.23 will be held valid not only when $\epsilon_{kk}$ is the asymptotic (equilibrium) deformation caused by changes in applied pressure or temperature, but also when it corresponds to the contribution to the equilibrium change due to the instantaneous or time-dependent response.

It will be assumed that, at low strains, the constitutive response of an amorphous and isotropic polymer can be formulated with the aid of two material functions, namely with the time-dependent bulk and shear moduli‡, and that the time scale of relaxation or creep is governed by a free volume induced time shift. Above the glass transition, the free volume changes will be assumed to be a constant fraction of the total deformation, as given by Eq. 1.1.23. Under isothermal conditions, the governing equations can then be summarized as follows:

$$\sigma_{ij} = \int_{-\infty}^{t} 2G\Big(\xi(t) - \xi(\tau)\Big)\frac{\partial \epsilon'_{ij}(\tau)}{\partial \tau} d\tau + \delta_{ij}\int_{-\infty}^{t} K\Big(\xi(t) - \xi(\tau)\Big)\frac{\partial \epsilon_{kk}}{\partial \tau} d\tau \ , \quad (1.1.24)$$

$K(t)$ and $G(t)$ being the time-dependent bulk and shear moduli,

$$\epsilon'_{ij} \ = \ \epsilon_{ij} - \frac{1}{3}\delta_{ij}\epsilon_{kk} \ , \quad (1.1.25)$$

---

** These assumptions will be relaxed in the next section 1.1.3 in order to address the rheological behavior of polymers below the glass transition; in particular, the parameter $\delta$ will result to be a function of the fractional free volume (*cf.* Eq. 1.1.73).

† The initial condition is a reference one, but it must not be confused with the reference condition related to the reference fractional free volume $f_0$, which is representative of the state of the material in which the time-dependent properties were measured.

‡ Large strain viscoelastic behavior, not addressed here, is complicated by the fact that the material response would be in general an isotropic function of the deformation tensor, such as a function of the invariants of the right Cauchy-Green deformation tensor, and, furthermore, possibly the time scale itself of the viscoelastic behavior could be affected by the increasingly anisotropic orientation of the molecules.

denoting the deviatoric part of the strain tensor field, and $\xi(t)$ representing the internal time of the material, as given by Eq. 1.1.10, with a dependence of the time shift on the current value of free volume as given by Eq. 1.1.11.

The model is completely general, but it can be helpful to visualize it through a mechanical analogy for the viscoelastic behavior. In particular, if one approximates the bulk behavior in terms of a Prony series, *i.e.*,

$$K(t) = K_\infty + \sum_i K_i e^{\frac{-t}{\tau_i}} , \qquad (1.1.26)$$

where $K_\infty$ represents the asymptotic, (long term) equilibrium response, the $K_i$'s are the components of the relaxation spectrum and the $\tau_i$'s are the corresponding relaxation times, then the constitutive behavior can be visualized through the mechanical model shown in Fig. 1.4, where each of the spring-dashpot assemblies represents one component of the spectrum and the series of the elastic springs takes care of the asymptotic material response.

The model expresses the volumetric part of the mechanical behavior as the sum of a time-independent response, corresponding to the equilibrium interaction of the molecules, and a time-dependent one that can be related to nonequilibrium behavior. If one wanted to look at the micromechanics of the volume deformation, then the elastic and time-dependent parts of the response could be attributed to local interaction*, as in the case where the material is pressurized and molecules are pressed against each other, and to entropic contributions stemming from the rubbery behavior of the polymer. At the present stage, no distinction is made between these two separate effects, though, in a more complete theory, this separation would need to be taken into account (Matheson, 1987), possibly through the

* Denoted here as energetic contribution, since it is the same phenomenon as the hydrostatic pressure in a gas, which is directly related to its internal energy.

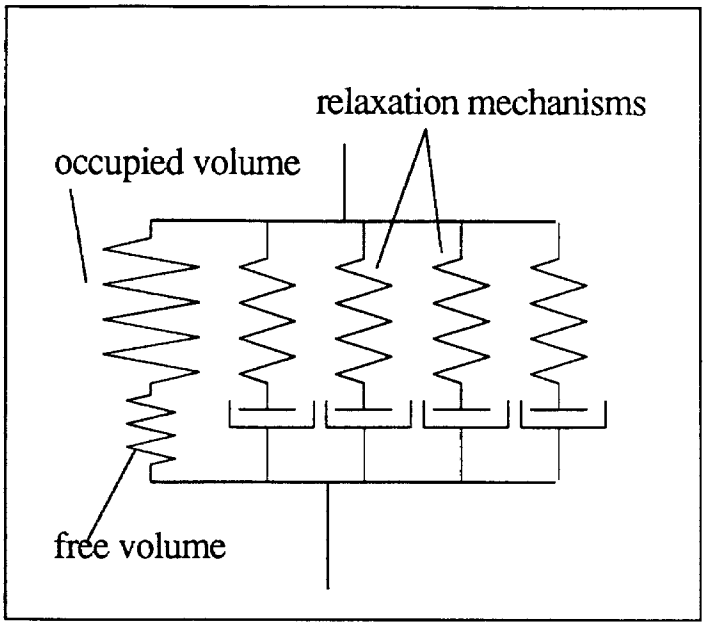


FIGURE 1.4 Mechanical analogue for nonlinearly viscoelastic bulk behavior.

subdivision of the elastic component into entropic and energetic parts. The free volume elastic response, related to the amount of deformation that contributes to changing the volume of holes in the network, is not supposed to attribute elastic properties to vacuum, which is ultimately the material of which the holes in between the molecules are made. Instead, it purposely corrects (increases) the compliance of the total volume by noting that some of the deformation does not result in forcing the molecules closer, but it merely allows the shuffling of vacancies around while changing their total volume. Under the assumption that the compliances of the free and occupied volume are simply additive and that their ratio is constant**, their values determine the constant fraction of the total deformation that contributes to a change of one or the other. If one denotes by $\beta_{fo}$ the ratio between the compli-

** Such assumption is reflected in the particular way in which the occupied and free volume elastic elements are arranged in the mechanical analogue. This hypothesis will be relaxed in section 1.1.4 in order to account for the change in material properties which occurs when the material passes through the glass transition.

ance of the free volume, $C_{free}$, and that of the occupied volume, $C_{occ}$, which is also the ratio between free and occupied volume changes occurring when the material is subjected to an external pressure variation, *i.e.*,

$$\beta_{fo} = \frac{C_{free}}{C_{occ}} = \frac{\Delta V_{free}}{\Delta V_{occ}} , \tag{1.1.27}$$

then the parameter $\delta$ of Eq. 1.1.23 is determined by the relation

$$\delta = \frac{\Delta V_{free}}{\Delta V_{free} + \Delta V_{occ}} = \frac{\beta_{fo}}{1 + \beta_{fo}} . \tag{1.1.28}$$

Attention shall now be devoted to the effects which temperature variations have on the material behavior. Temperature changes influence the mechanical state of the polymer in two different ways: on the one hand, there are variations in the mechanical properties such as those which are expressed by Eq. 1.1.11 or those which follow from passing through a glass transition†; on the other hand, a state of stress is induced in the material if all motion is restrained or, conversely, a thermal expansion follows a temperature change under isobaric conditions. The latter aspect, *i.e.*, the direct effect of temperature on the stress and displacement fields, will be addressed here, while the former one will be discussed in section 1.1.4.

In the case of elastic materials such as metals, it is generally assumed that the thermal expansion is instantaneously dependent on the temperature changes. However, experimental observations (*e.g.*, Kovacs, 1958) seem to indicate a different behavior characteristic of polymers, notably a behavior which has time-dependence associated with it. For such materials, the relation between the mechanical state and the temperature history needs to be expressed in terms of functionals of the

† The effects of the glass transition on the mechanical properties will be specifically addressed in section 1.1.4; in the same section, a method of inferring the parameter $\beta_{fo}$ from experimental data is suggested.

latter. One can deduce some indications about the nature of the stress field dependence on temperature variations by means of rational thermodynamics. Within such a framework, if one assumes that the material (Helmholtz) free energy can be expressed in terms of linear and quadratic functionals of the strain and temperature histories, then the satisfaction of the Clausius-Duhem inequality for the entropy production (*e.g., cf.* Christensen and Naghdi, 1966) results in an expression for the stress state which reads

$$\sigma_{ij}(t) = \int_{-\infty}^{t} 2G\Big(\xi(t)-\xi(\tau)\Big)\frac{\partial \epsilon'_{ij}(\tau)}{\partial \tau}d\tau + \delta_{ij}\int_{-\infty}^{t} K\Big(\xi(t)-\xi(\tau)\Big)\frac{\partial \epsilon_{kk}}{\partial \tau}d\tau - \\ -\delta_{ij}\int_{-\infty}^{t}\Theta\Big(\xi(t)-\xi(\tau)\Big)\frac{\partial T}{\partial \tau}d\tau \ , \qquad (1.1.29)$$

where $\Theta(t)$ is a (possibly) time-dependent material function. If one postulates a time-dependent coefficient of thermal expansion, namely a material function $\alpha(t)$ which gives the thermal strains $\epsilon_\theta(t)$ under isobaric conditions and initial equilibrium (*i.e.*, $\sigma_{kk}=0$), as

$$\epsilon_\theta(t) = \int_{-\infty}^{t}\alpha\Big(\xi(t)-\xi(\tau)\Big)\frac{\partial T}{\partial \tau}d\tau \ , \qquad (1.1.30)$$

then one deduces from Eq. 1.1.29 a relationship between $K(t)$, $\alpha(t)$, $\Theta(t)$, which reads

$$\Theta(t) = \int_{-\infty}^{t} K\Big(\xi(t)-\xi(\tau)\Big)\frac{\partial \alpha}{\partial \tau}d\tau \ . \qquad (1.1.31)$$

A straightforward derivation of Eq. 1.1.31 transforms Eq.s 1.1.29 and 1.1.30 in the Laplace domain. If bar quantities are used to denote the Laplace transformed functions, then the transformed Eq. 1.1.31 and volumetric component of Eq. 1.1.29 read

$$\bar{\epsilon}_{kk}(s) = s\,\bar{\alpha}(s)\,\bar{T}(s) \ , \qquad (1.1.32a)$$

$$\bar{\sigma}_{kk}(s) = 3\,s\,\bar{K}(s)\,\bar{\epsilon}(s) - 3\,s\,\bar{\Theta}(s)\,\bar{T}(s) \ . \qquad (1.1.32b)$$

Upon substitution of Eq. 1.1.32a in 1.1.32b, one obtains for the isobaric case ($\bar{\sigma}(s) = 0$)

$$\Theta(s) \;=\; s\,\bar{K}(s)\,\bar{\alpha}(s) \;\;, \tag{1.1.33}$$

which yields Eq. 1.1.31 upon inverse Laplace transformation.

It is useful to place bounds on the time-dependent function $\Theta(t)$. If one considers a monotonically increasing coefficient of thermal expansion, *i.e.,*

$$\alpha(t) \;=\; \alpha_0 + \Delta\alpha(t) \;\;;\;\; \frac{d\Delta\alpha(t)}{dt} \geq 0 \;\;, \tag{1.1.34}$$

where $\alpha_0$ is the initial value[‡] of such coefficient and $\Delta\alpha(t)$ is its time-dependent component, then Eq. 1.1.31 implies

$$\Theta(t) \geq \alpha_0\, K(t) \;\;. \tag{1.1.35}$$

On the other hand, it is reasonable to assume that the stress state due to temperature variations is a nonincreasing function of time, *i.e.,*

$$\frac{d\Theta}{dt} \leq 0 \;\;, \tag{1.1.36}$$

which in turn implies

$$\Theta(t) \leq \alpha_0\, K_0 \;\;, \tag{1.1.37}$$

$K_0$ being the instantaneous value of the bulk modulus. The above inequalities combined read

$$K(t) \leq \frac{\Theta(t)}{\alpha_0} \leq K_0 \;\;, \tag{1.1.38}$$

---

‡ $\alpha_0$ and $K_0$ denote here the instantaneous values of coefficient of thermal expansion and bulk modulus, which **are not** the same as the glassy values which are characteristic of the polymer below the glass transition. As presented in section 1.1.4, the glassy values are additionally affected by the lack of free volume deformability, which results in $\alpha_g \leq \alpha_0$ and $K_g \geq K_0$.

which means that the functional $\Theta(t)$ is characterized by an initial value of $\alpha_0 K_0$ and, if the coefficient of thermal expansion is time-dependent, decays as a viscoelastic modulus but possibly not as fast as the bulk modulus, since its values need to stay above the curve $\alpha_0 K(t)$.

The following observations can give further insight into the characteristics of the function $\Theta(t)$. This function expresses the isotropic part of the stress state when all volumetric deformations are restrained, *i.e.,* when $\epsilon_{kk} = 0$. Macroscopic deformations play a significant role in the time-dependent nature of the viscoelastic response, which is conceivably the result of short-range rearrangements of the polymer chains, such as bond rotation or local readjustments of position, and also of long-range motion, which involves a drift of the entire polymer molecule. If macroscopic deformation is restrained, it is conceivable that the long-range motions of the polymer chains are strongly impaired by the lack of deformability of the network, which in turn implies that the time-dependence of the resulting stress state might not be as significant as when the material can expand or contract freely.

As a result of these observations, it will be assumed that, when macroscopic motions are restrained, the stress state following a temperature change is time-independent, *i.e.,* the function $\Theta(t)$ is taken to be constant. This situation would hold true if the restraint imposed on the macroscopic deformation implied a total absence of rearrangements in the molecular network, such as the trading between the occupied volume and the volume of the vacancies. Since such a trading can conceivably occur, the assumption of a time-independent stress state under isocoric conditions still contains a margin of error in it, but seems to be superior to assuming a constant coefficient of thermal expansion, since the former hypothesis effects a time-dependent volume change. The temperature effects are therefore

translated into an equivalent, time-independent "thermal pressure" $\hat{p}(T)$ acting on the viscoelastic material *, so that the constitutive equation can be rewritten in the form

$$\sigma_{ij} = \delta_{ij}\hat{p}(T) + \int_{-\infty}^{t} 2G\Big(\xi(t)-\xi(\tau)\Big)\frac{\partial \epsilon'_{ij}(\tau)}{\partial \tau}d\tau + \delta_{ij}\int_{-\infty}^{t} K\Big(\xi(t)-\xi(\tau)\Big)\frac{\partial \epsilon_{kk}}{\partial \tau}d\tau \ . \tag{1.1.39}$$

Since the isocoric stress change due to temperature rise is assumed to be time-independent, it can be computed as the stress state which, in the rubbery regime characteristic of temperatures above the glass transition, gives an asymptotic volume deformation equal to the product of the rubbery coefficient of thermal expansion $\alpha_l$ times the temperature increment. Recalling that $K_\infty$ is the asymptotic value of the bulk modulus, the thermal pressure can then be written as

$$\hat{p}(T)_{equil} = \hat{p}(T) = -K_\infty \alpha_l \Delta T \ . \tag{1.1.40}$$

Eq. 1.1.39 can also be written in a different form, in which the thermal strains are subtracted from the dilatational history, which reads

$$\sigma_{ij} = \int_{-\infty}^{t} 2G\Big(\xi(t)-\xi(\tau)\Big)\frac{\partial \epsilon'_{ij}(\tau)}{\partial \tau}d\tau + \delta_{ij}\int_{-\infty}^{t} K\Big(\xi(t)-\xi(\tau)\Big)\frac{\partial (\epsilon_{kk}-\epsilon_\theta)}{\partial \tau}d\tau \ , \tag{1.1.41}$$

where $\epsilon_\theta$ is given by

$$\epsilon_\theta(t) = \int_{-\infty}^{t} M\Big(\xi(t)-\xi(\tau)\Big)\frac{\partial (K_\infty \alpha_l T)}{\partial \tau}d\tau \ , \tag{1.1.42}$$

$M(t)$ being the viscoelastic bulk compliance, related to the bulk modulus by the equation (*cf.* Appendix B)

$$\int_{-\infty}^{t} K(t-\tau)M(\tau)d\tau = t \ . \tag{1.1.43}$$

---

* Such thermal pressure is representative of the isotropic state of stress characterizing the polymer when all volume changes are restricted and the material is subjected to a temperature variation.

It can also be noted that, since a direct correspondence is assumed between temperature changes and pressure, an applied pressure change is equivalent to a temperature change of

$$\Delta T = -\frac{1}{K_\infty \alpha_l}\Delta p \ . \tag{1.1.44}$$

Such equivalence will be used in section 1.1.7, where the pressure dependence of the glass transition will be discussed.

The presented model reduces the thermal contribution to the stress state to a constant term, easily computable in terms of other known quantities. On the other hand, if the stress state dependence on temperature had been constructed through an appropriate functional of the thermal history, the experimental measurement of the corresponding viscoelastic function would be required and such a measurement is, to say the least, almost unattainable due to the constant presence of thermal transients (heat conduction in a specimen of finite size). Although the model contains some approximations, such as the already mentioned neglect of possible "trading" between free and occupied volume under isocoric conditions, it is certainly an improvement over assuming that the isobaric coefficient of thermal expansion, commonly denoted with $\alpha_l$ or $\alpha_g$ depending on the temperature range, is time or history independent. In fact, one of the consequences of the model is the time-dependent thermal expansion under isobaric conditions, governed by the bulk behavior and by the free volume induced change in relaxation times, as was suggested by Kovacs's experiments (1958). Furthermore, the extension of the proposed constitutive assumptions into the range of metastable equilibrium (below the glass transition) will require, as shown in Section 1.1.4, no second coefficient of thermal expansion besides $\alpha_l$.

Some comments on the consequences of the constitutive assumptions on the

relaxation behavior are in order. The time scale of the material relaxation is taken to be affected by the instantaneous free volume through the time shift computed via Eq. 1.1.11. Since the free volume changes are a part of the total deformation, this assumption effects a coupling between the strain and stress fields and the internal time scale of the polymer, as shown by Knauss and Emri (1981). It follows that high tensile stresses (dilatation) produce an acceleration of the creep process, due to the increase in free volume, and this feature has been proposed to be one of the main factors influencing the "yielding-like" phenomenon in glassy polymers. Conversely, high pressures effect a decrease in the void volume, with a shift of the viscoelastic spectra towards the glassy behavior, and longer times needed for the material to reach equilibrium.

The constitutive model presented in this section is built within the framework of the well-known nonlinear viscoelastic theory based on free volume considerations. The extensions of this model to the treatment of the problems of the residual free volume and the second order glass transition will introduce some new, additional elements to such theory. These aspects will be addressed in the coming sections, and the residual free volume will be considered first.

### 1.1.3 The residual free volume

The concept of residual free volume arises from experimental observations of the rheological behavior of polymers at temperatures below the glass transition, *i.e.*, when the polymer can at best achieve a state of metastable equilibrium. The notion of a state of metastable equilibrium** is intended here as a state in which

** McKinney and Goldstein (1974) adopt the terminology "isoviscous" state.

there is no time-dependent change in the condition of the polymer, but the material is far from thermodynamic equilibrium. Conditions of metastable equilibrium typically occur below the glass transition, *e.g.,* in the case where crystallization is prevented and the polymer remains in an amorphous state, or when the volume of the vacancies is larger than the equilibrium free volume fraction. The latter aspect will be investigated next.

It is established experimentally that the time shift predicted by Eq. 1.1.11, with the free volume $f$ linearly dependent on temperature, fails to conform to measured values below the glass transition. The experimental time-temperature shift for PVAc, as measured by L. Heymans (Heymans, 1983), is shown by the discrete points in Fig. 1.5. It is easy to see that a fit of Eq. 1.1.11 to the experimentally measured values, assuming a linear dependence of free volume on temperature, diverges from the experimental curve below the glass transition temperature, which is about 29 $C$ for PVAc.

There are two plausible explanations for this discrepancy, the simplest one being, perhaps, that the parameter $B$ of the Doolittle equation has a discontinuity across the glass transition. Experimental observations seem, however, to favor the opposite point of view, namely that the parameters and the form of the Doolittle equation are continuous across the transition, and the discrepancy between the experimental and computed time shifts has to be explained in terms of a different dependence of the free volume on temperature. Rusch (1968) confirmed experimentally that volume-recovery data, *i.e.,* asymptotic contraction upon cooling below $T_g$, are consistent with the time shift if one considers the excess volume, defined as the amount of volume which the material possesses above some equilibrium curve, as frozen-in free volume, which affects the relaxation behavior through Eq. 1.1.11.

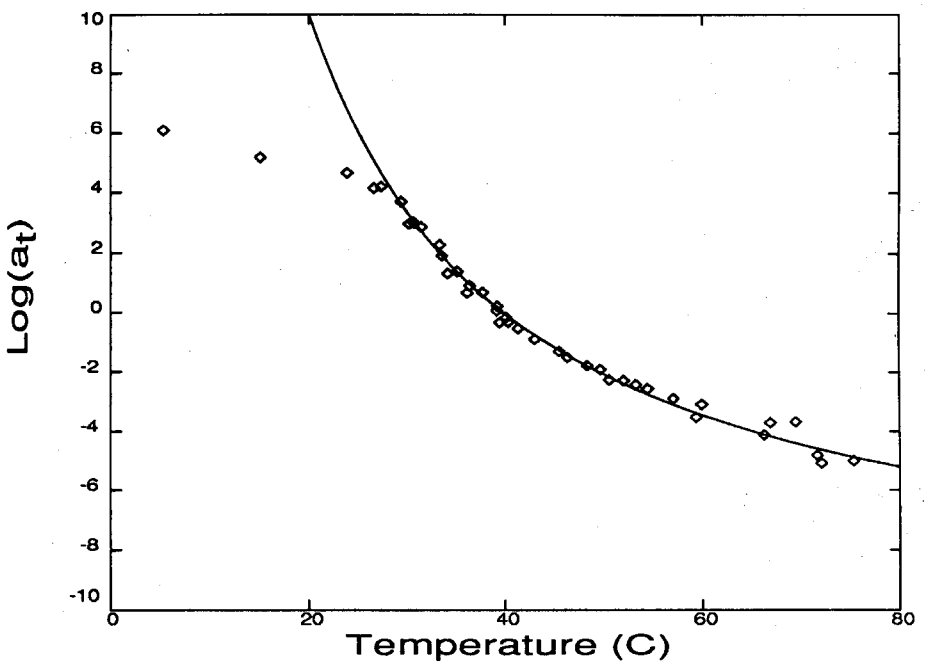


FIGURE 1.5 Logarithm (base 10) of the experimental time shift for PVAc, referenced to 40 C (squares). The WLF fit to the experimental data is shown by the continuous line, with the following choice of parameters: reference free volume at 40 $C$ = .0095; $\frac{\partial f}{\partial T} = \alpha_f = 2.32 \times 10^{-4} C^{-1}$; $B$ (parameter of the Doolittle equation)= .10.

That situation is depicted in Fig. 1.6, where the appropriate volume-temperature curve for PMMA is shown. The dashed lines represent the (thermodynamic) equilibrium curves for the free and occupied volume, whereas the continuous one represents the experimentally measured values† which are attained when the polymer settles into a state of metastable equilibrium. It is assumed that the equilibrium free volume vanishes at some temperature $T_2$ below the glass transition, which can be computed from the reference conditions and the equilibrium change of free volume with temperature; $T_2$ is shown in Fig. 1.6 by the intersection of the occupied and free volume equilibrium curves and equals about 50 $C$. If this excess volume is

† Below $T_g$, the values were measured after a 10,000-sec annealing at each temperature.

taken to represent free volume which has been left in the polymer and which will not disappear in time, the time shift is well predicted through this metastable value of $f$ and the unchanged (from above the glass transition) Doolittle equation. The finite volume of the vacancies below $T_2$, determined where the linear temperature dependence above $T_g$ would predict a null free volume content, will be denoted here as residual, since it does not vanish where the high-temperature behavior of the polymer indicates that it should.

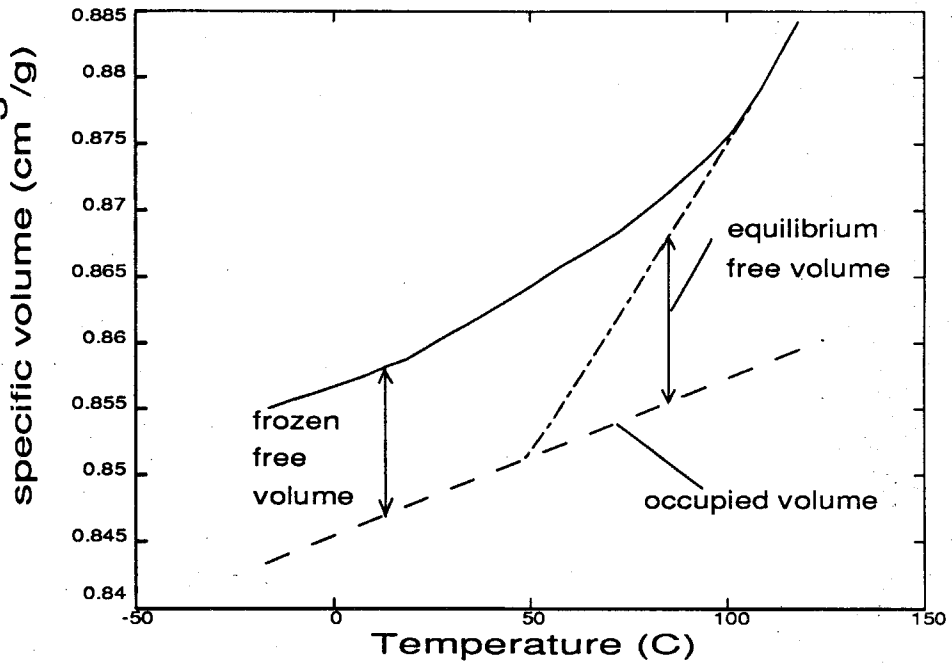


FIGURE 1.6 Experimental volume recovery data for PMMA (Rusch, 1968).

Rusch (1968) does not indicate the reasons for the existence of a residual free volume. A tentative explanation is given here with the intent of extending the phenomenological model presented in the previous Section 1.1.2 to the range of metastable equilibrium. Such a simple explanation arises naturally from the consideration that random thermal vibrations of the polymer chains are unlikely to

destroy the disorder in the network as embodied in the distribution of defects or vacancies. There is thus a need to quantify random motion and its relationship to the macroscopic material behavior.

What appears to be a continuous process on a macroscopic scale, such as creep or relaxation, is in fact, on a molecular level, the superposition of a slow drift of the chains and of the ensemble of thermal collisions between neighboring molecules. These two aspects are not physically separable from each other, because there would be no drifting without thermal motion, which provides the "engine" for the relaxation process. However, for the temperature range of interest, the two processes can be considered superimposed on each other‡. A simple schematization of a viscous process and of the process as it would appear on a very small spatial and temporal scale is shown in Fig. 1.7. Given the physical characteristics of this phenomenon, the best way to approach it is through the theory of continuous Markov processes*.

At first, one should consider the phenomenon of volume changes as it appears on a macroscopic scale when the amplitude of the random fluctuations is small compared with the time-dependent viscous changes. This task can be accomplished by considering the viscoelastic laws for the evolution of the polymer from a nonequilibrium state to a stable one.

For instance, consider the free volume changes due to an arbitrary pressure

---

‡ For temperatures low enough to drastically change the vibrational modes of the polymer chains, this might not be true. It is assumed here that in the temperature range of interest, not extending to cryogenic values, this problem does not arise. This assumption also implies the absence of strong discontinuities in the equilibrium internal energy of the polymer, as would be the case when a first order transition is present.

* A continuous Markov process is a particular kind of process which is partly governed by one or more stochastic (random) variables, *e.g.*, white noise. A short introduction to stochastic analysis and Markov processes is given in Appendix C; for a more thorough exposure, see Gardiner, 1985.

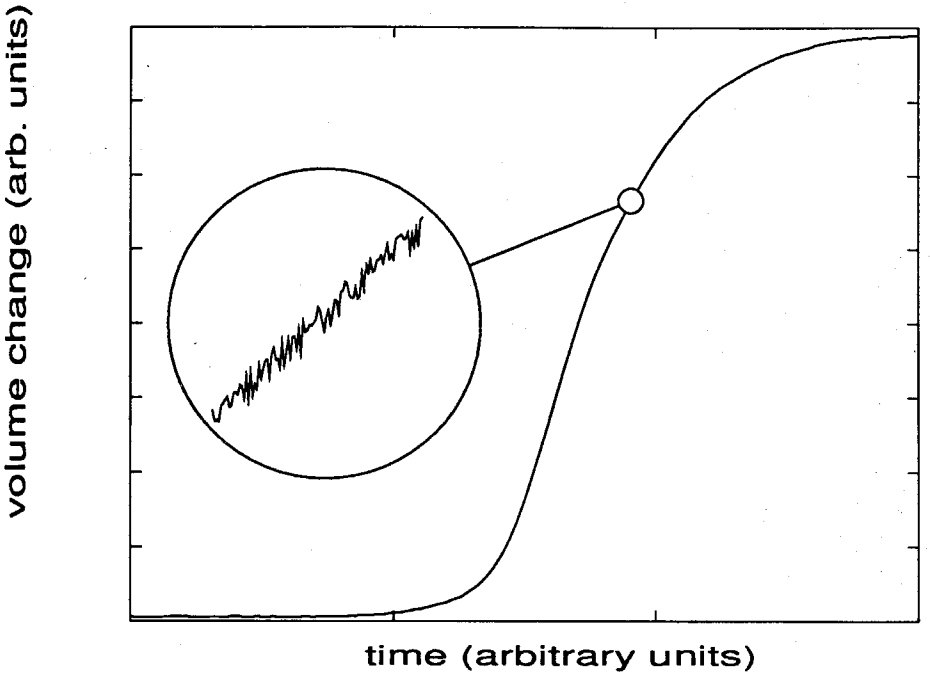


FIGURE 1.7 Schematic representation of a Markov process. The figure presents a viscous process as it appears on a macroscopic scale; the large circle shows how the process would appear if a very small volume, as the one occupied by a few molecules, and a fine temporal resolution were characterizing the observation.

history which, in the linearly viscoelastic case, can be written as

$$f(t) \;=\; \delta \cdot \int_{-\infty}^{t} M(t-\tau)\frac{\partial p}{\partial \tau} d\tau \;\;, \tag{1.1.45}$$

where $\delta$ is the fraction of the total deformation that contributes to free volume changes, as formulated in Eq. 1.1.23. If one adopts a Prony series expansion for the bulk compliance, *i.e.*,

$$M(t) \;=\; M_0 + \sum_i M_i (1. - e^{-\frac{t}{\tau_i}}) \;\;, \tag{1.1.46}$$

then the same equation can be rewritten without loss of generality in the form

$$f(t) \;=\; \delta \cdot \left[ M_0 \Delta p + \sum_i \int_{-\infty}^{t} M_i (1 - e^{-\frac{t-\tau}{\tau_i}}) \frac{\partial p}{\partial \tau} d\tau \right] \;. \tag{1.1.47}$$

Differentiating Eq. 1.1.47 and by virtue of the vanishing of $M(t)$ for $t < 0$, one obtains

$$\frac{df}{dt} = \delta \cdot \Big[\frac{dp}{dt}M(0) + \sum_i \int_{-\infty}^{t} \frac{M_i}{\tau_i} e^{-\frac{t-\tau}{\tau_i}} \frac{dp}{d\tau} d\tau\Big] =$$

$$= \delta \cdot \frac{dp}{dt} M_0 + \sum_i \frac{1}{\tau_i}(f_{i,\infty} - f_i) \ , \tag{1.1.48}$$

where

$$f_i = \delta \cdot \int_{-\infty}^{t} M_i (1 - e^{-\frac{t-\tau}{\tau_i}}) \frac{dp}{d\tau} d\tau \tag{1.1.49}$$

is the current deformation of each component of the creep spectrum, and

$$f_{i,\infty} = \delta \cdot \int_{-\infty}^{t} M_i \frac{dp}{d\tau} d\tau \ = \ \delta \cdot M_i \ p(t) \tag{1.1.50}$$

is the corresponding (long term) asymptotic deformation. In differential terms, one may write

$$df \ = \ \Big[\sum_i \frac{1}{\tau_i}(f_{i,\infty} - f_i) + \delta \cdot M_0 \frac{dp}{dt}\Big] dt \ . \tag{1.1.51}$$

Eq. 1.1.51 is valid only at the reference condition in which the time-dependent bulk compliance has been measured. For values of temperature or pressure different from those in the reference state, one has to observe that the free-volume induced time shift operates, therefore the above equation needs to be recast in the form

$$df \ = \ \Big[\sum_i \frac{1}{\tau_i}(f_{i,\infty} - f_i)\frac{dt}{a_t} + \delta \cdot M_0 \frac{dp}{dt} dt\Big] \ =$$

$$= \ \Big[\sum_i \frac{1}{\tau_i}(f_{i,\infty} - f_i) e^{-B(1/f - 1/f_0)} + \delta \cdot M_0 \frac{dp}{dt}\Big] dt \ , \tag{1.1.52}$$

by virtue of Eq. 1.1.11.

As suggested previously in this section, it is of interest to investigate the consequences of adding randomness to the molecular motion represented by Eq. 1.1.52. A consistent way of concretizing that intention is to consider the viscoelastic changes as the superposition of an average viscoelastic motion, such as that expressed by Eq. 1.1.52, and a random Brownian disturbance incorporating the stochastic features of thermal vibration. If one considers each individual contribution of the creep spectrum to the total deformation, an extension of the viscoelastic model which includes such random features incorporates a term describing stochastic motion (white noise) in Eq. 1.1.52, *i.e.*,

$$df_i = \frac{1}{\tau_i}(f_{i,\infty} - f_i)e^{-B(1/f-1/f_0)}dt + \sqrt{\frac{A}{\tau_i}}f_i d\underline{b} \quad . \tag{1.1.53}$$

The term $d\underline{b}$ represents uncorrelated random fluctuations with the following features

$$E(d\underline{b}) = 0 \quad , \tag{1.1.54}$$

and

$$E([d\underline{b}]^2) = dt \quad , \tag{1.1.55}$$

where $E(\underline{x})$ denotes the expected value of the random variable $\underline{x}$. The above equations simply state that the mean value of the fluctuations is zero and their variance is proportional to time. Eq. 1.1.55 also gives some information about the nature of mathematical white noise, namely that it has dimensions of $(\text{time})^{1/2}$. Consequently, a few adjustments are necessary to introduce this term into Eq. 1.1.52 in a dimensionally proper way. These adjustments are the scaling of white noise by the square root of a characteristic time scale and the multiplication by the fractional free volume $f_i$ **. These two terms can also be interpreted in a qualitative manner:

** Technically speaking, the multiplication by $f_i$ is not necessary since $f$ denotes fractional free volume, which is dimensionless; but then the same equation cast in terms of total or fractional free volume would have two completely different meanings; thus the reason for the introduction of the multiplicative factor $f_i$.

the multiplicative factor $f_i$ arises from the probability of thermal motion affecting the pre-existing free volume, probability which has to be proportional to the fractional free volume; or it can arise from the proportionality of the fluctuations to the current number or size of the vacancies. Since the above equation is to be valid for each component of the relaxation spectrum, the characteristic time scale was chosen as the corresponding relaxation time. $A$ is a (dimensionless) parameter, assumed to be constant throughout the whole relaxation spectrum.

If one integrates the stochastic differential equation 1.1.53, the expected value of the free volume deformation†, according to the Stratonovich integral‡, is

$$E(\Delta f_i) = \left[\frac{1}{\tau_i}(f_{i,\infty} - f_i)e^{-B(1/f-1/f_0)} + \frac{A}{2\tau_i}f_i\right]\Delta t \,. \qquad (1.1.56)$$

Given the values of $f_{i,\infty}$, *i.e.*, $\delta\ M_i p$, which represent the values of free volume achievable in the absence of random motion, one can compute the (metastable) equilibrium free volume $f_{i,e}$ as the value for which $E(\Delta f_i)$ is zero, which yields

$$\frac{1}{\tau_i}(f_{i,\infty} - f_{i,e})e^{-B(1/f_e-1/f_0)} + \frac{A}{2\tau_i}f_{i,e} = 0 \,, \qquad (1.1.57)$$

or

$$f_{i,e}(e^{-B(1/f_e-1/f_0)} - \frac{A}{2}) = f_{i,\infty}e^{-B(1/f_e-1/f_0)} \,. \qquad (1.1.58)$$

Since the total free volume $f$ is given by the sum of the individual time-dependent components $f_i$ and the time-independent one associated with the quantity $\delta \cdot M_0 \frac{dp}{dt}$, one can write an expression which predicts the (metastable) equilibrium free volume below the glass transition. In order to distinguish among the different contributions

---

† *i.e.*, the average quantity one could measure through an ensemble average of all the changes occurring at the different free volume sites.

‡ A brief introduction to stochastic integration is given in Appendix C. A more detailed exposition of the subject is given in Gardiner (1985).

to the residual free volume, the time-dependent components will be denoted by a superscript $v$ and the time-independent one by a superscript $g$. One thus has

$$f_e = \sum_i f^v_{i,e} + f^g = \frac{f^v_\infty}{1 - \frac{A}{2} e^{B(1/f_e - 1/f_0)}} + f^g \ , \qquad (1.1.59)$$

where $f^v_\infty = \sum_i f_{i,\infty}$ is the asymptotic value of the time-dependent component of free volume in the absence of Brownian motion. If one denotes by $\zeta$ the ratio of the instantaneous free volume change to the overall asymptotic one, *i.e.*, $\frac{\Delta f^g}{\Delta f_\infty}$, one has

$$f^g = \zeta f_\infty = \zeta(f_0 + \Delta f_\infty) \ , \qquad (1.1.60)$$

and

$$f^v_\infty = (1 - \zeta) f_\infty = (1 - \zeta)(f_0 + \Delta f_\infty) \ ; \qquad (1.1.61)$$

here $\Delta f_\infty$ is the *total* equilibrium free volume change in the absence of random molecular motion, which can be computed through the equilibrium material description, *i.e.*, $\frac{\partial f}{\partial T}$, which is characteristic of the polymer above the glass transition. The quantity $\zeta$ can be computed* from the initial and asymptotic values of the bulk modulus; the bulk modulus of PVAc as measured by McKinney and Belcher (1963) was characterized by an initial value of 41500 bars and by an asymptotic one of 25250 bars, which gives a value of $\zeta$ equal to

$$\zeta = \frac{K_{initial} - K_{asymptotic}}{K_{initial}} = \frac{41500 - 25250}{41500} = 0.392 \ . \qquad (1.1.62)$$

The free volume $f_e$ in conditions of metastable equilibrium is given implicitly as a function of $f_\infty = f_0 + \Delta f_\infty$ through the nonlinear Eq. 1.1.59. $f_\infty$ can be considered as the value of the (thermodynamic) equilibrium free volume in the

---

* This trivial calculation can be performed by considering the combined stiffness of two springs in series, which represent, respectively, the time-dependent and constant part of the response. The relative amount of deformation which affects one of the springs, say the second one, is given by $\zeta_2 = \epsilon_2/(\epsilon_1 + \epsilon_2) = k_1/(k_1 + k_2)$.

absence of Brownian motion, *i.e.*, if randomness of thermal motion did not exist and if the molecules "knew" the positions of the holes that could be filled; $f_e$ is the value of the free volume that is actually achieved after an infinite period of time. For very small values of $f_\infty$ there is always a nonzero positive value of $f_e$ that satisfies Eq. 1.1.59; we identify these values of $f_e$ as the residual free volume of the material.

The validity of Eq. 1.1.59 also extends to the case when the parameter $A$ is temperature or pressure dependent, under the assumption that the free volume fluctuations do not affect the temperature or pressure field; Appendix C will consider the consequences on Eq. 1.1.56 of a situation in which such an assumption does not hold. A temperature and pressure dependence of the Markov parameter $A$, *i.e.*, a dependence of the amplitude of the random thermal vibrations on temperature and pressure, has effects on the pressure dependence of the glass transition, if the onset of the latter is related to a critical value of free volume; the effect of a pressure dependence of $A$ will be addressed in section 1.1.7.

Fig. 1.8 shows the residual value of free volume below the glass transition computed from the experimentally measured time shifts (Heymans, 1983) and the parameters of the Doolittle equation. Along with the experimental values, the solid curve represents the prediction ** of Eq. 1.1.59, with $f_\infty = f_0 + \alpha_f(T - T_{ref})$, $f_0 = .0095$, $T_{ref} = 40\ C$ and $\alpha_f = 2.32 \times 10^{-4}\ C^{-1}$. The curve was fitted to the measured data by choosing a parameter $A = 2. \times 10^{-6}$. As can be seen, the

---

** It has to be remarked here that the parameters chosen to fit the time shift data by means of the Doolittle equation differ from the usual ones employed in the literature. In particular, instead of using the "universally accepted" value of 1 for $B$ and the difference $(\alpha_l - \alpha_g)$ for $\alpha_f = \frac{\partial f}{\partial T}$ (*cf.* Fig. 1.5), the value of $\alpha_f$ was taken as that derived later in section 1.1.4; the consequent fit required the choice $B = 0.1$. These choices effect a value for the fractional free volume at the glass transition of about six tenths of a percent, differing from the value of two and a half percent proposed by Williams, Landel and Ferry (1955).

shape of the solution $f_e$ to Eq. 1.1.59 has a strikingly good agreement with the the experimental data.

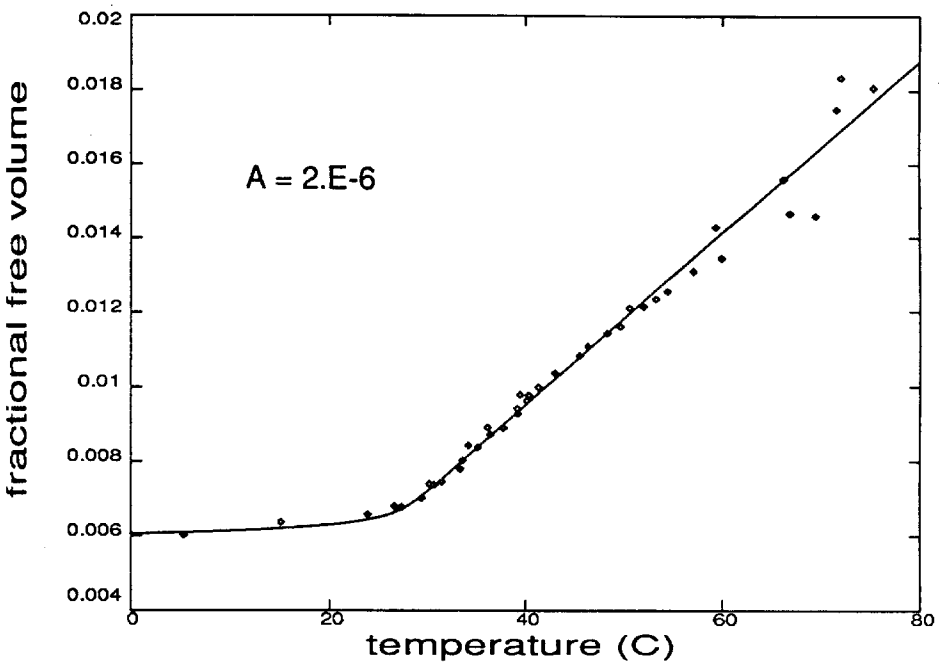


FIGURE 1.8 Experimental and Predicted Free Volume in conditions of metastable equilibrium below $T_g$, about 29 $C$ for PVAc.

In an earlier stage of preparation of this work, no distinction was made between the time-dependent and the instantaneous free volume changes, which now appears in Eq. 1.1.59. The time-independent component was then treated as any other viscous one, on the basis that Eq. 1.1.58 does not depend on any relaxation time, and the equation corresponding to Eq. 1.1.59 was written in the form

$$f_e = \frac{f_\infty}{1 - \frac{A}{2} e^{B(1/f_e - 1/f_0)}} \,. \tag{1.1.63}$$

The different predictions of Eq.s 1.1.59 and 1.1.63 are shown in Fig. 1.9, for the same choice of the parameter $A$, *i.e.*, $A = 2. \times 10^{-6}$. The difference is very marginal†

† The computations presented in Sect. 1.2 are actually carried out on the basis of Eq. 1.1.63 for

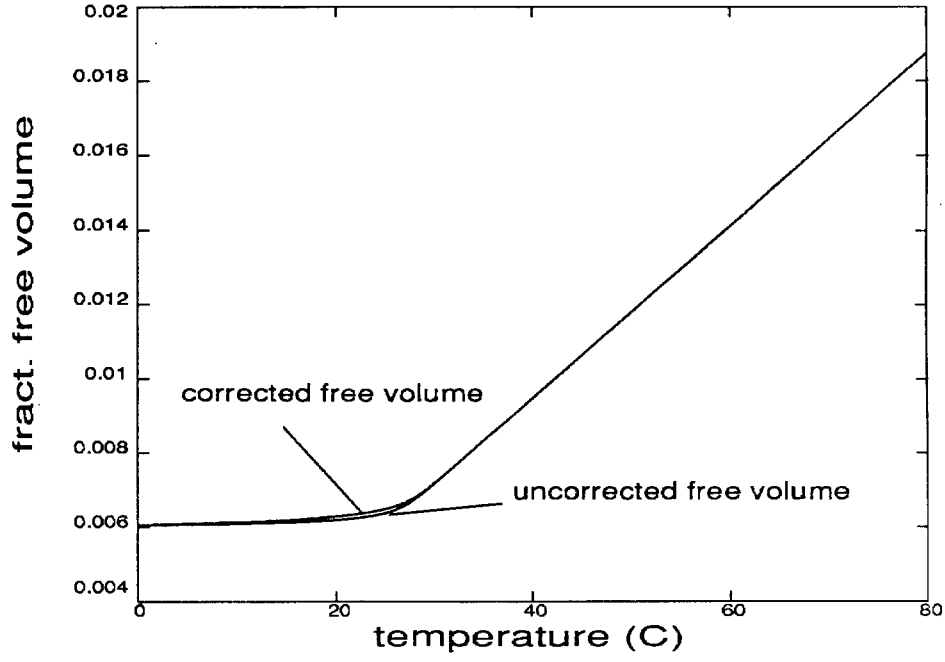


FIGURE 1.9 Comparison between the different predictions for the residual free volume upon different treatment of the time-independent component. The "corrected free volume" curve is the one predicted by Eq. 1.1.59, while the "uncorrected" curve shows the predictions of Eq. 1.1.63.

### 1.1.4 The mechanical properties and the glass transition

The mechanical response of a polymer is not, in general, a simple linear function of the strain or strain history. Among the several factors which can influence the constitutive behavior, this section will consider two which are responsible for changes in the long-term, asymptotic response such as that represented by the asymptotic bulk modulus, $K_\infty$. These two factors are, on the one hand, the possible presence of thermodynamic transitions in the equilibrium state of the polymer and the departure of the polymer from thermodynamic equilibrium below the glass transition, as encountered in the freezing-in of the free volume sites and of the relax-

the description of residual free volume. Since the values predicted by Eq.s 1.1.59 and 1.1.63 are very close to each other, the computations in section 1.2 and based on Eq. 1.1.63 are judged fully representative of the physics of the problem.

ation mechanisms. This section will attempt to assess their relative importance by considering the consequences that each factor alone has on the asymptotic response of the material.

First consider what would be the asymptotic material behavior under equilibrium conditions but in the presence of a thermodynamic transition (*i.e.*, a discontinuity in the values or in the derivatives of the thermodynamic potentials). In the case of an elastic material passing through a second order transition[‡], one can derive two equations, commonly called Ehrenfest relations, which express the change of the transition temperature $T_c$ with variations in the applied pressure $p$ in the form

$$\frac{\partial T_c}{\partial p} = \frac{\frac{1}{K_+} - \frac{1}{K_-}}{\alpha_+ - \alpha_-} \tag{1.1.64}$$

and

$$\frac{\partial T_c}{\partial p} = \frac{T \cdot (\alpha_+ - \alpha_-)}{C_{p+} - C_{p-}} \tag{1.1.65}$$

Here $T$ is the absolute temperature, $K_+$ and $K_-$ represent the bulk moduli above and below the transition, $\alpha_+$ and $\alpha_-$ are the corresponding isobaric coefficients of thermal expansion and $C_{p+}$ and $C_{p-}$ the heat capacities per unit volume and at constant pressure. From Eq. 1.1.64 and Eq. 1.1.65 it follows that

$$\frac{1}{K_+} - \frac{1}{K_-} = T\frac{(\alpha_+ - \alpha_-)^2}{C_{p+} - C_{p-}} \quad . \tag{1.1.66}$$

Since the nature of the glass transition in polymers is thought to be indicative of the presence of an equilibrium second order transition, one would need to apply Eq. 1.1.66 to the elastic (equilibrium) response of the material, *i.e.*, to the changes of the asymptotic bulk modulus, $K_\infty$.

---

‡ A second order transition is defined as a transition in which the derivatives of the thermodynamic potentials have a discontinuity but the potentials themselves are continuous. The glass transition in polymers has sometimes been considered indicative of a second order transition.

Besides these effects originated by the changes in the thermodynamic equilibrium state, there are additional ones caused by the relaxation behavior of the polymer practically frozen for low values of free volume and from the fact that the material can at best achieve a state of metastable equilibrium below the (assumed) second order transition. In order to assess the relative importance of (thermodynamic) equilibrium and nonequilibrium effects on the mechanical response, one can investigate the consequences of nonequilibrium by initially neglecting the presence of a thermodynamic transition of any kind at $T_g$, *i.e.*, the constitutive behavior would not obey Eq. 1.1.66.

With this assumption in mind, one can consider the effects of temperature on the isobaric expansion/contraction of the material which, as mentioned in section 1.1.2, are cast in terms of an equivalent "thermal pressure', assumed to be linearly dependent on temperature but not affected by any equilibrium transition and time-independent. The implications of this assumed lack of a transition with respect to the constitutive behavior in the glassy and rubbery regime and as exemplified by the differences in thermal expansion coefficients need to be considered now. In the long term (equilibrium) rubbery regime the relaxation mechanisms, symbolized in the mechanical model by the dashpots, have no effect on the material response, and the corresponding equilibrium dilatation is only affected by the elastic free and occupied volume response. The second partial derivative of the internal energy of the system with respect to temperature and volume can be computed by differentiating the thermal pressure with respect to temperature, resulting in

$$\left[\frac{\partial^2 U}{\partial V \partial T}\right]_{T_g+} = \frac{\partial \hat{p}(T)}{\partial T} = K_\infty \alpha_l \,, \tag{1.1.67}$$

where $\alpha_l$ is the thermal expansion coefficient of the rubbery (sometimes denoted as "liquid") state, and $K_\infty$ is the (long-time) asymptotic bulk modulus, given by the

elastic characteristics of the free and occupied volume springs in series.

Far below the glass transition the deformation of the free volume is completely absent, as explained in section 1.1.3. This lack of free volume deformation affects the equilibrium response of the total (free + occupied) volume, and one can try to compute this change in accordance with the intuitive mechanical model shown in Fig. 1.4, by considering the stiffness of the free and occupied volume springs in series. If $C^*_{free}$ is the (equilibrium ) compliance of the free volume above the glass transition, *i.e.,* in conditions of thermodynamic equilibrium, then

$$C_{free}\Big|_{(T>>T_g)} = C^*_{free} = \frac{\partial f}{\partial \sigma_{kk}} \ , \tag{1.1.68}$$

where $f = f_e$, since the distinction between residual (metastable) and equilibrium free volume vanishes above the glass transition. Below the glass transition, the effective free volume compliance is affected by the conditions of metastable equilibrium; therefore one has

$$C_{free} = \frac{\partial f_{eq}}{\partial \sigma_{kk}} = \frac{\partial f_{eq}}{\partial f_\infty}\frac{\partial f_\infty}{\partial \sigma_{kk}} = C^*_{free}\frac{\partial f_{eq}}{\partial f_\infty} \ . \tag{1.1.69}$$

An expression for $\frac{\partial f_{eq}}{\partial f_\infty}$ can then be obtained by differentiating Eq. 1.1.63, which yields

$$C_{free} = \frac{C^*_{free}}{1 - \frac{A}{2} exp(\frac{B}{f_e} - \frac{B}{f_0})[1 - \frac{B}{f_e}]} \ . \tag{1.1.70}$$

Eq. 1.1.63 was obtained by considering the time-independent states of the polymer (*cf.* Eqs. 1.1.56 and 1.1.57). It appears reasonable to extend the validity of this relation into time-dependent behavior by substituting the current value of the fractional free volume $f$ in place of the asymptotic value $f_e$. If one does so, then Eq. 1.1.70 can be concisely written in the form

$$C_{free} = C^*_{free}\phi(f) \ , \tag{1.1.71}$$

where

$$\phi(f) = \frac{1}{1 - \frac{A}{2} exp(\frac{B}{f} - \frac{B}{f_0})[1 - \frac{B}{f}]} \tag{1.1.72}$$

is a function which is near unity for sufficiently large values of $f$ but vanishes as the latter becomes small. If one denotes by $\beta_{fo}$ the ratio* between the compliances of the free and occupied volume in the rubbery regime, $\beta_{fo} = \frac{C^*_{free}}{C_{occ}}$, the equation expressing the free volume changes as a function of the total deformation, Eq. 1.1.23, needs to be reformulated as

$$f = f_{init} + \delta(f) \cdot \epsilon_{kk} \ , \tag{1.1.73}$$

where

$$\delta(f) = \frac{\beta_{fo}\phi(f)}{1 + \beta_{fo}\phi(f)} \ . \tag{1.1.74}$$

Above the glass transition, the value of the asymptotic bulk modulus is given by

$$K_\infty = \frac{1}{C^*_{free} + C_{occ}} = \frac{1}{C_{occ}(1 + \beta_{fo})} \ (T \gg T_g) \ . \tag{1.1.75}$$

Much below the transition, where the compliance of the free volume vanishes completely, a simple calculation shows that the asymptotic response, characterized here by the symbol $\hat{K}_\infty$, becomes

$$\hat{K}_\infty = \frac{1}{C^*_{free}\phi(f) + C_{occ}} = \frac{1}{C_{occ}[1 + \beta_{fo}\phi(f)]} = K_\infty \frac{1 + \beta_{fo}}{1 + \beta_{fo}\phi(f)} \ , \tag{1.1.76}$$

and, since $\phi(f)$ goes to zero as $f$ becomes small

$$\hat{K}_\infty = K_\infty(1 + \beta_{fo}) \ (T \ll T_g) \ . \tag{1.1.77}$$

In addition, the relaxation mechanisms are frozen much below $T_g$, and that fact has to be considered, too. The effective value of the bulk modulus for any deformation sufficiently below the glass transition is therefore given by

$$K_{T<<T_g} = K_\infty(1 + \beta_{fo}) + \sum_i K_i \ , \tag{1.1.78}$$

---

* This is also the ratio between free volume and occupied volume change in the total deformation above $T_g$.

where the $K_i$'s are the same quantities that appear in Eq. 1.1.26. If one focuses attention on the glassy state characterized by a bulk modulus given by Eq. 1.1.78 and a glassy coefficient of thermal expansion $\alpha_g$, the second partial derivative of the internal energy of the glass with respect to volume and temperature can now be written as

$$\left[\frac{\partial^2 U}{\partial V \partial T}\right]_{T_g-} = [K_\infty(1+\beta_{fo}) + \sum_i K_i]\alpha_g \ . \tag{1.1.79}$$

Under the (initial) assumption that the glass transition is not indicative of a thermodynamic transition, this derivative has to take on equal values in the rubbery and in the glassy regime. If one compares Eq. 1.1.67 with Eq. 1.1.79, one finds

$$\alpha_g = \frac{\alpha_l}{1+\beta_{fo}+\sum_i \frac{K_i}{K_\infty}} \ . \tag{1.1.80}$$

Since $\alpha_g$ and $\alpha_l$ are usually measured, the unknown value of $\beta_{fo}$ can be extracted as

$$\beta_{fo} = \frac{\alpha_l}{\alpha_g} - \sum_i \frac{K_i}{K_\infty} - 1 \ . \tag{1.1.81}$$

Recall that the parameter $\beta_{fo}$ was defined as the ratio of the free to the occupied volume changes sufficiently far above the glass transition. From the relaxation data for PVAc by McKinney and Belcher (see Appendix B), and the values of $\alpha_l$ and $\alpha_g$ by Sandberg and Bäckström (1980),** Eq. 1.1.81 renders the value of this quantity for this particular material as $\beta_{fo} = 0.63$.

It is useful to stress once again the most important aspect of this theory: the difference in the value of the coefficient of thermal expansion, across the glass transition, is dictated by the purely nonlinear viscoelastic behavior of the material, which brings about a difference in the effective asymptotic bulk modulus. The

** Using the values of $\alpha_l = 5.5 \times 10^{-4}$ and $\alpha_g = 2.3 \times 10^{-4} K^{-1}$, as given by McKinney and Simha (1974), changes the result by less than a 1%.

parameters† which govern the material behavior are the rubbery ("liquid") coefficient of thermal expansion, $\alpha_l$, and the time-dependent rubbery bulk modulus, $K(t) = K_\infty + \sum K_i exp(-t/\tau_i)$. The glassy thermal behavior is predicted through the freezing of the mechanical relaxation plus the locking of the residual free volume, and both of these phenomena affect the compliance of the total volume to yield a glassy coefficient of thermal expansion below $T_g$.

It can now be shown that nonequilibrium effects are predominant over the consequences of equilibrium phase changes. If one considers in the Ehrenfest relation, Eq. 1.1.66, $T \approx 300\ K$, and allows for the properties of PVAc (Sandberg and Bäckström, 1980), *i.e.*,

$$\alpha_l = 6. \times 10^{-4}\ K^{-1}$$

$$\alpha_g = 2.5 \times 10^{-4}\ K^{-1}$$

$$C_{pl} = 2.09 \times 10^6\ \frac{J}{m^3 K}$$

$$C_{pg} = 1.29 \times 10^6\ \frac{J}{m^3 K}\ ,$$

then the predicted change in bulk modulus based on the idea of thermodynamic equilibrium can be compared with the values of the experimentally determined bulk modulus (McKinney and Goldstein, 1974). The typically measured values of 17000 bars for the rubbery modulus and 37000 bars for the glassy one correspond to a change in compressibility of around $2.9 \times 10^{-5}$ bar$^{-1}$, which is almost *six* times greater than the one predicted for the thermodynamic transition by Eq. 1.1.66, namely $4.5 \times 10^{-6}$bar$^{-1}$. This discrepancy has been for a long time a thorny problem in the studies of the glass transition in polymers: experimental evidence shows that the predictions of equilibrium thermodynamics are insufficient to explain the constitutive behavior of glasses. A first attempt to solve this discrepancy was made

---

† The quantity $\beta_{fo}$ is not considered a parameter, since it is computable through Eq. 1.1.81.

by Davies and Jones (1953), who recast Eq. 1.1.66 into the inequality form

$$\frac{1}{K_{\infty,rubbery}} - \frac{1}{K_{\infty,glassy}} \geq T\frac{(\alpha_l - \alpha_g)^2}{C_{pl} - C_{pg}} \quad . \tag{1.1.82}$$

In the Davies/Jones approach to the glass transition, the excess amount of the difference in compressibilities originates from the presence of additional variables, other than pressure, temperature and specific volume, which are presumed to be needed to describe the thermodynamic states of glasses. In the language of nonequilibrium thermodynamics, such variables are often called internal variables, due to their elusiveness in experimental measurements.

Although at this stage of development one may argue about elegance in argumentation, the work presented here has similarities with the approach of nonequilibrium thermodynamics, with one substantial difference: instead of referring to general internal variables, the physical significance of which is sometimes not fully characterized, the free volume content of polymers is considered as a more or less recognizable physical internal variable which is needed to fully describe their thermomechanical state; the consequences of this assumption on the time-independent mechanical behavior are then derived. The results show that a much better agreement with experimental data can be achieved if one keeps track of both this additional parameter (free volume) and of the vanishing of material relaxation at low temperatures. Among other aspects, future work will have to assess whether the additional possible presence of an equilibrium thermodynamic transition significantly alters the thermomechanical behavior of polymers, as far as the predictions of residual stresses and durability are concerned.

Current studies of the constitutive behavior of glasses often do not address the possible existence of a thermodynamic transition (Christensen and Naghdi, 1967; Oden and Armstrong, 1971), or try to explain it in terms of a set of viscoelastic

functionals (Shay and Caruthers, 1986). The approach presented here has the appealing feature of accommodating at least two important aspects of the problem, namely the nonlinearly viscoelastic behavior and the change in thermodynamic properties, by suggesting a model which is prevalently dependent on the viscoelastic properties of polymers but that can conceivably be expanded to include entropy jumps or discontinuities in its derivatives (therefore the heat capacity) at the glass transition.

The last comment concerns an aspect which more properly belongs to an equilibrium thermodynamics treatment of the glass transition; nonetheless, it needs to be mentioned here because it shows how equilibrium and nonequilibrium aspects might be related to each other. The ratio between the heat capacities in the rubbery and glassy phase of PVAc (Sandberg and Bäckström, 1980) is, within experimental error, equal to the ratio of the elastic compliances of the total volume ($2.09/1.29 = 1.62 \approx 1 + \beta_{fo}$) in the rubbery and glassy regime, which ratio has just been found within the framework of a nonequilibrium approach. Rather than being considered a confirmation of this simple theory, this agreement has to be considered an interesting subject of discussion, in which one could ask if the heat capacities have a connection to the free and occupied volume deformabilities and, if so, why. An approximate explanation of this connection would consider the energy change associated with the free volume deformation (as it is done, for a different purpose, in Section 1.1.6). How can the energy of a hole be evaluated? As long as the vacancies represent part of the total volume in which the polymer molecules can migrate freely and exchange free volume, it is possible to evaluate the energy associated with the hole distribution by filling up the vacancies, ending up with a homogeneous continuum and computing the energy spent in the process. If one could do that, then the energy spent would be equal to the energy associated with the occu-

pied volume times the volume of the holes. Above the glass transition, a positive temperature change effects an increase in both the free and the occupied volume, with a corresponding energy expenditure[‡]. Below the transition, there exists a residual amount of vacancies (residual free volume, due to nonequilibrium effects) but this space is energetically unattainable for the polymer molecules, because of their low energy levels. The energy associated with the free volume deformation is therefore essentially zero, since such deformation is restrained; the corresponding value for the heat capacity is affected by the thermal properties of the occupied volume only; that seems to be the case as shown by the simple results derived in this section.

### 1.1.5 The kinetic aspects of the glass transition

In section 1.1.4 the nonequilibrium and, in part, the equilibrium aspects of the glass transition have been addressed. In this section some further features of a third component of the transition, namely its kinetic or rate dependence, will be considered. This aspect, which is more closely connected with experiments such as cooling or heating at fixed or variable rates, is a consequence of the viscoelastic material response which requires a certain amount of time (increasing with decreasing temperature) to bring the polymer to an equilibrium state. Such a phenomenon can be explored for example in experiments in which the thermal contraction is measured

---

‡ It is appealing from an intuitive point of view to model the holes and the occupied volume as two different species of gas, thoroughly mixed. Above the glass transition, both gases are present and active; below it, only one (the occupied volume) takes part in the thermal and mechanical processes, while the other is kept in a frozen state. The heat capacity above the transition would be given by the sum of the heat capacities of each phase, while below $T_g$ it would be equal to the heat capacity of the only phase still active. One can also draw an analogy with the behavior of diatomic gases at high temperatures, where an increase in the heat capacity is effected by the additional degree of freedom which the two atoms experience by oscillating along the axis of the molecule.

under a fixed rate of cooling. If one considers in such experiments the temperature $\hat{T}_g$ at which the slope of the volume-temperature curve changes as indicative of the glass transition*, one observes a shifting of the transition to higher temperatures with increasing cooling rate. In particular, in experiments on monomeric glasses such as $As_2Se_3$, $B_2O_3$ and potassium silicate, Moynihan *et al.* (1974) have observed a linear dependence of the fictive temperature $\hat{T}_g$ on the logarithm of the cooling rate.

The question arises whether free volume theory is consistent with such an observed dependence of this transition temperature on the logarithm of the cooling rate. Very often critical observations are offered in this regard by noting that, under nonequilibrium conditions, the viscoelastic free volume changes at a given temperature are a decreasing function of the cooling rate; less time needed to reach the final temperature implies a larger nonequilibrium free volume fraction, and therefore, in cooling, a larger total free volume at that temperature. If one were to make the hypothesis that the onset of the glass transition is closely related to a critical value of free volume, this critical value would be reached at lower temperatures with increasing cooling rate (because the nonequilibrium fraction would be larger) and, so the argument proceeds, this fact would correspond to a lowering of the glass transition with a rate increase, which is precisely the opposite of what is observed experimentally.

In order to give a qualitative rebuttal to those remarks, one can estimate the volume change for a simple viscoelastic material subject to cooling from some temperature $T_0$ above $\hat{T}_g$. If considerations are simplified by using a relaxation spectrum

---

* $\hat{T}_g$ is often called a fictive transition temperature, since it is primarily a consequence of the kinetics of molecular rearrangements.

possessing a single component **, *e.g.*,

$$K(t) = K_\infty + K_1 exp(-\frac{t}{\tau}) \ , \tag{1.1.83}$$

then the differential equation describing the viscoelastic material response can be written as†

$$(K_\infty + K_1)\frac{d\epsilon_{kk}}{dt} + \frac{1}{\tau}K_\infty \epsilon_{kk} = \frac{1}{3}\frac{d\sigma_{kk}}{dt} + \frac{1}{3\,\tau}\sigma_{kk} \ . \tag{1.1.84}$$

For constant mechanical pressure (isobaric conditions) the thermal effects can be described in terms of the equivalent thermal pressure $\hat{p}(T) = \frac{1}{3}\sigma_{kk} = K_\infty \alpha_l \Delta T = K_\infty \alpha_l (T - T_0)$; Eq. 1.1.84 can then be rewritten as

$$\frac{d\epsilon_{kk}}{dt} = \frac{K_\infty}{K_\infty + K_1}\left[\frac{1}{\tau}(\alpha_l \Delta T - \epsilon_{kk}) + \alpha_l \frac{dT}{dt}\right] \ . \tag{1.1.85}$$

If one observes furthermore that the relaxation time has to be also modified according to the free volume induced time shift, one obtains

$$\frac{d\epsilon_{kk}}{dt} = \frac{K_\infty}{K_\infty + K_1}\left\{\frac{1}{\tau\ exp[B(\frac{1}{f} - \frac{1}{f_0})]}(\alpha_l \Delta T - \epsilon_{kk}) + \alpha_l \frac{dT}{dt}\right\} \ . \tag{1.1.86}$$

The first term on the right hand side is a consequence of the viscous material behavior, and is proportional to the "distance" $(\alpha_l \Delta T - \epsilon_{kk})$ of the polymer from its equilibrium state, while the second one can be seen as the "glassy" (short term) response to the temperature variations. The glassy term is linearly proportional to the cooling rate, while the first one makes its presence felt only when the effective relaxation time of the material, *i.e.*, $\tau\ exp[B(\frac{1}{f} - \frac{1}{f_0})]$, is short compared to the experimental time scale. In order to present a qualitative idea of how the volume

---

** This simplification is actually very well representing the experiments on monomeric glasses by Moynihan *et al.*, since monomeric glasses tend to have, rather than a complete spectrum as polymers, single values for the bulk and shear viscosity.

† For a material having a more complicated relaxation behavior, *e.g.*, $N$ relaxation times, the equation would change into a differential equation of N-th order.

behavior changes with the cooling rate, one can consider a situation - as indicative of the transition - in which the two terms are of the same order, *i.e.*,

$$\frac{1}{\tau\ exp[B(\frac{1}{f}-\frac{1}{f_0})]}(\alpha_l\Delta T-\epsilon_{kk})\ \sim\ -\alpha_l\frac{dT}{dt}\quad . \tag{1.1.87}$$

Furthermore, one can make the reasonable assumption that the term $(\alpha_l\Delta T-\epsilon_{kk})$ is somehow proportional to the absolute value of cooling rate $\frac{dT}{dt}$, or, more generally, to some power $\zeta$ of it, *i.e.*,

$$(\alpha_l\Delta T-\epsilon_{kk})\sim\left|\frac{dT}{dt}\right|^{\zeta}\quad . \tag{1.1.88}$$

Eq. 1.1.87 can then be rewritten as

$$exp[-B(\frac{1}{f}-\frac{1}{f_0})]\ \sim\ \left|\frac{dT}{dt}\right|^{1-\zeta}\quad . \tag{1.1.89}$$

Eq. 1.1.89 shows‡ that, as the rate of cooling increases, the fractional free volume at which the fictive transition occurs also increases, in contrast to the assumption that such a transition occurs at a critical value of $f$. In order to make a qualitative statement on how the free volume at the transition changes with the cooling rate, one can observe that in a cooling experiment the low material viscosity in the rubbery state is such that the free volume of the material is not too far from its equilibrium curve given by $f=f_0+\alpha_f(T-T_0)$, where $\alpha_f$ is the equilibrium rate of change of free volume with temperature. Therefore, if the value of free volume $\hat{f}$ at the transition temperature is approximated as the equilibrium value at the transition*, *i.e.*, $\hat{f}\sim f_0+\alpha_f(\hat{T}_g-T_0)$, then, upon taking the logarithm of the above expression 1.1.89 and considering only the terms dependent on the cooling rate, one obtains

$$\frac{1}{f_0+\alpha_f(\hat{T}_g-T_0)}\approx\frac{1}{f_0}\Big(1-\frac{\alpha_f(\hat{T}_g-T_0)}{f_0}\Big)\sim(1-\zeta)log\left|\frac{dT}{dt}\right|\ , \tag{1.1.90}$$

‡ *e.g.*, by taking the logarithm of both sides of the equation.

* This would correspond to a cooling experiment which starts from a temperature not too far from the transition temperature, so that $\frac{f-f_0}{f_0}$ can also be considered small.

from which one derives

$$\hat{T}_g - T_0 \sim log\left|\frac{dT}{dt}\right| . \qquad (1.1.91)$$

It has thus been shown that the present model is at least consistent with the experimental observations by Moynihan *et al.*

### 1.1.6 A closer look at free volume: its transient distribution

It has been assumed so far that the time scale of material relaxation and the instantaneous fractional free volume are connected by the Doolittle equation. This assumption should now be reconsidered in a critical manner. Eq. 1.1.11 was derived by assuming that the distribution of free volume maximizes the entropy of the material, *i.e.*, it was derived with underlying equilibrium assumptions about the size and the density of the vacancies. After the material has settled into a time-independent equilibrium state, such a hypothesis seems appropriate; however, when a time-dependent volume change is taking place, the distribution of free volume might not be the same as that given by Eq. 1.1.6, since the latter indicates an equilibrium distribution. In this section the effect of a nonequilibrium distribution on the material viscosity will be addressed by adapting a qualitative model connecting the changes in the hole volume to the time-dependent evolution from one equilibrium state to another.

One can conceive of (at least) two principal mechanisms for creating and destroying free volume. The first one would be a "glassy"** mechanism, such as the response of the material to a sudden compression, and the other one would be a time-dependent rearrangement of the distribution of vacancies in the solid. At first

** The word "glassy" is used here with the meaning of "instantaneous".

one can consider what happens upon sudden deformation, assuming the material to be initially ($t = 0^-$) characterized by the (exponential) equilibrium distribution of free volume $p(v) = (1/v_{f0})exp(-v/v_{f0})$, which corresponds to a value of the overall fractional free volume equal to $f_0$. If the sudden compression destroys all the sites of size smaller than a hypothetical value $\hat{v}$ and at the same time removes a corresponding amount from the larger ones, two distinct effects can be isolated, namely:

i. the number (*i.e.*, the density per unit volume of the polymer) of free volume sites changes, since all the vacancies of size $v \leq \hat{v}$ are removed;

ii. the distribution of the size of the remaining vacancies might change.

To evaluate the consequences of these two aspects on the instantaneous value of the time shift, *i.e.*, to compute the new material viscosity, one has to modify the Cohen-Turnbull considerations and observe that the probability which a particle has of accessing free volume in excess of a certain amount, say $v_{min}$, is proportional to the product of the probability for a given site (hole) of being larger than $v_{min}$ times the density of sites in the material (number of sites per molecule or per volume), which will be denoted by $\rho$. Assuming, as was done in section 1.1.1, that the material viscosity is inversely proportional to such a probability, one writes

$$\eta^{-1} \sim \rho \int_{v_{min}}^{\infty} p(v)\, dv \ . \tag{1.1.92}$$

Let the initial density of free volume sites be given by $\rho_0$. If a certain amount $\hat{v}$ is removed from all vacancies, the number of the sites still active after the removal will be proportional to the previous density times the fraction of sites having free volume in excess of $\hat{v}$. Consequently, the new density is given by

$$\rho = \rho_0 \int_{\hat{v}}^{\infty} p(v)dv = \rho_0 exp\Big(-\frac{\hat{v}}{v_{f0}}\Big) \ . \tag{1.1.93}$$

Paradoxically, the probability distribution of free volume does not change; this invariance is a consequence of the property of the exponential function which, upon shifting and renormalization†, remains unchanged. If one denotes as $v'$ the new free volume after the initial compression, the new probability distribution $p(v')$ must be calculated taking into account the elimination of all the holes of volume less than $\hat{v}$ and the subtraction of the amount $\hat{v}$ from the volume of the larger ones, which yields

$$p(v') = \frac{\frac{1}{v_{f0}} exp(-\frac{v'+\hat{v}}{v_{f0}})}{\frac{1}{v_{f0}} \int_0^\infty exp(-\frac{v'+\hat{v}}{v_{f0}}) dv'} = \frac{1}{v_{f0}} exp(-\frac{v'}{v_{f0}}) \quad . \tag{1.1.94}$$

Eq. 1.1.94 states that, although the number of sites has changed, the average volume‡ per site is the same as before. The new macroscopic fractional free volume will be different though, since the density of sites has changed (some of them, namely those with volume less than $\hat{v}$, have been removed). The time shift with respect to the initial condition can then be computed through a size distribution which still has the form of the equilibrium distribution, as given by Eq. 1.1.6, but with a different density (total number of available vacancies per total number of molecules) of sites. Since the distribution of the size of the vacancies has the exponential (*i.e.*, equilibrium) form, the Cohen-Turnbull result, Eq. 1.1.11, remains valid upon the substitution

$$f = f_0 exp(-\frac{\hat{v}}{v_{f0}}) \quad , \tag{1.1.95}$$

which is the value of the new fractional free volume after sudden deformation. The relation between the time shift and the macroscopic free volume change still holds, even if the material is far from its equilibrium state.

---

† A continuous probability distribution has to be normalized so that its integral over the domain of definition yields unity.

‡ The average free volume is intended here as the average size of the vacancies over the existing population of holes.

The time-dependent free volume changes will now be considered. It is of interest to examine the effects of the local disequilibrium on the macroscopic behavior of the material; in particular, one can investigate the validity of the Doolittle-type dependence of the relaxation times on the macroscopic free volume changes. For the sake of simplicity, assume that the density of sites does not change and that only the distribution of the site sizes varies*, *i.e.*, the time-dependent changes in the macroscopic, average free volume are exclusively due to variations in the size distribution of free volume sites. For the purpose of analyzing the consequences of this assumption, a simplified model may be used which contains the equilibrium distribution of free volume as a stationary solution and which can be justified by considering the local equilibrium of molecules constrained in the holes of the network. Following the general approach to free volume theory of Cohen and Turnbull, this model does not take into account the chain-like nature of polymer molecules but considers instead the interaction between an isolated, "monomeric" molecule and the rest of the solid which surrounds the "cage" in which such a particle is constrained.

On a very small scale, the volume of the cage constraining a molecule depends on the interaction between the latter and the outside medium, *i.e.*, the rest of the material which will here be assumed to behave as a homogeneous continuum. Locally, the volume of each hole will be such that the sum of the two energies, one characterizing the particle and the other one associated with the energy stored in the outside medium, will reach a minimum. This picture resembles that of a gas of particles contained in a reservoir, and in which (picture) the pressure exerted by the gas on the walls of the container deforms them and stores mechanical energy

* This assumption is truly crucial but, since only qualitative results are attempted here, it should not affect the conclusions in a drastic manner.

through their elastic deformation.

The objective is now to consider what happens to the local equilibrium when it is disturbed, such as in the case of a temperature or pressure change. In order to do so, it is expedient to make the following simplified assumptions:

- the local interaction can be uncoupled: one may consider the total energy as the sum of the energy which is stored in the particle constrained in the cage, plus the energy which is stored in the outside medium;
- the initial equilibrium state of the hole volume corresponds to a deformed configuration, *i.e.*, the walls of the cage have already been moved in order to accommodate the particle;
- such deformed configurations correspond to nonzero energies stored in both the medium surrounding the cage and in the constrained particle;
- the changes in the volume of the cage are small in comparison to its total volume; one can therefore linearize the dependence of the energy of the surrounding medium and of the particle with respect to the hole volume changes;
- the interaction between the particle and the medium can be represented in terms of the Brownian, random collisions of the particle against the walls of the cage and of a continuum-type response of the outside solid;
- the response of the outside medium can therefore be modeled as governed by a change in the stored energy which, for small variations of the hole volume, can be considered a linear function of these variations;
- the fluctuations of the hole volume are mainly fluctuations in the free volume of the cage, given the initial loose packing of the particle in the

hole;

- one also has to take into account the viscoelastic nature of the material, for which there is a damping of the oscillations of the hole volume.

The above observations can be reformulated more precisely as follows:

i. the effect of the thermal collisions of the particle on the walls of the containing cage can be represented by a Brownian term (white noise)** in the equation for the equilibrium of the free volume of the cage;

ii. there is a natural tendency of the holes to close, due to the already present deformation of the containing medium;

iii. the random variations of the hole (free) volume due to the Brownian collisions of the particle against the walls of the cage have a characteristic variance, $\sigma$;

iv. there exists also an intrinsic viscous damping which smooths out the oscillations of the volume of the vacancy.

Under these assumptions, one can represent the energy of the containing medium with a linear dependence on the hole volume, *i.e.*,

$$U = c\, v_{tot} = c(v_{occ} + v_f) \ . \tag{1.1.96}$$

For the sake of simplicity and for consistency with the notation adopted in section 1.1.1, denote the free volume of the cage enclosing the particle by $v$; then, for small variations of such a volume, the force which tries to close the holes will be given by

** For more information about the analysis of stochastic processes, see Gardiner, 1985.

the gradient of the potential energy, $\frac{\partial U}{\partial v}$, where $U$ is given by Eq. 1.1.96. One can therefore consider the volume of a hole as the coordinate of a particle subjected to such a conservative force and, in addition, to Brownian collisions $d\underline{b}(t)$ and to an intrinsic viscous damping $\mu\frac{dv}{dt}$. The system of equations for such a particle can be written as

$$\frac{dv}{dt} = \dot{v} \tag{1.1.97}$$

$$\frac{d^2v}{dt^2} = -\mu\dot{v} - \frac{dU}{dv} + \sqrt{\sigma}d\underline{b}(t) \ , \tag{1.1.98}$$

where the effect of thermal collisions has been taken to be proportional to some scaling parameter $\sqrt{\sigma}$[†]. The viscosity $\mu$ is indicative of the reluctance of the viscoelastic polymer to engage in a random, Brownian dance governed by the thermal collisions. Eq. 1.1.98 has the same form as the equation of volume change of a monomeric glass, for which $\mu$ would represent the bulk viscosity; in the case of a polymer having a relaxation behavior characterized by several relaxation times, the corresponding equation would contain higher derivatives of the dilatational rate. In the limit of large $\mu$, *i.e.*, in the limit of a relaxation time that is large compared to the characteristic time scale of thermal motion, Eq. 1.1.98 can be approximated as[‡]

$$\dot{v} \simeq -\frac{1}{\mu}\left[\frac{dU}{dv} - \sqrt{\sigma}d\underline{b}(t)\right] \ . \tag{1.1.99}$$

Upon substitution in Eq. 1.1.97, one obtains

$$\frac{dv}{dt} = -\frac{1}{\mu}\frac{dU}{dv} + \frac{1}{\mu}\sqrt{\sigma}d\underline{b}(t) \ . \tag{1.1.100}$$

---

† The symbol $\sigma$ is used here because the quantity it represents will turn out to be proportional to the variance of the volume increments.

‡ This solution technique is often denoted as adiabatic elimination of fast variables. Gardiner (1985) provides some information about the approximation which is achieved by following this approach.

Eq. 1.1.100 contains a random variable, *i.e.*, $d\underline{b}(t)$. If one considers the expected increment and variance of the function $v(t)$, one obtains*

$$E(\Delta v) = -\frac{1}{\mu}\left[\frac{dU}{dv}\right]dt \quad , \tag{1.1.101}$$

and

$$E((\Delta v)^2) = \frac{\sigma}{\mu^2}dt \quad . \tag{1.1.102}$$

The theory of stochastic processes asserts that Eq. 1.1.101 and 1.1.102 are equivalent to a differential equation, known as the forward Fokker-Planck equation**, which describes the changes in the probability distribution for the position of the particle

$$\frac{\partial p(v,t)}{\partial t} = \frac{1}{\mu}\left\{\frac{\partial}{\partial v}\left[\frac{dU}{dv}p(v,t) + \frac{\sigma}{2\mu}\frac{\partial p(v,t)}{\partial v}\right]\right\} \quad , \tag{1.1.103}$$

in which $\frac{dU}{dv} = c$ by Eq. 1.1.96. The equation can be scaled if one divides by $c$, and lets $t' = t/\mu$, $v_{f0} = \frac{\sigma}{2\mu c}$; one obtains then

$$\frac{\partial p}{\partial t'} = \frac{\partial p}{\partial v} + v_{f0}\frac{\partial^2 p}{\partial v^2} \quad . \tag{1.1.104}$$

The stationary solution of this differential equation is the equilibrium size distribution of free volume corresponding to a value of the macroscopic free volume equal to $v_{f0}$, *i.e.*,

$$p(v) = \frac{1}{v_{f0}}exp(\frac{-v}{v_{f0}}). \tag{1.1.105}$$

Therefore, at least in the stationary case, this simple model represents the features of the distribution of holes in amorphous materials rather well. It is also of interest to examine the predictions of the Chapman-Kolmogorov equation in the case when the equilibrium value of the macroscopic free volume is suddenly changed from

---

* Appendix C contains some information about the features of mathematical white noise.

** This is the basic theorem of stochastic analysis. For one version of the proof, see Gardiner, 1985.

$v_{f0}$ to, say, $v_{f1}$, as can happen when the material is suddenly thrown into a non-equilibrium state by a sudden compression or cooling†. That examination amounts to consider the new version of Eq. 1.1.104, written as

$$\frac{\partial p}{\partial t'} = \frac{\partial p}{\partial v} + v_{f1} \frac{\partial^2 p}{\partial v^2} \ , \qquad (1.1.106)$$

which has, as a stationary solution, the new equilibrium distribution $p(v) = \frac{1}{v_{f1}} exp(\frac{-v}{v_{f1}})$. The differential equation 1.1.106 can be integrated in time, with the initial condition given by Eq. 1.1.105. The corresponding probability distributions at different times are shown in Fig. 1.10, where the (arbitrary) case $v_{f0} = 1$ and $v_{f1} = .5$ has been considered.

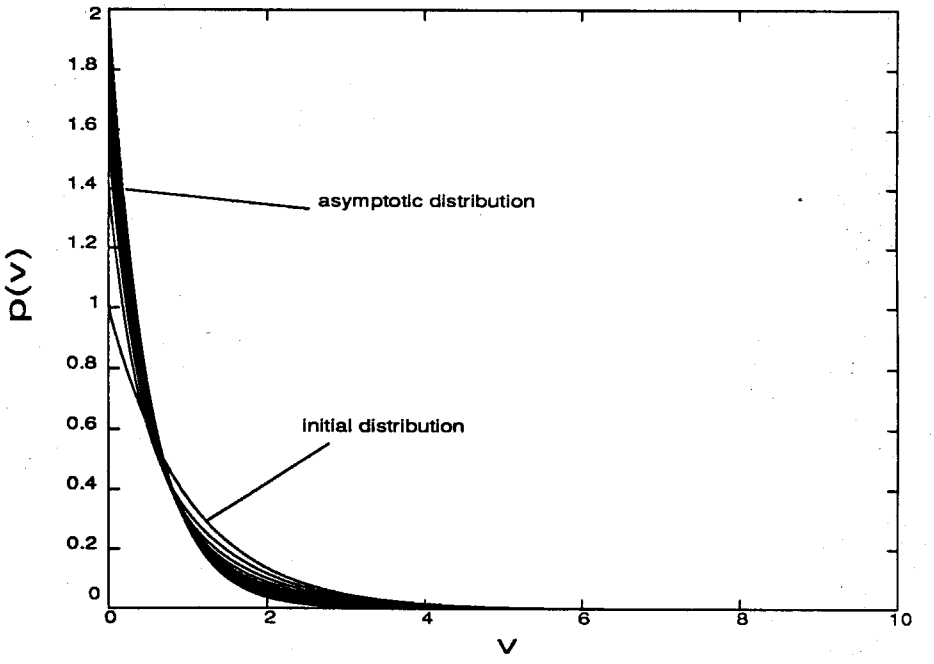


FIGURE 1.10 Diffusion in probability space

† Such changes are assumed to imply a change in the amplitude of the thermal collisions of the particle against the walls of the cage, *i.e.*, a variation in the Brownian term amplitude, $\sqrt{\sigma}$.

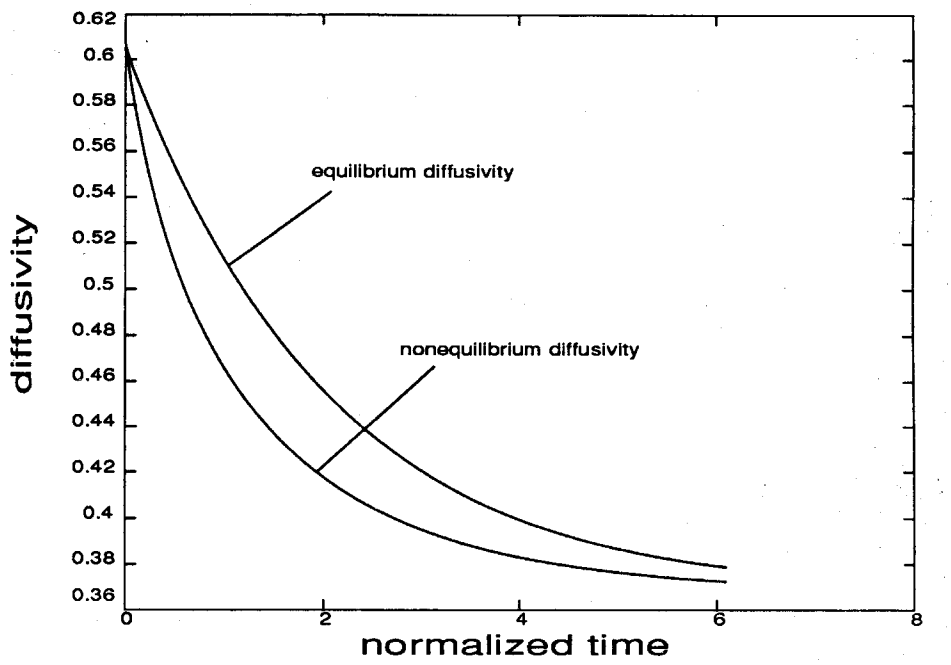


FIGURE 1.11 Prediction of intrinsic diffusivity.

Having examined the transient distribution of the free volume, it is next of interest to consider the consequences of such distribution on the material viscosity. The values of viscosity computed through the instantaneous distributions at different times and Eq. 1.1.1 can be compared with those values predicted by the equilibrium theory as a function of the instantaneous average value of free volume. If one adopts a form ‡ of the Doolittle equation which is convenient for these considerations, *i.e.*,

$$log(\eta) \sim \frac{B'}{v_f} \quad , \tag{1.1.107}$$

or, with $D$ as the material diffusivity (reciprocal of viscosity),

$$log(D) = log(\frac{1}{\eta}) = -\frac{B'}{v_f} \quad ; \tag{1.1.108}$$

‡ The following equation differs from Eq. 1.1.11 in the direct dependence of the viscosity on the average free volume instead of its fractional value.

then sizable differences can be found between the two predicted viscosities, as shown in Fig. 1.11*. One observes that the viscosity computed through Eq. 1.1.1 and the instantaneous distribution is higher than that predicted by Eq. 1.1.107, which assumes an exponential shape for the distribution function**. The differences in values of the viscosity (which for a polymer would correspond to an error in the evaluation of the time shift) are of the order of some fraction of the correct, nonequilibrium solution, far smaller than the exponential changes seen in polymers in equilibrium at different temperatures. Thus, even if the time shift does not depend on the instantaneous value of the nonequilibrium free volume as given by Eq. 1.1.11, the error incurred by assuming the validity of that equation is small compared to the variations in the time shift due to temperature changes.

### 1.1.7 The pressure dependence of the glass transition

The proposed constitutive model now allows the consideration of the pressure dependence of the glass transition and the behavior of the entropy across that transition. In the previous sections, two relevant features of the glass transition have already been addressed, and they are summarized here for convenience:

- the glass transition is characterized by the polymer deviating from thermodynamic equilibrium and settling into a metastable state;
- there is a kinetic aspect to the glass transition, and this aspect is particularly evident when experiments are conducted at different rates of cooling or heating through the transition range.

---

* The parameter $B'$ of the same equation was set to unity for the sake of simplicity, therefore the viscosity changes from $e^{-1}$ to $e^{-2}$.

** Fig. 1.11 shows a lower diffusivity characterizing the instantaneous (nonexponential) size distribution.

In addition to these two features, there are additional ones which might help to further illuminate this complicated phenomenon. For example, hysteretic effects in cooling and heating cycles have been experimentally observed (Sharonov and Vol'kenshtein, 1964; Sandberg *et al.*, 1977, 1980). A typical example of these effects is shown in Fig. 1.12, where the apparent heat capacity of PVAc is shown upon heating across the glass transition. The three different curves correspond to different, prior annealing (holding) times below the transition, and they show that aging below $T_g$ induces higher peaks in the heat capacity upon reheating. Whether this phenomenon can be justified merely through a free volume description of the material viscosity will require further investigation. The different possible explanations for this phenomenon include the admissible different natures of the transition ( *(a)* second order, *i.e.*, with a change in the slope of the equilibrium entropy, or *(b)* first order, with a finite entropy jump at $T_g$), time-dependent changes in the ordering parameter† which determines the onset of the transition, or a direct dependence of the entropy of the material on the number and size of holes in the "network" (*cf.* the discussion at the end of section 1.1.6). Also, the assumed step change in the heat capacity might not be entirely correct; recent studies, in the framework of percolation theory for liquids (Cohen and Grest, 1979), indicate that a smoother variation should take place, mainly because the material is experiencing not a single value of free volume, but rather a distribution of free volume sites. For such a situation, the theory of critical phenomena (*cf.* Domb and Green, 1972) suggests a variation of the heat capacity as $\xi^{\gamma}$, where $\xi$ is an ordering parameter and $\gamma$ an exponent which, for a three dimensional cluster, is equal to 0.4.

---

† An ordering parameter is intended as a parameter which describes the onset of the glass transition upon reaching a critical value; in the simplest theory, one would consider temperature as the ordering parameter and assume that the glass transition occurs at a given temperature, independent of pressure or rate of straining and cooling.

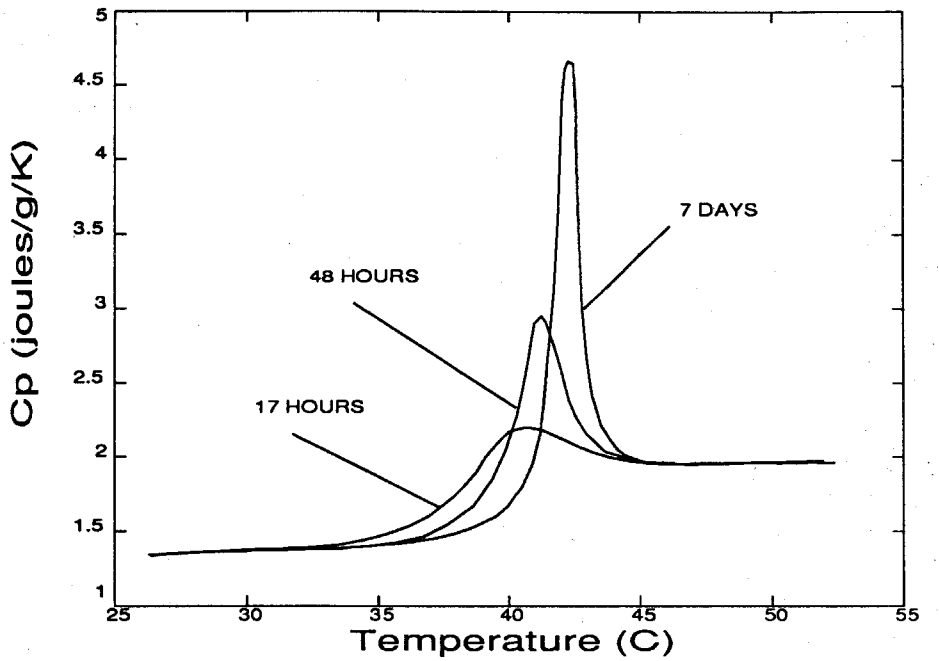


FIGURE 1.12 Apparent heat capacity of PVAc upon reheating across $T_g$, for different annealing times at low temperature (Sharonov and Vol'kenshtein, 1964).

It is also evident (*cf*. McKinney and Goldstein, 1974, for experiments on PVAc) that the glass transition is a pressure dependent phenomenon. One can recall that the model presented here (*cf*. section 1.1.3) recognizes two components of free volume changes, namely a viscoelastic term and a Brownian noise term, resulting a non-zero residual free volume in conditions of metastable equilibrium below $T_g$; this result holds even for infinitesimally low rates of cooling. While it may be premature to consider the present theory to be a complete theory for the glass transition process, it would be of interest to connect those aspects that are related closely to equilibrium thermodynamics (such as the change in heat capacity) to what has been developed so far within the framework of this phenomenological model. For instance, one could consider that the onset of the glass transition in polymers occurs when the molecular relaxation, represented by the viscoelastic, or "drifting"

term in the constitutive behavior symbolized by Eq. 1.1.56, achieves the same order of magnitude as the thermal agitation of the molecules, which is represented by the second term on the right hand side of the same equation. This approach is not mere speculation, since one can also think of the problem in the terms of the percolation model of the glass transition by Cohen and Grest (1979), by which a significant portion of the entropy of the material above $T_g$ arises as configurational entropy from the migration of the molecules within "liquidlike" cells which in turn are connected to form an infinite percolation cluster. In the Cohen-Grest model the "drifting" capability of the molecules is the main cause for the change in heat capacity, through affecting the configurational entropy of the material. It is not clear whether the Cohen-Grest theory of the glass transition can be applied directly to polymers, since the original theory seems to apply principally to complex but monomeric glass forming substances. The presence in the polymeric material of a chain backbone which imposes constraints on the drifting motion of the individual members of the chain undermines somehow the "simple" derivation for the configurational entropy in the Cohen-Grest developments, and this feature could explain the discrepancy between the fact that their theory predicts a first order transition while experiments seem to indicate it to be of second order. The main assertions of the Cohen-Grest theory can however be maintained, namely the fact that the diffusive capability of the molecules is strictly connected to the change in heat capacity.

The predictions of the proposed phenomenological model will be considered now. The predicted curve for the equilibrium free volume, as represented through Eq. 1.1.59, is shown in Fig. 1.8. If one hypothesizes that a "critical" value of free volume, $f_{crit}$, characterizes the onset of the glass transition, some interesting predictions can be obtained. Fox and Flory (1950) suggested that the viscosity of

amorphous polymers may be written in the product form

$$\eta \;=\; g(T)\, z(f) \;\;, \tag{1.1.109}$$

where $z(f)$ has the usual Doolittle-type dependence on fractional free volume, and $g(T)$ is a function which depends on temperature only; the onset of the glass transition can then be related to a critical value of viscosity. According to the simplifications adopted in the present work, the direct effect of temperature will be ignored; next, the consequences of assuming a critical value of free volume characterizing the onset of the glass transition will be investigated within the framework of the proposed phenomenological model. Under general thermal and mechanical histories, the total differential of the free volume at equilibrium is given by

$$df \;=\; \frac{\partial f}{\partial T} dT + \frac{\partial f}{\partial p} dp \;\;, \tag{1.1.110}$$

which can be expressed in terms of the model parameters (above the glass transition)

$$df \;=\; \delta \cdot \left( \alpha_l dT + \frac{dp}{K_\infty} \right) \;\;. \tag{1.1.111}$$

If the free volume at the glass transition is taken as a material constant, then $df \;=\; 0$ at $T_g(p)$. One thus obtains

$$\left( \frac{\partial T}{\partial p} \right)_{T_g} \;=\; \frac{1}{K_\infty \alpha_l} \;\;, \tag{1.1.112}$$

which, for PVAc, predicts a value of .06 Kelvin per Bar. This value is reasonably close to the values ranging from .02 to .04 as measured by McKinney and Goldstein (1974) for the same polymer species. The equilibrium curves corresponding to the model predictions are shown in Fig. 1.13 for different values of pressure[‡].

---

‡ Since the effect of temperature is felt through the action of the equivalent thermal pressure, the equilibrium curves at different mechanical pressure need to take the latter into account, *i.e.*, they need to be horizontally shifted by an amount $\Delta T \;=\; \Delta p [K_\infty \alpha_l]^{-1}$.

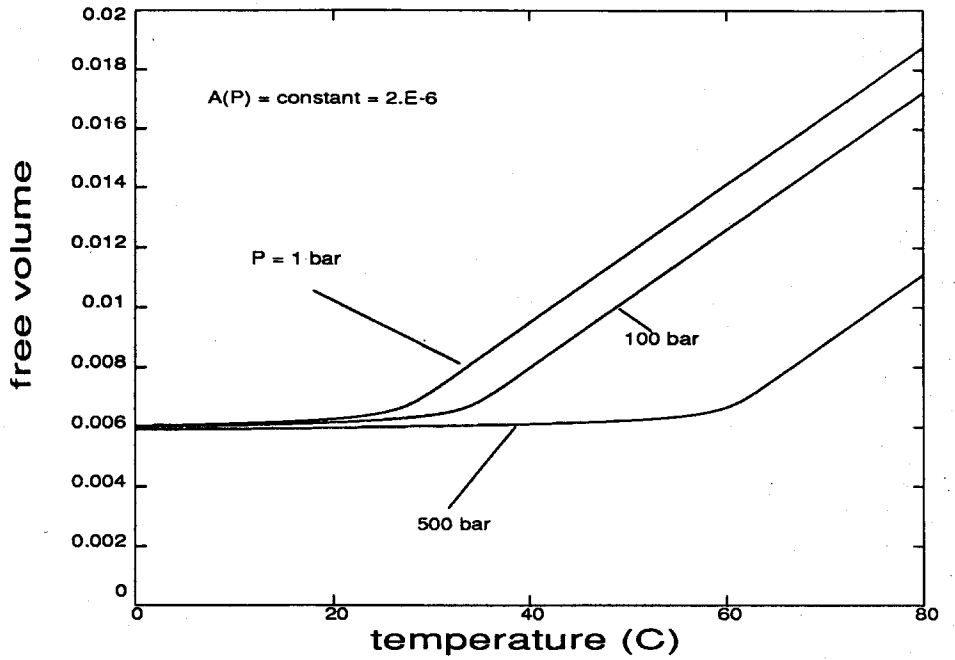


FIGURE 1.13 Predicted equilibrium curves at different pressures

It has to be noted that the parameter $A$ of Eq. 1.1.59 has been considered so far to be a constant. If one were to use an equation of state for the thermal vibration of the polymer molecules, which is equivalent to introducing a pressure and temperature dependence for $A$, the agreement between the predicted values and the ones measured by McKinney and Goldstein could be even better, as shown in Fig. 1.14, where a simple pressure dependence for this parameter has been used in the form

$$A(p) \;=\; 2.1 \times 10^{-6}\; exp(-.0465p) \quad . \tag{1.1.113}$$

Such a pressure dependence of $A$ would imply that the amplitude of the thermal vibrations is a decreasing function of pressure. Fig. 1.14 shows that for this simple choice the points where the equilibrium curve changes in slope are more closely gathered, *i.e.*, $\frac{\partial T_g}{\partial p} < .06$, thus closer to the measured values (.02 to .04 Kelvin per Bar) than in the previous case, where the same parameter was considered to be

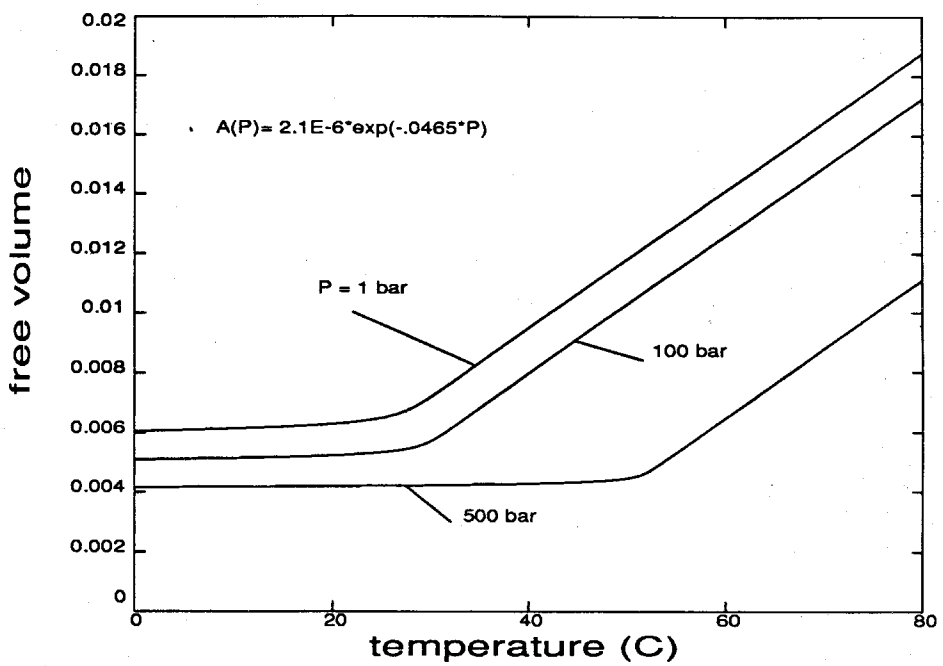


FIGURE 1.14 Predicted equilibrium curves with pressure dependence of the Markov parameter A.

constant.

Keeping these observations in mind, it can also be said that the present model performs very well if one considers the case of cooling only. This good behavior of the model is a consequence of the fact that, as the material cools down, the internal time scale continuously slows down and eventually stops. This means that small errors in evaluating the thermal transients (such as those generated from a misrepresentation of the entropy curve) have increasingly marginal effects as the temperature drops, since the error in cooling time drops far below the relaxation times of the polymer, which times increase as the temperature decreases. Additional studies for the cooling case, not presented here, indicate that ignoring the change in heat capacity across the glass transition yields a distribution of residual stresses that is quite similar to that computed through the full-fledged material description.

On the other hand, the same argument applied to heating cycles predicts that the errors amplify as temperature increases, for which a complete theory of thermal stresses under the most general temperature histories will require some additional refinement. This improvement would consist in allowing the possibility of discontinuities in the entropy curve at $T_g$ and will also need careful experimentation in order to be validated.

It needs to be stressed that the theory presented here is strictly a small deformation model of nonlinearly viscoelastic behavior. No distinction is made between current and reference configuration, the displacement gradients are supposed to be small compared to unity, thus the constitutive behavior of an isotropic polymer can be described in terms of only two quantities, the bulk and shear moduli. It is recognized that large strains will induce anisotropy in the molecule orientation, and a study on large strain viscoelasticity will have to take that into account, since not only the equilibrium dilatational behavior will be modified, but also the time shift will be affected; given a preferential orientation of the polymer chains, a deformation that involves sliding of the molecules along that particular direction will experience a lower value of viscosity than that associated with another type of motion, and this will have to be taken into account. Furthermore, it has been frequently stressed throughout this work that the effects of a thermodynamic transition on the mechanical properties (*cf.* Eq. 1.1.66) have been ignored. It is intended to include such features in a more advanced model, *e.g.,* through the use of an appropriate equation of state for the time-independent material response.

With the above limitations in mind, it is nonetheless felt that the theory presented so far allows a reasonable degree of accuracy for the usual manufacturing conditions, in which the material is cooled through the glass transition, and this

is probably enough for the formulation of an engineering judgment on the material properties after the manufacturing process.

## 1.2 Numerical analysis

The preceding section 1.1 has addressed the construction of a constitutive model for the time and temperature dependent properties of amorphous polymers. It is now of interest to evaluate the predictions of the constitutive assumptions in model engineering problems, such as the determination of transient and residual thermal stresses in a polymer cooled across the glass transition. This particular case has a relevant practical interest since such stresses always arise during the manufacturing process of polymeric structural components. In addition, the predictions of the presented constitutive model need to be compared with those of different, sometimes less accurate material description, in order to assess the benefits, inconveniences or inaccuracies involved in the use of one or the other.

The constitutive model was implemented in a finite element code, FEAP, originally devised by R. J. Taylor of U.C. Berkeley and made available to our research group through the courtesy of Dr. Ravichandran of Brown University. As outlined in Appendix A, the code was modified so it could accomodate materials with nonlinearly viscoelastic properties. Since the thermal diffusion problem had to be addressed concurrently, the numerical code was structured so that it solved the two problems separately and then iterated the solution until convergence was obtained for each time step. This iteration scheme was found to be more convenient than solving the two problems simultaneously since, given the asymmetric nature of the laws of mechanical equilibrium and thermal conduction with respect to the temperature and displacement fields, this latter approach would have led to the solution of an asymmetric system of equations, which system is notoriously more demanding on computating time. The thermal problem was solved using a three-step method, known as Gear's method with an averaged Crank-Nicolson start, which is well suited

to address integration of parabolic equations with discontinuous initial boundary conditions (Wood and Lewis, 1975), such as the case of a sudden drop or rise in surface temperature.

In order to examine the effect of different features of the proposed material model and to compare the predictions with previous analyses of thermo-viscoelastic behavior, two additional simpler material models are considered. The first one is similar to that used by Muki and Sternberg (1961)*, in which the temperature effects reduce to subtraction of the quasi-elastic thermal strains from the mechanical strain history, in the form

$$\sigma_{ij} = \int_{-\infty}^{t} 2G\Big(\xi(t) - \xi(\tau)\Big)\frac{\partial \epsilon'_{ij}(\tau)}{\partial \tau}d\tau + \delta_{ij}\int_{-\infty}^{t} K\Big(\xi(t) - \xi(\tau)\Big)\frac{\partial(\epsilon_{kk} - \epsilon_{\theta})}{\partial \tau}d\tau \quad , \tag{1.2.1}$$

where

$$\epsilon'_{ij} = \epsilon_{ij} - \frac{1}{3}\delta_{ij}\epsilon_{kk} \tag{1.2.2}$$

is the deviatoric part of the strain tensor, $K(t)$ and $G(t)$ are the time dependent bulk and shear moduli, and $\xi(t)$ is representative of the internal time scale, related to that in reference conditions through Eq. 1.1.18. The shear modulus was computed from Heymans's data (Heymans, 1983) and the bulk modulus from data by McKinney and Belcher (McKinney and Belcher, 1963) through a numerical procedure presented in Appendix B. In this model, which from now on will be referred to as the "elementary" model, the glass transition temperature was considered to be constant at 29 $C$, and the coefficient of thermal expansion and the heat capacity were characterized by a discontinuity across $T_g$. The thermal strains were therefore

---

* The original model used by Sternberg and Muki did not take into account a discontinuity in the heat capacity across the glass transition.

computed from

$$\begin{aligned} \frac{d\epsilon_\theta}{dT} &= \alpha_l = 6.0 * 10^{-4} K^{-1} \; for \; T > T_g = 29.C \\ &= \alpha_g = 2.5 * 10^{-4} K^{-1} \; for \; T < T_g \; . \end{aligned} \tag{1.2.3}$$

The Fourier law of heat conduction is written in the form**

$$\kappa \nabla^2 T = \rho C_p \frac{dT}{dt} \; , \tag{1.2.4}$$

where (Sandberg and Bäckström, 1980)

$$\kappa = .19 \; \frac{Watt}{mK} \; , \tag{1.2.5}$$

$$\begin{aligned} \rho C_p = \rho C_{pl} &= 2.09 * 10^6 \frac{J}{m^3 K} \; for \; T > T_g \; , \\ &= \rho C_{pg} = 1.29 * 10^6 \frac{J}{m^3 K} \; for \; T < T_g \; . \end{aligned} \tag{1.2.6}$$

In this elementary model, the heat conductivity $\kappa$ was taken to be constant. The bulk and shear moduli were referenced to 40 $C$ and the time shift was computed from Heymans's data, shown in Fig. 1.5, with a linear dependence of the free volume on temperature, represented by the solid curve in the same figure†.

Before introducing the second simple model, a brief summary of the model presented in this work is necessary, since the two material descriptions are closely related. The equilibrium equations have the same form as Eq. 1.2.1, the only difference being the change in the time-independent part of the volumetric response resulting from the freezing-in of the free volume sites (*cf.* section 1.1.4, Eq. 1.1.76).

---

** The effect of material energy dissipation resulting from viscoelastic behavior was not taken into account in the energy equation, of which the Fourier law of heat conduction is a simple form. The justification for this neglect comes from the model validity being restricted only to small strain deformations; the dissipated energy, which is a quadratic function of the strains, is therefore very small in comparison to the other terms of the energy equation, such as the change in the internal energy of the material.

† This implies that the time-temperature shift of the elementary model diverged from the experimental one below the glass transition.

Because of this variation, the convolution integrals of Eq. 1.2.1 had to be reduced to differential equations which were then solved in the discretized time domain‡. The coefficient of heat capacity was taken to have a discontinuity at the glass transition, but the glass transition itself was considered to occur at a critical value of fractional free volume, as explained in section 1.1.7, resulting in a pressure and rate dependent transition temperature*. The transition was assumed to be of second order, *i.e.*, no finite jump in the equilibrium entropy was allowed. As explained in section 1.1.4, the only required coefficient of thermal expansion was the rubbery coefficient $\alpha_l$, since the glassy behavior follows automatically from the freezing of the free volume sites and of the relaxation mechanisms. The coefficient of heat conduction was kept constant. The value of the time shift was assumed to depend on the instantaneous value of the free volume, the changes of which are affected by the mechanical and thermal histories. The initial value for the fractional free volume ($T_{initial}$ = 65 C) was taken to be .0142, as suggested by the Doolittle equation fit to the experimentally measured time shift (Heymans, 1983) and the choice $\frac{\partial f}{\partial T} = 2.32 \times 10^{-4} C^{-1}$.

In this context, the question arises as to what are the consequences of considering a material scale of relaxation which depends on the nonequilibrium fractional free volume, *i.e.*, the history-dependent volume of the vacancies. Within a simplified approach to the problem, one could assume that the internal time scale depends on the local value of temperature only, which is equivalent to a dependence of the time shift on the equilibrium (asymptotic) value of free volume. This approach would not take into account the viscoelastic "lag" between the temperature changes and

‡ The replacement of convolution integrals by differential equations is also extremely advantageous for the reduction in computational time, as explained in Appendix A.

* In these calculations, the critical value of fractional free volume was set to be .0065, *i.e.*, .65 per cent.

the morphological changes in the polymer, which lag causes the instantaneous time shift to differ from the "equilibrium" one at a given temperature; in addition, the stress and strain fields would have no influence on the variations in the time scale of material relaxation, since the latter would only be temperature-controlled. It should be noted that the effect of the stress field is an acceleration of the relaxation process where high tensile stresses are present; these stresses induce a dilatation which increases the local free volume, resulting in a higher molecular mobility (compared with that which would be present in the case where free volume depended on temperature only).

In order to examine the importance of the coupling between the stress field and the time scale of relaxation, a second simple material description, denoted here as semi-elementary, was considered. In this model, the time shift governing the local relaxation behavior was assumed to depend on the local temperature according to the experimental data shown in Fig. 1.5**. All the other features, such as the discontinuity in the heat capacities and the dependence of the glass transition on pressure, were the same as in the model presented in section 1.1.

Two example cases were initially considered: 1) the case of an infinitely long circular cylinder, restrained axially and uniformly at the ends, and 2) that of a sphere; in both cases the material (PVAc) experiences a sudden temperature drop at the surface. Both the cylinder and the sphere were taken to have a radius of two centimeters. The initial temperature was chosen to be $+65\ C$ and the final one $-5\ C$, so that the glass transition temperature ($T_g \sim +29\ C$ for PVAc) fell in between the two extremes. Some of the predictions of the three different models are shown in the following figures.

---

** In the elementary model the fitted continuous curve, also shown in the same figure, was used.

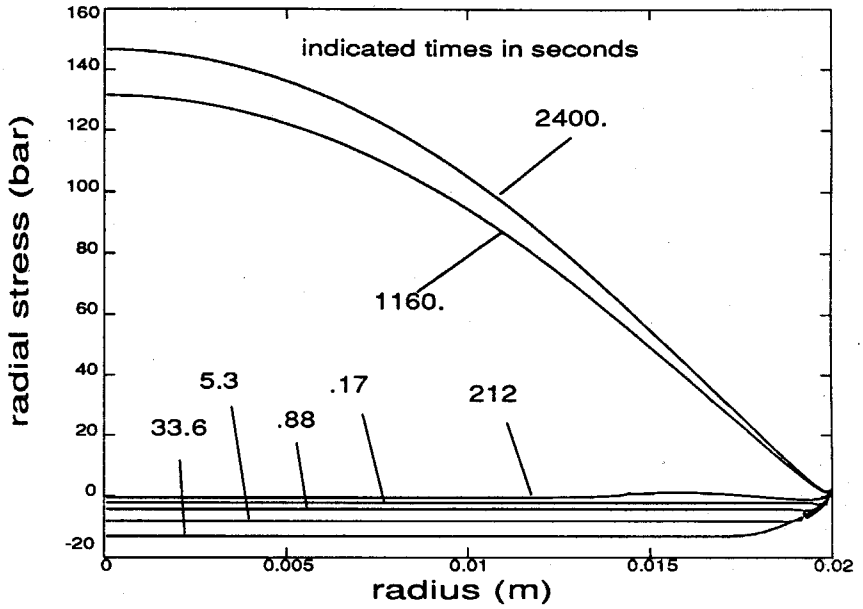


FIGURE 1.15 Radial stress in the infinite cylinder (elementary model).

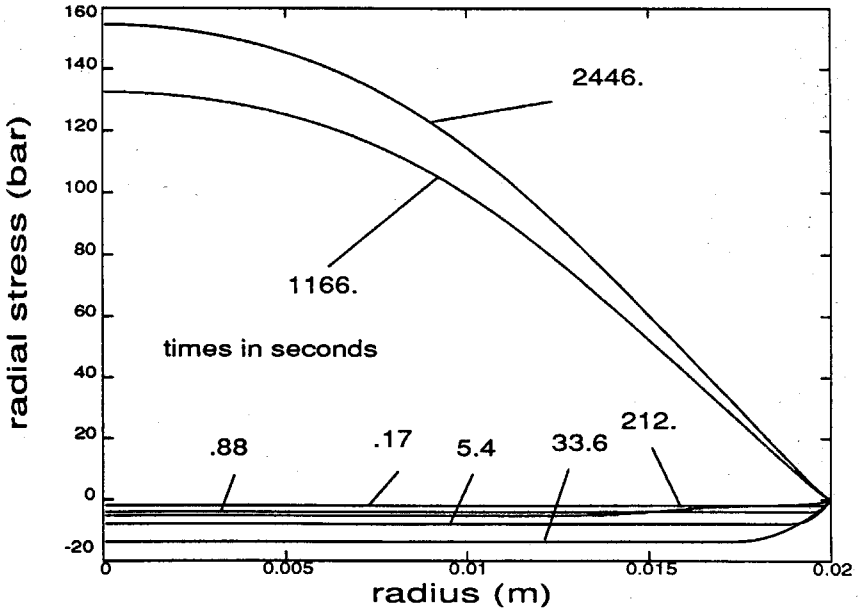


FIGURE 1.16 Radial stress in the infinite cylinder (proposed model).

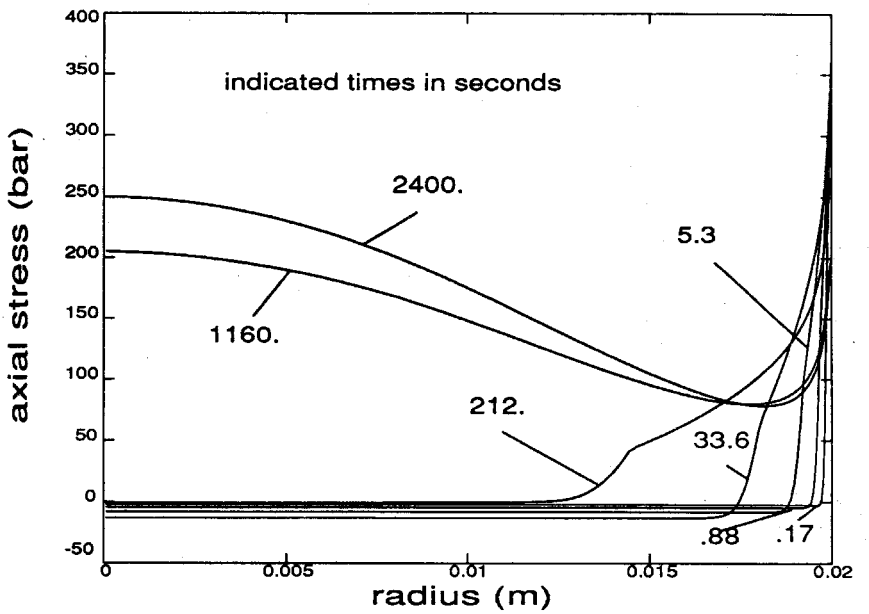


FIGURE 1.17 Axial stress in the infinite cylinder (elementary model).

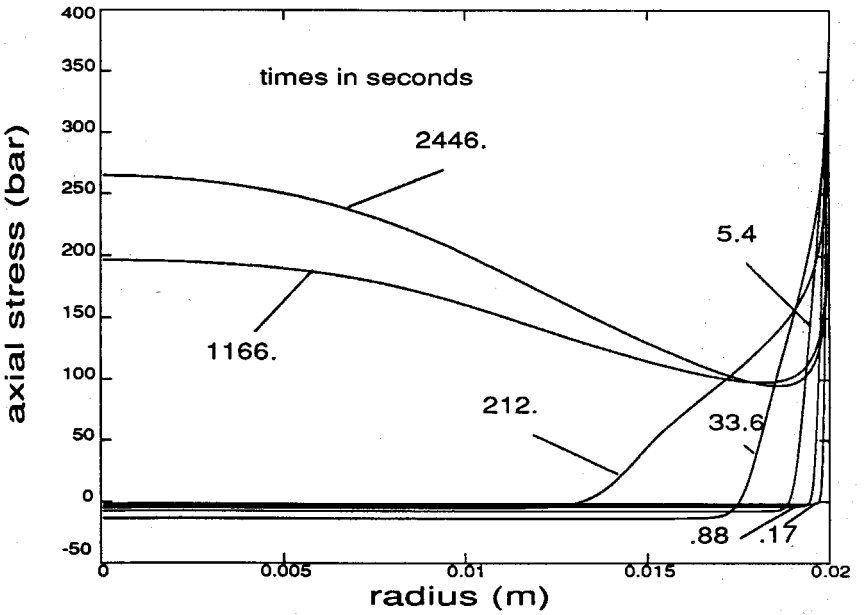


FIGURE 1.18 Axial stress in the infinite cylinder (proposed model).

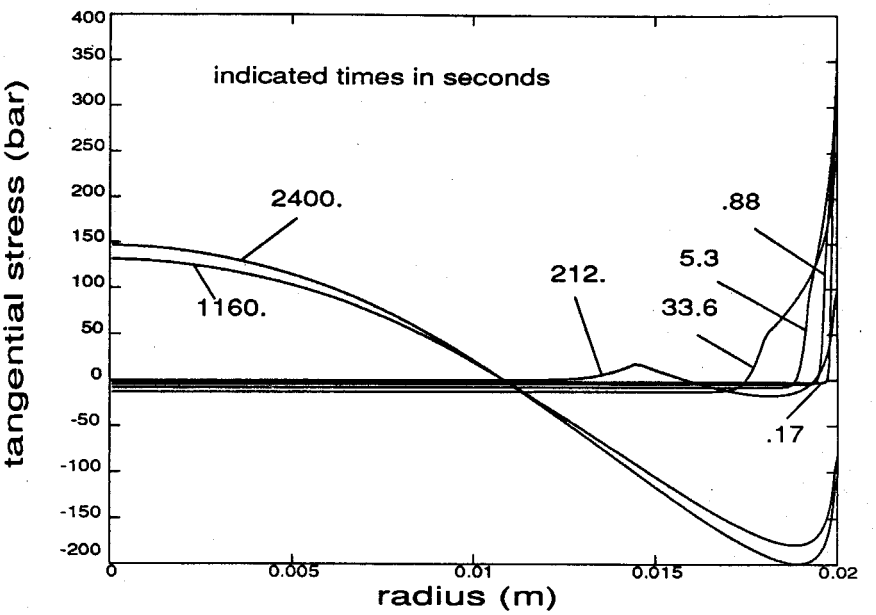


FIGURE 1.19 Hoop Stress in the infinite cylinder (elementary model).

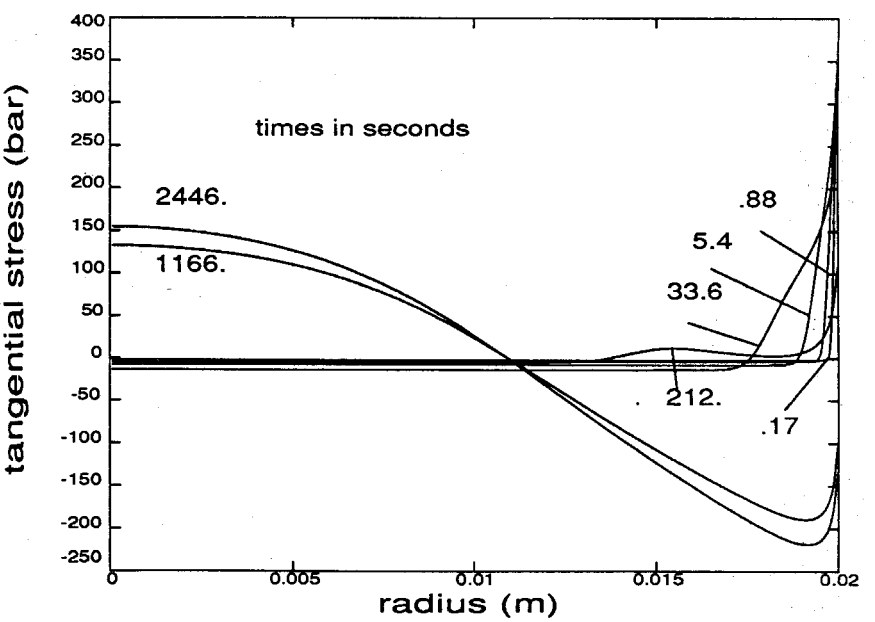


FIGURE 1.20 Hoop Stress in the infinite cylinder (proposed model).

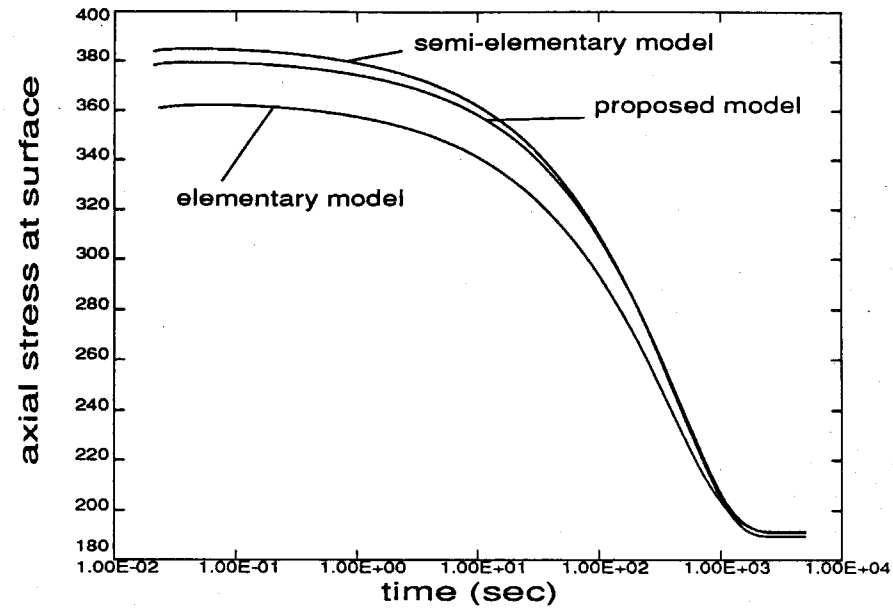


FIGURE 1.21 Comparison of the three model predictions for the axial stress at the surface.

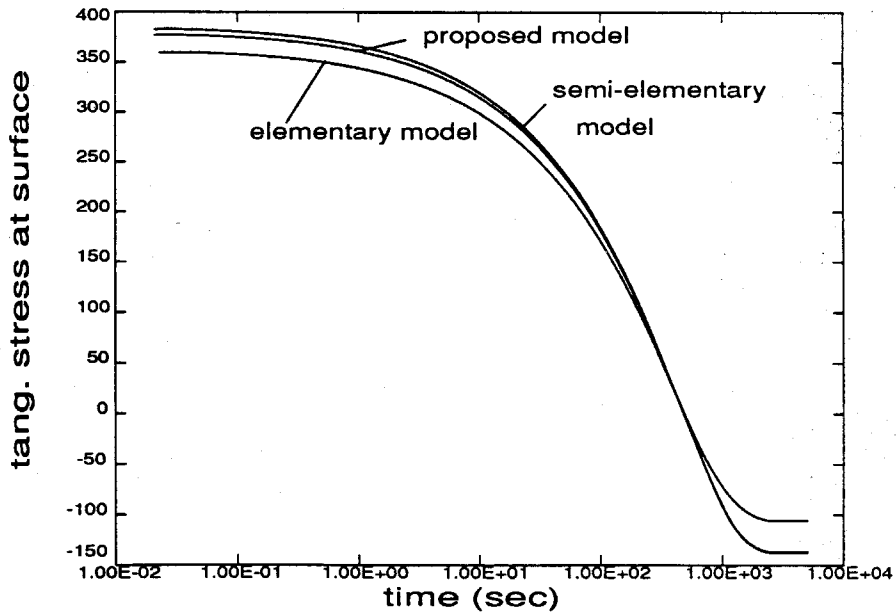


FIGURE 1.22 Comparison of the three model predictions for the tangential stress at the surface.

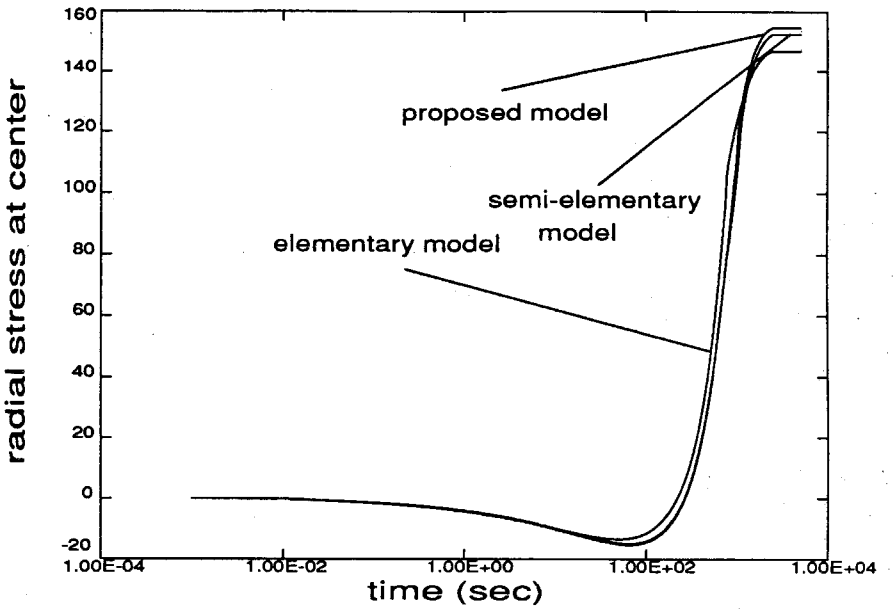


FIGURE 1.23 Comparison of the three model predictions for the radial stress at the cylinder axis.

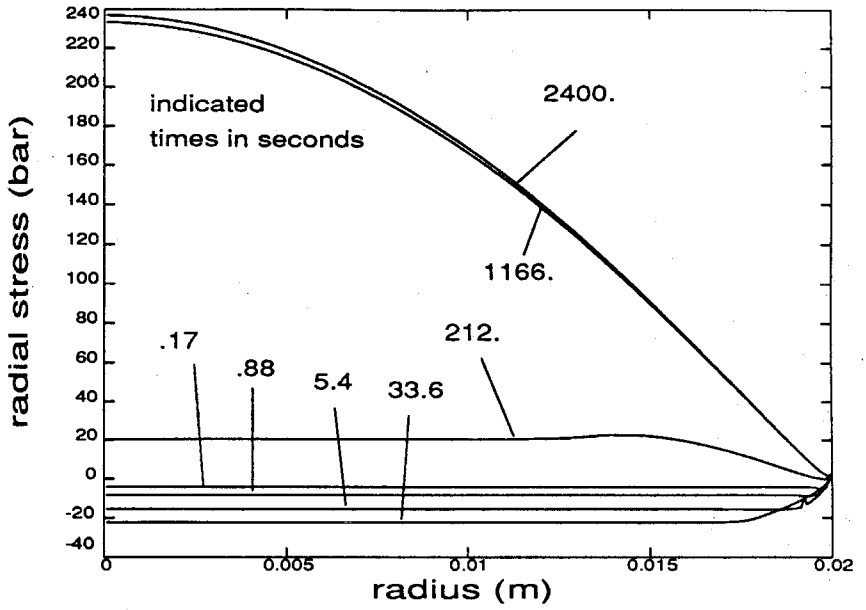


FIGURE 1.24 Radial stress in the sphere (elementary model).

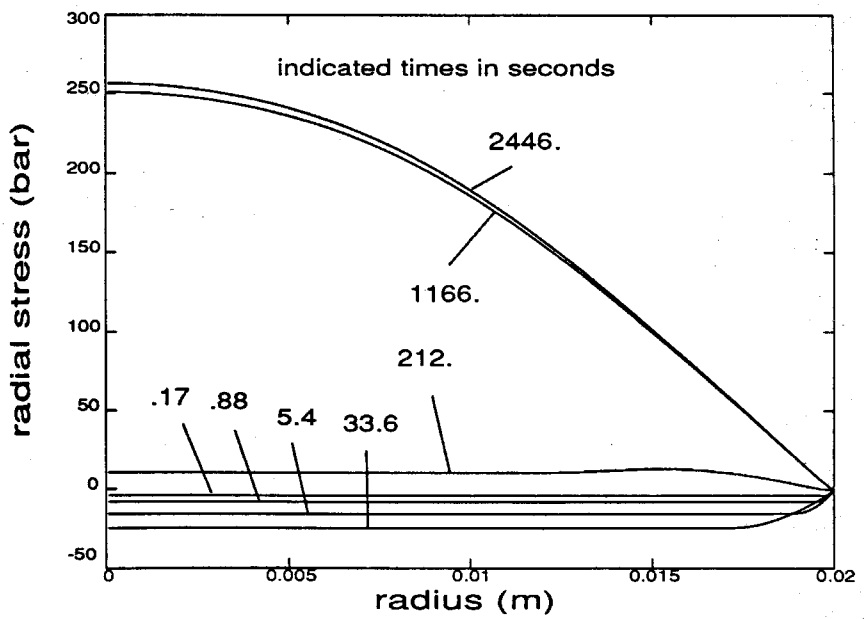


FIGURE 1.25 Radial stress in the sphere (proposed model).

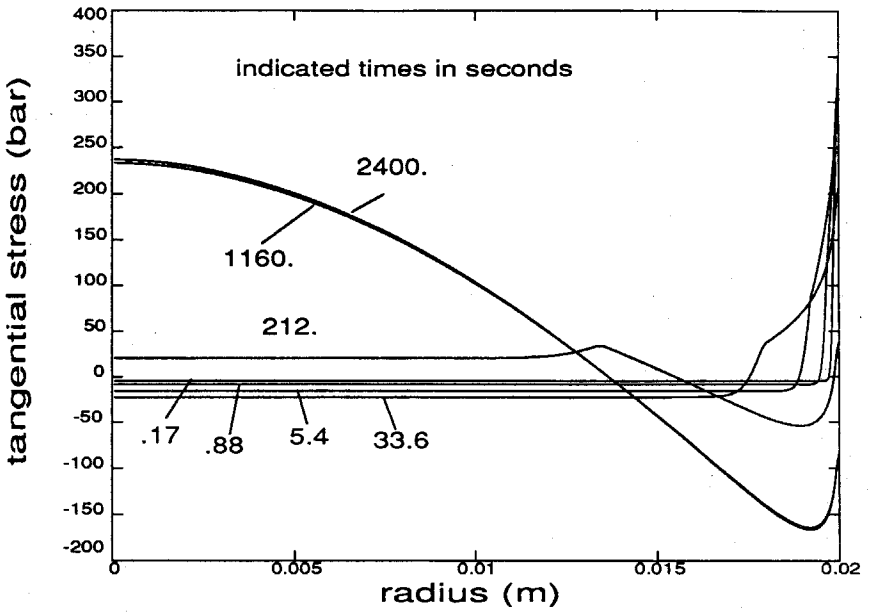


FIGURE 1.26 Tangential stress in the sphere (elementary model).

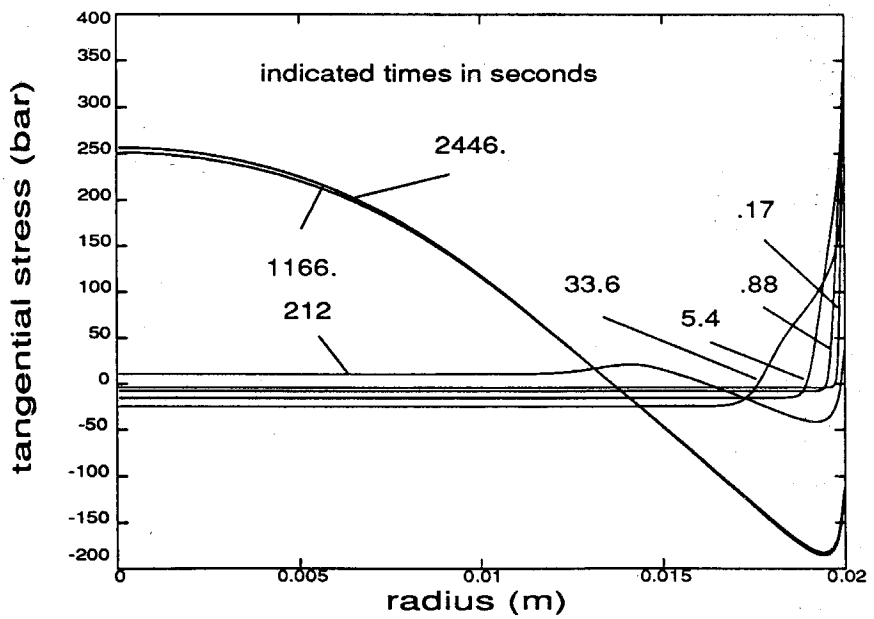


FIGURE 1.27 Tangential stress in the sphere (proposed model).

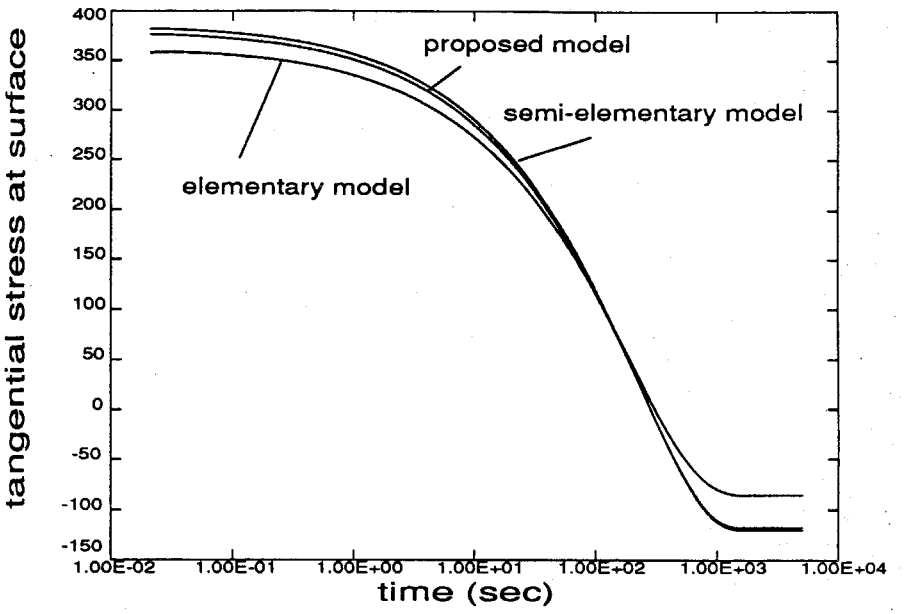


FIGURE 1.28 Comparison of the three model predictions for the tangential stress at the surface.

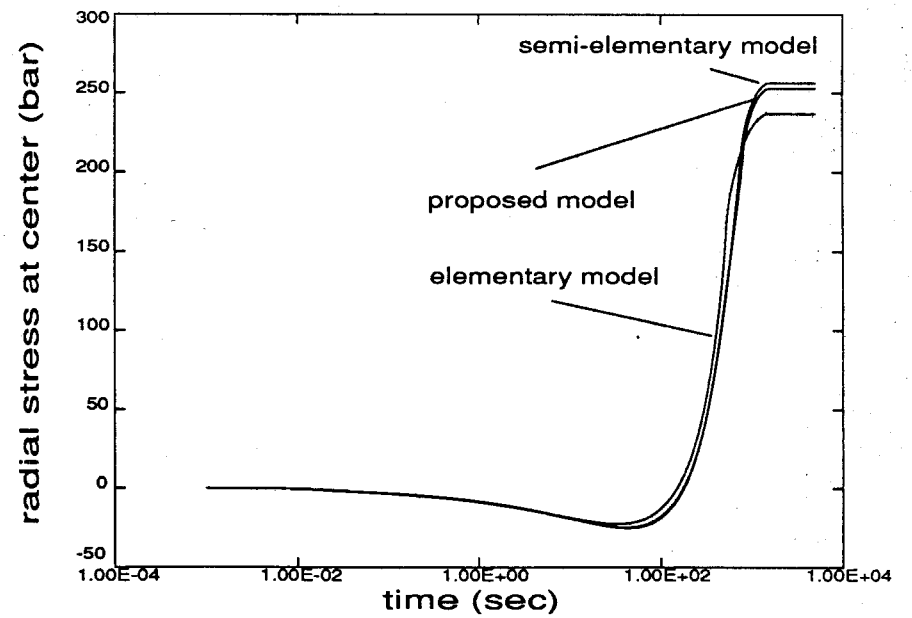


FIGURE 1.29 Comparison of the three model predictions for the radial stress at the center.

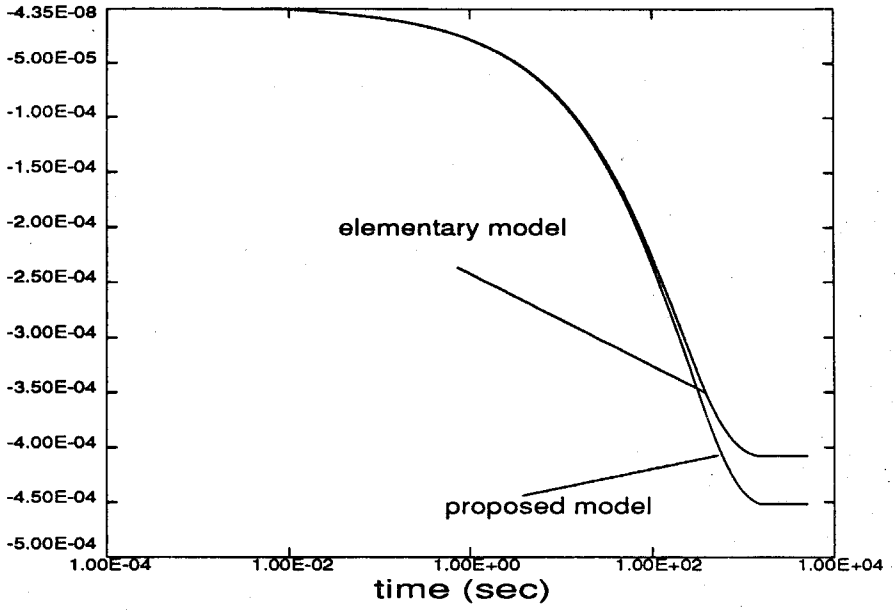


FIGURE 1.30 Reduced volume contraction ($\Delta V/[V|T_{initial} - T_{final}|]$) of the PVAc sphere cooled from +65 to −5 C.

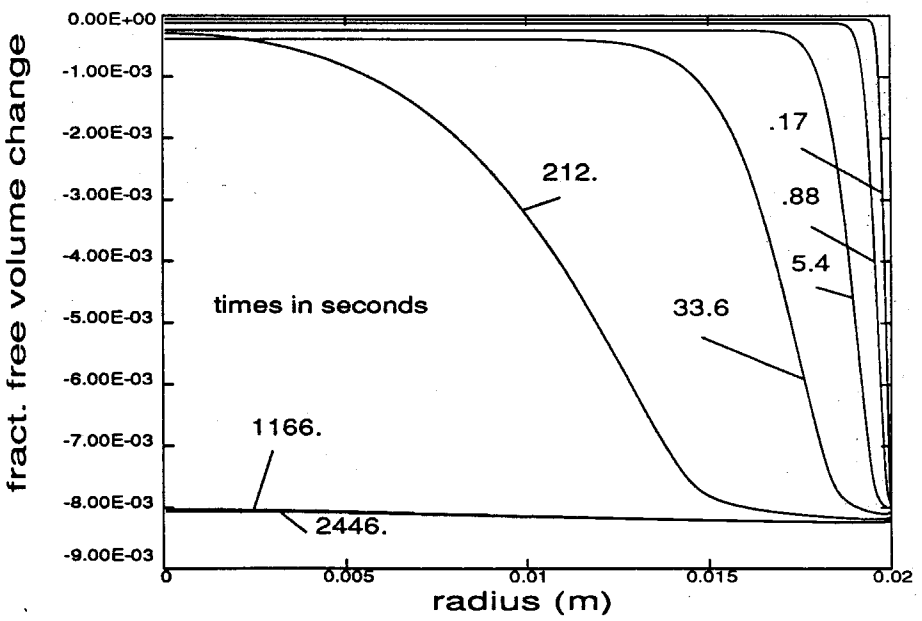


FIGURE 1.31 Time dependent fractional free volume change in the sphere (proposed model).

Some special characteristics of the numerical solution are of interest. The elementary model predicts a moving discontinuity in the gradient of the stress distribution, which discontinuity occurs at the point where the material passes through the glass transition (*cf.* Figs. 1.17, 1.19, 1.26). The "cusp" in the stress distribution is noticeably smoothed if the predictions of the proposed model are considered (*cf.* Figs. 1.18,1.20,1.27). Also, dealing with two different coefficients of thermal expansion gives rise to difficulties in the numerical analysis, as indicated by the occasional "glitches" in the stress distribution in Figs. 1.16, 1.25. The predictions of the three different models differ by an amount which increases as the time scale of the local thermal transients becomes shorter. As shown by Figs. 1.21, 1.29, the differences in the predicted radial stress on the axis of the cylinder or at the center of the sphere, *i.e.,* at the position where the temperature drop is slowest, are almost negligible. In contrast, these differences are larger at the surface (*cf.* Figs. 1.22, 1.23, 1.28) where the thermal transients closely follow the initial, instantaneous drop in surface temperature. This fact indicates an additional aspect of the residual stress problem, namely the interaction between the local relaxation time scale and the time scale of the thermal diffusion. In particular, if one considers the time dependence of the bulk modulus of PVAc (McKinney and Belcher, 1963), shown in Fig. 1.32, one can see that at a temperature of 40 C the volumetric response of the polymer reaches equilibrium approximately after $10^{-2}$ seconds. Near the surface of the sphere and of the cylinder, the material experiences a temperature drop in a time interval of the order of few milliseconds and, furthermore, the relaxation times become longer once the solid reaches the lower temperatures. At the center of the sphere, thermal equilibrium is reached in about an hour (the cylinder takes a little longer), and most of this time is spent at temperatures at which the polymer can reach voluminal equilibrium within a second or less. As a consequence, the

departure of the material from an equilibrium curve, characterized by the rubbery (asymptotic) values of dilatation as a function of temperature, is greater near the surface than at the center, *i.e.,* is larger where the "distance" of the polymer from its equilibrium state is more significant; the differences are also larger between the predictions of the three material models.

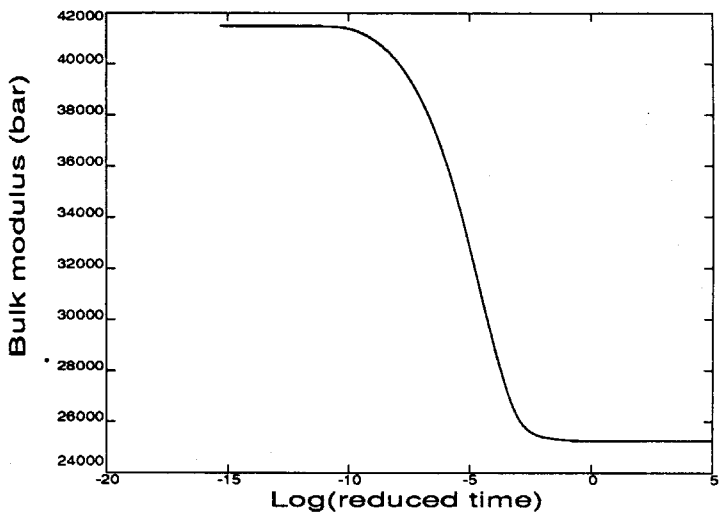


FIGURE 1.32 Bulk modulus of PVAc, referenced to $T_{ref} = 40$ C.

In order to investigate the interaction between the thermal transients and the relaxation behavior, the case of the sphere, one millimeter in radius, cooled from 40 to 35 C and heated from 30 to 35 C, was considered. The choice of temperatures was made with the desire of comparing the numerical results with experiments conducted by Kovacs (1958) on the time-dependent thermal expansion of PVAc. Those experiments were conducted in the following manner: a PVAc specimen was introduced under vacuum into a glass reservoir, which was connected to a capillary. The reservoir was subsequently filled with mercury at some initial temperature and then dropped into a liquid bath at a different temperature; from the position of

the mercury meniscus in the capillary, the time-dependent volume changes were measured. While it is not our intention to reproduce Kovacs's results exactly†, a qualitative comparison is certainly possible. Kovacs's experimental results are shown in Fig. 1.33.

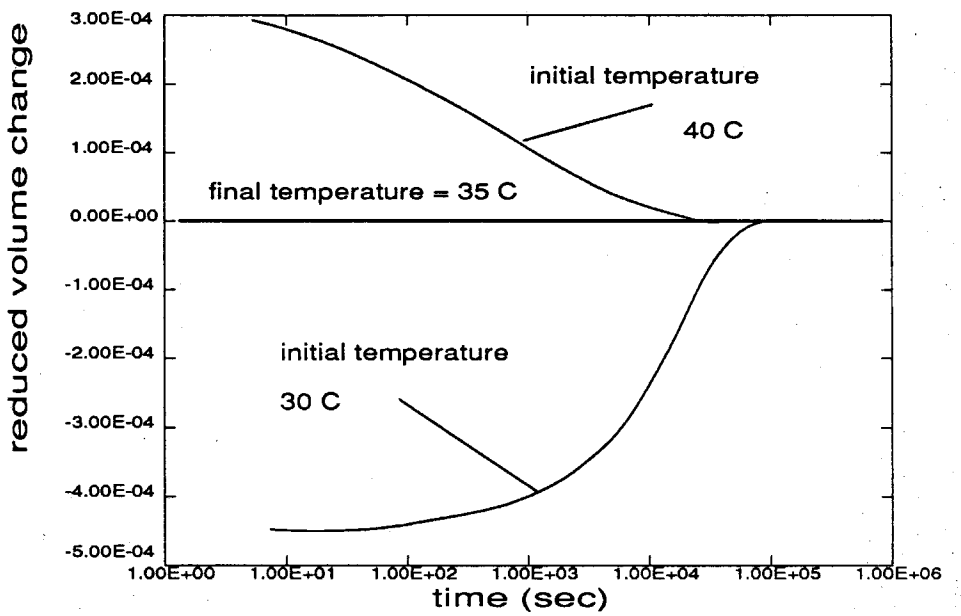


FIGURE 1.33 Reduced volume change $\frac{V-V_\infty}{V|T_{init}-T_\infty|}$ of PVAc, plotted vs. time; data obtained by Kovacs (1963).

A relevant feature of the data in Fig. 1.33 is the difference between the heating and cooling curves, which can only be explained in terms of free volume controlled relaxation behavior (Kovacs, 1963). Furthermore, the time required to reach voluminal equilibrium can be estimated, from the cooling curve, to be about $10^4$ seconds, much larger than the 10 seconds predicted by the time-temperature shift of PVAc associated with the time-dependent bulk modulus measured by McKinney

† This would require the exact knowledge of the geometry of the specimen, glass container and of the volume of mercury, none of which have been reported in Kovacs's publication.

and Belcher (1963)[‡]. As a result, some questions arise about the conditions of the material (PVAc) of which McKinney and Belcher measured the bulk modulus. It is possible that the polymer was in a swollen state, perhaps due to contamination by water or solvents; this suspicion is strengthened by the observation that the material had a glass transition of about 17 C at atmospheric pressure, far from being in the neighborhood of 29 C which several other measurements (*e.g.*, Heymans, 1983) indicate as the transition temperature. Consequently, it was decided to consider a "modified" bulk modulus in addition to the one extracted from McKinney's and Belcher's data. This bulk modulus was obtained from that used in the calculations so far through a shift of 2.5 decades along the logarithmic time scale*. For the case of the sphere of 1 mm in radius, the predictions of the proposed and semi-elementary models are presented in the following figures.

---

‡ The time shift between 40 and 30 C is, for PVAc, of the order of $10^3$; the bulk modulus measured by McKinney and Belcher reaches equilibrium at $t \approx 10^{-2}$ seconds, at a temperature of 40 C. This implies that about 10 seconds are required at 30 C.

* *i.e.*, all the relaxation times were multiplied by $10^{2.5} = 313$.

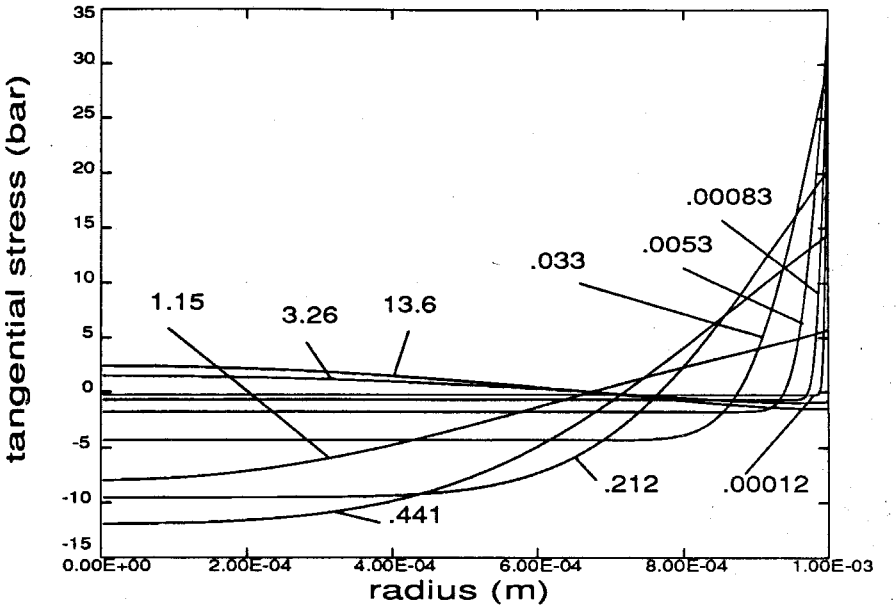


FIGURE 1.34 Tangential stress in the 1 mm radius sphere cooled from 40 to 35 C (proposed model, McKinney's and Belcher's bulk modulus).

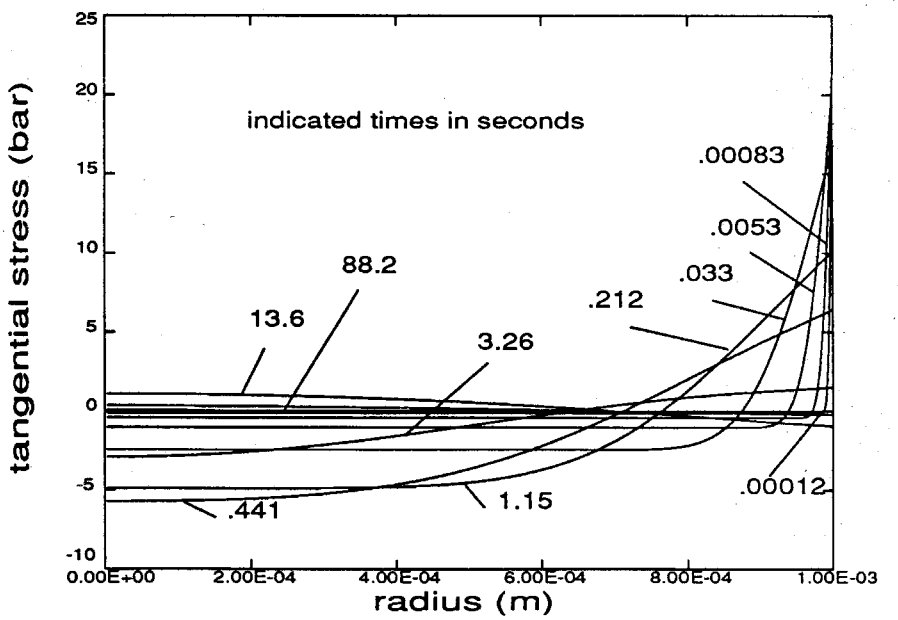


FIGURE 1.35 Tangential stress in the 1 mm radius sphere cooled from 40 to 35 C (proposed model, "modified" bulk modulus).

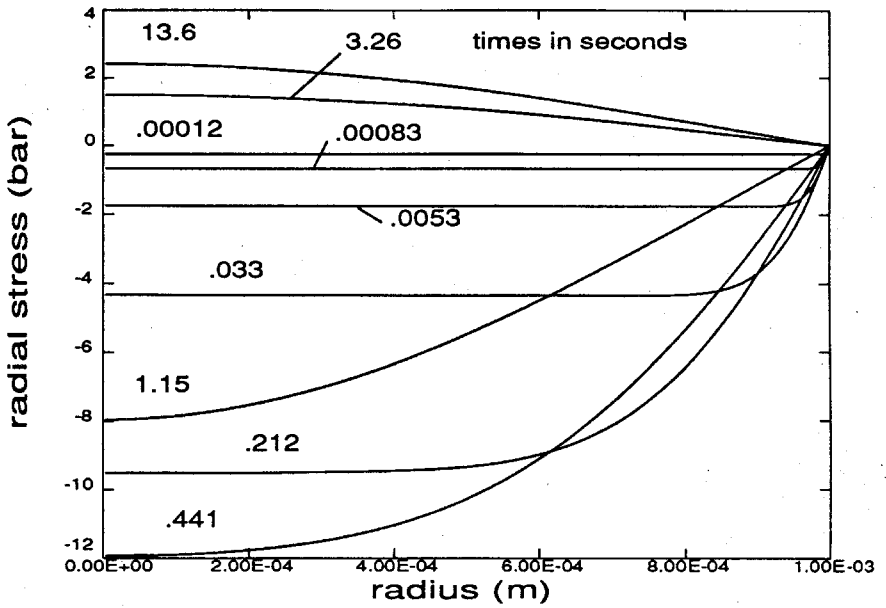


FIGURE 1.36 Radial stress in the 1 mm radius sphere cooled from 40 to 35 C (proposed model, McKinney's and Belcher's bulk modulus).

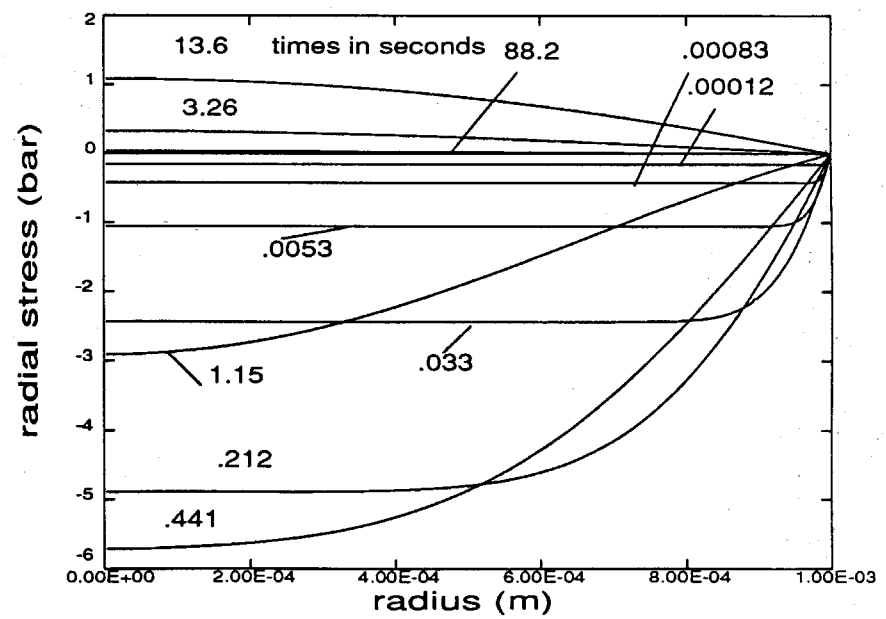


FIGURE 1.37 Radial stress in the 1 mm radius sphere cooled from 40 to 35 C (proposed model, "modified" bulk modulus.

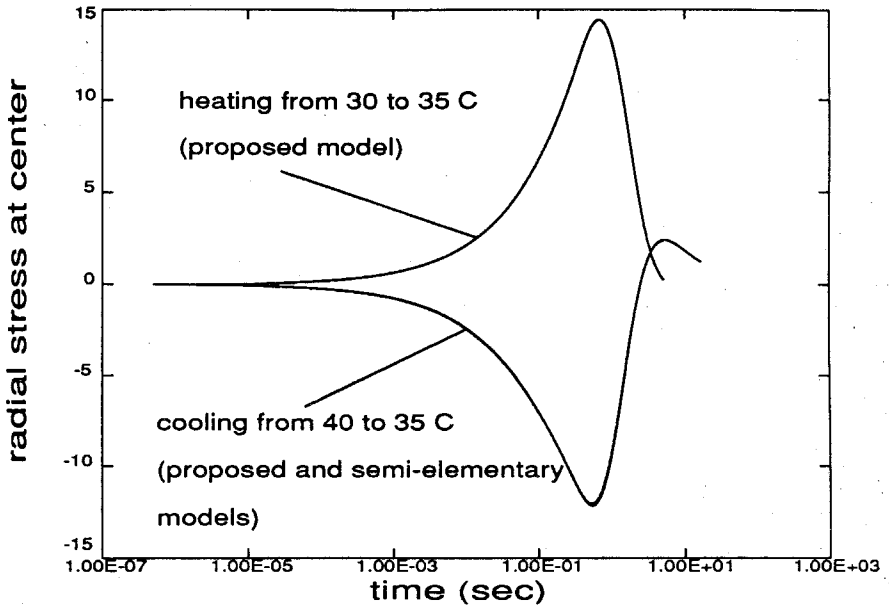


FIGURE 1.38 Predictions for the radial stress at the center of the 1 mm radius sphere (McKinney's and Belcher's bulk modulus).

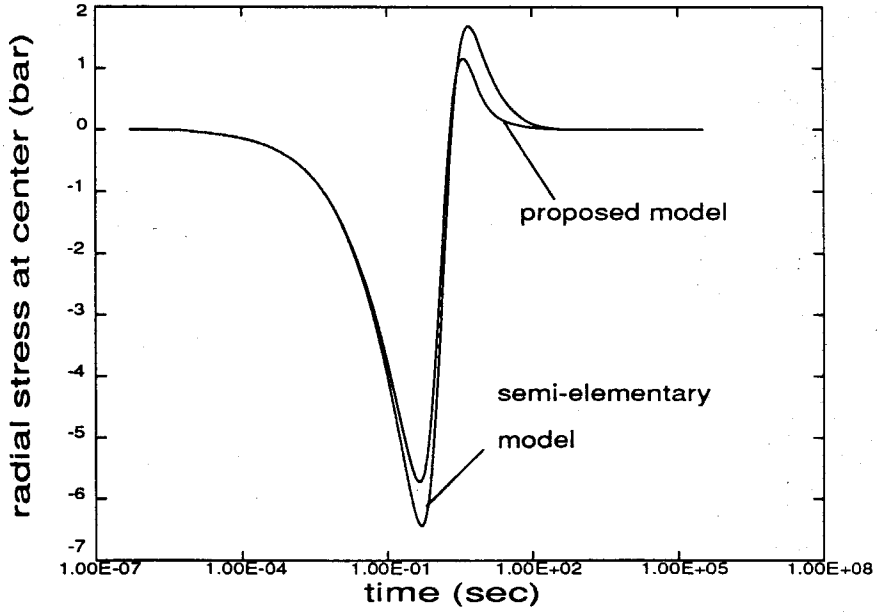


FIGURE 1.39 Predictions for the radial stress at the center of the 1 mm radius sphere cooled from 40 to 35 C ("modified" bulk modulus).

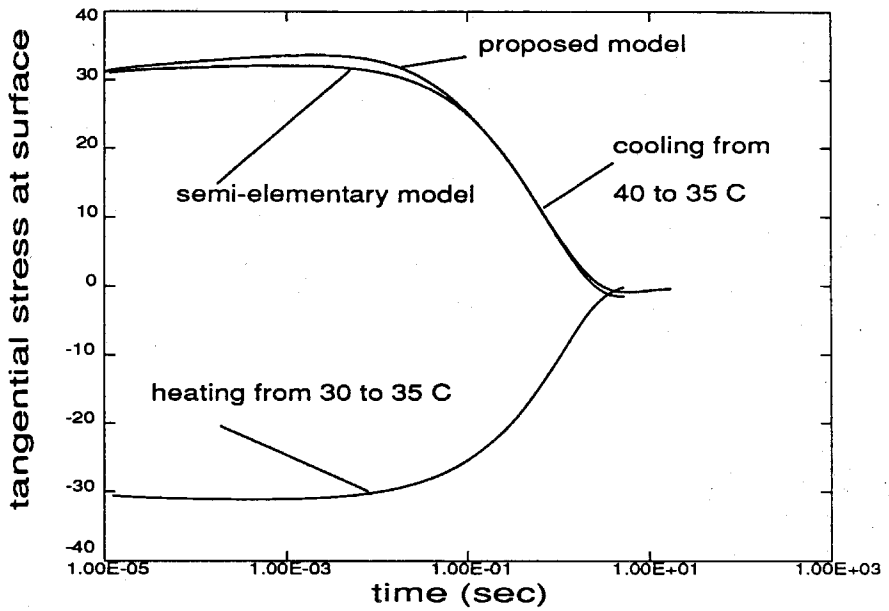


FIGURE 1.40 Predictions for the tangential stress at the surface of the 1 mm radius sphere (McKinney's and Belcher's bulk modulus).

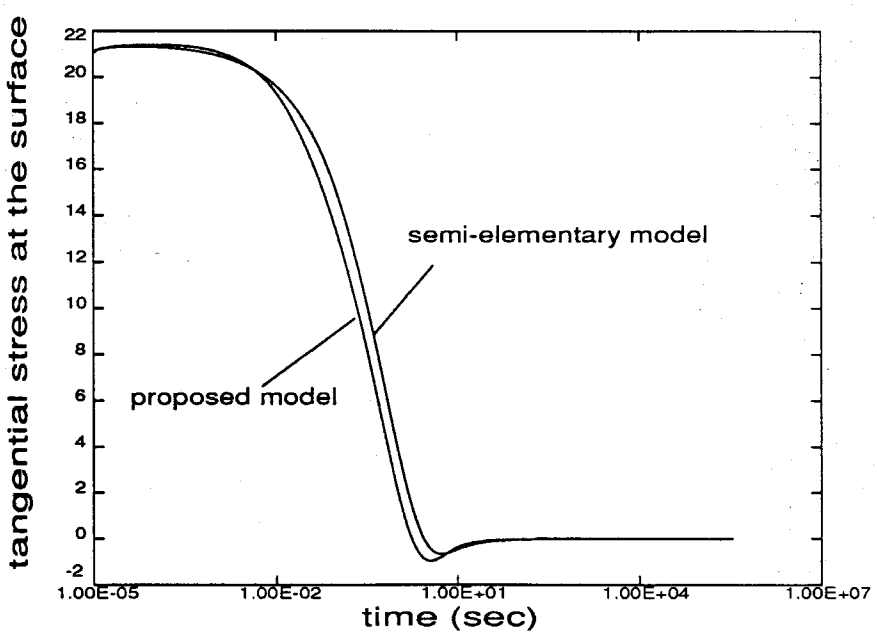


FIGURE 1.41 Predictions for the tangential stress at the surface of the 1 mm radius sphere cooled from 40 to 35 C ("modified" bulk modulus).

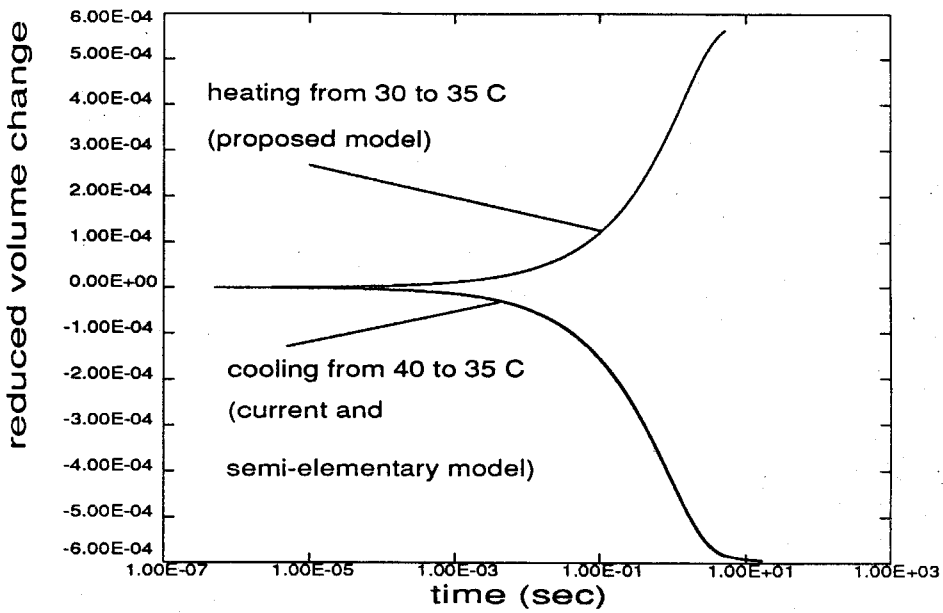


FIGURE 1.42 Reduced volume change $\Delta V/[V|T_{init} - T_{final}|]$ of the 1 mm radius sphere (McKinney's and Belcher's bulk modulus).

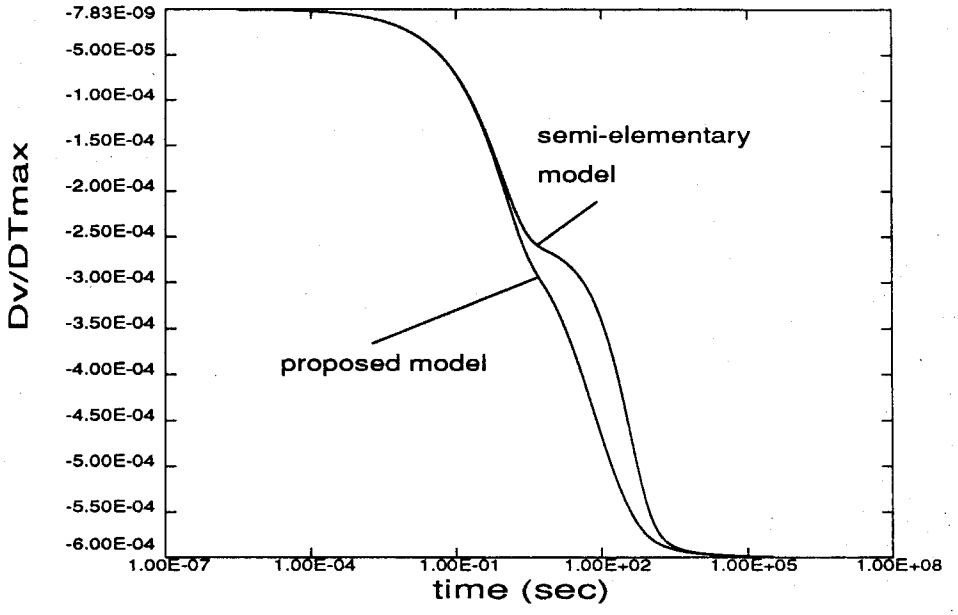


FIGURE 1.43 Reduced volume change $\Delta V/[V|T_{init} - T_{final}|]$ of the 1 mm radius sphere cooled from 40 to 35 C ("modified" bulk modulus).

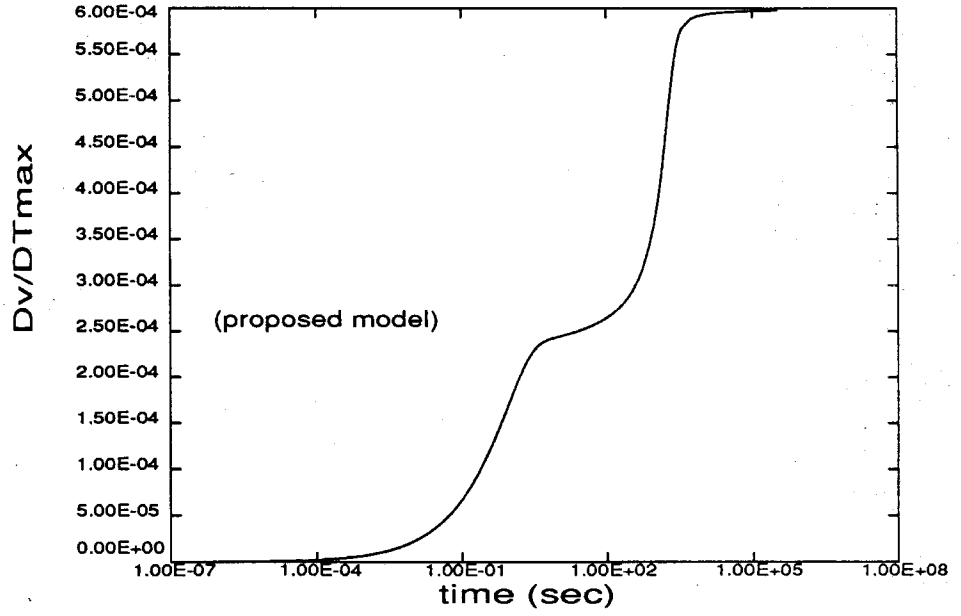


FIGURE 1.44 Reduced volume change $\Delta V/[V|T_{init} - T_{final}|]$ of the 1 mm radius sphere heated from 30 to 35 C ("modified" bulk modulus).

If one restricts attention to the case where the "modified" modulus was used, one can see that the differences between the predictions of the current and semi-elementary model are highlighted. In particular, Fig. 1.39 shows that at the center of the sphere cooled from 40 to 35 C, the highest tensile stress predicted by the semi-elementary model is about 50 per cent higher than that predicted by the present theory. Similarly, the cooling and heating curves of McKinney's and Belcher's material are only marginally affected by the choice of material representation, (*cf.* Fig. 1.42), whereas, in the case of the "modified" material, these differences are substantial (*cf.* Figs. 1.43, 1.44).

The predicted residual stresses, in the temperature range just examined, fade to zero since the final temperature (30 C) is above the glass transition and characterized by active relaxation mechanisms. In order to examine the differences in the residual stress distribution when the final temperature is low enough to freeze molecular relaxation, and the two time scales, the one of thermal diffusion and the one of viscoelastic behavior, are "close" to each other**, a rather extreme case was considered, namely the case of a PVAc sphere, 1 mm in radius, cooled from +60 to $-5$ $C$. The comparisons between the predictions of the three different models are shown in the next pages, and they show relevant differences in the magnitude of the residual stresses. These results suggest that, when the material is subjected to harsh cooling such as in this last case, the problem of transient and residual thermal stresses needs to be addressed with a lot of (scientific) care.

---

** This statement is intended only in a qualitative way, since the local rate of cooling depends on the global geometry and the distance from the boundaries of the solid, whereas the viscoelastic time scale is, as a first approximation, a function of the local, changing temperature.

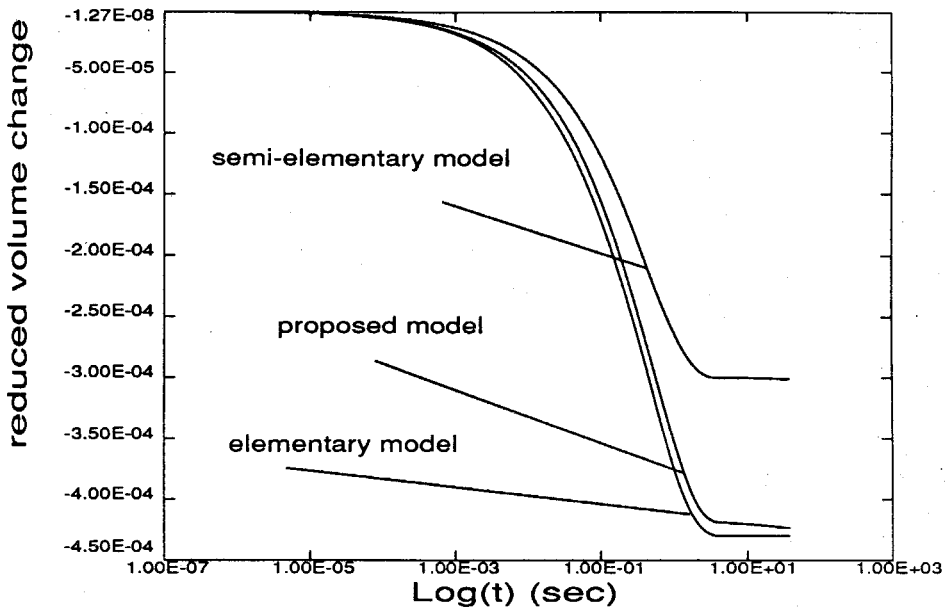


FIGURE 1.45 Reduced volume change $\Delta V/[V|T_{init} - T_{final}|]$ of the 1 mm radius sphere cooled from +60 to -5 C ("modified" bulk modulus).

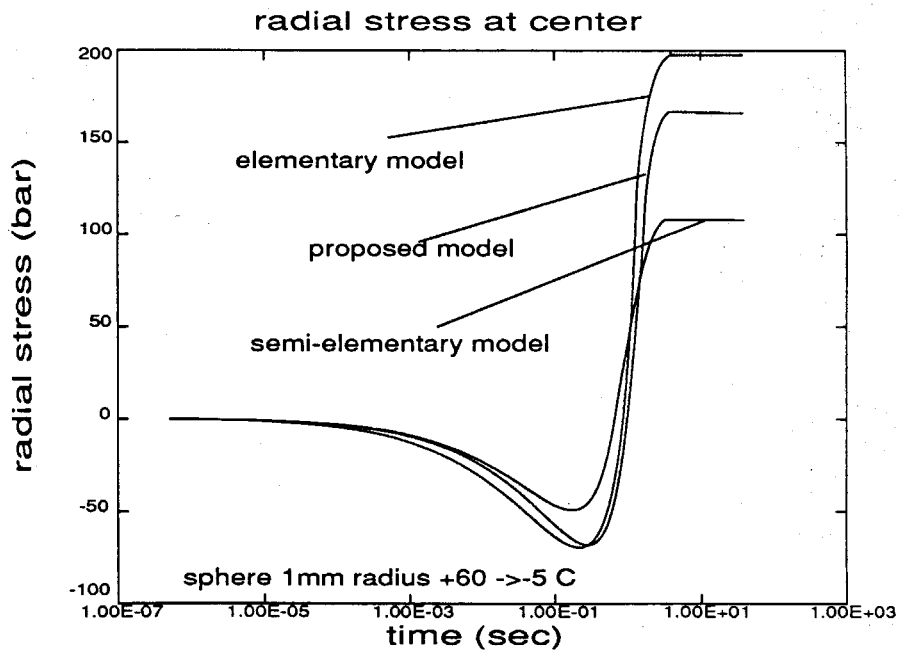


FIGURE 1.46 Predictions for the radial stress at the center of the 1 mm radius sphere cooled from +60 to -5 C ("modified" bulk modulus).

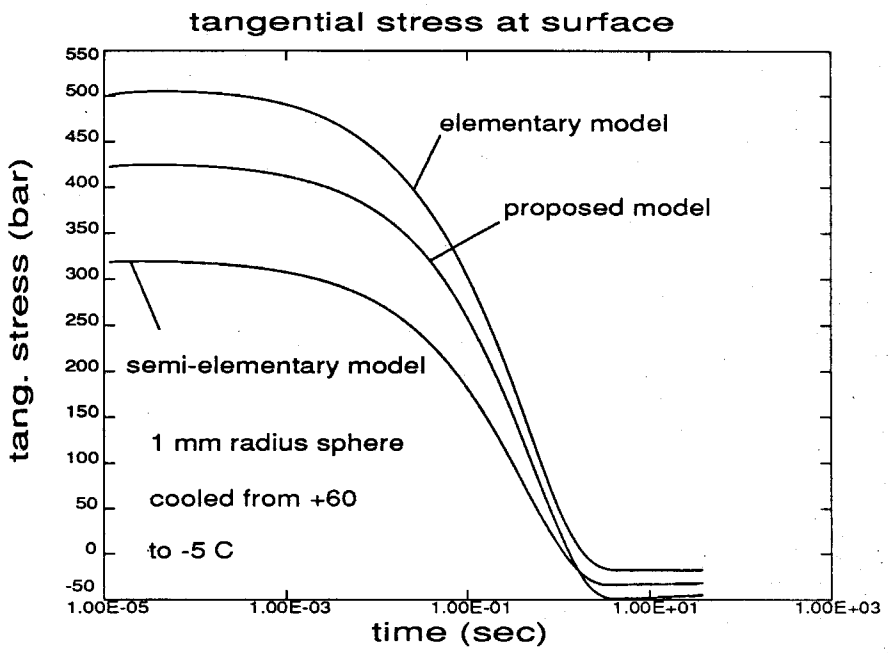


FIGURE 1.47 Predictions for the tangential stress at the surface of the 1 mm radius sphere cooled from +60 to -5 C ("modified" bulk modulus).

## 1.3 Conclusions

A model has been presented which has the capability of describing the changes in the rheological properties of a polymer at temperatures above and below the glass transition. The model is based on experimentally measurable parameters, such as the time-dependent bulk and shear moduli. The material behavior below the glass transition is fully described through the use of parameters typical of the rubbery state, such as the rubbery coefficient of thermal expansion $\alpha_l$ and the asymptotic value of the bulk modulus, $K_\infty$. No glassy coefficient of thermal expansion is required since the glassy behavior is effected by the freezing-in of the free volume and of the relaxation mechanisms. The consequences of the model with respect to the kinetic aspects of the glass transition have been investigated and found in essential agreement with experimental results. The problem of transient and residual thermal stresses has been addressed in the framework of this material representation and of two simpler constitutive theories. The difference between the predictions of the three models have been found to increase as the time scale of the thermal transients becomes of the same order or smaller than the time scale of viscoelastic relaxation. Experimental results for the time-dependent thermal expansion of PVAc have indicated that a careful measurement of the viscoelastic bulk modulus is needed; in particular, the predicted volume change sheds some concern on the conditions in which the experimental results of McKinney and Belcher (1963) were obtained.

The model neglects the effect of an equilibrium second order transition on the mechanical response, which could be accomplished readily. A more challenging task is the inclusion of the effects of molecular reorientation with increasing deformation on the isotropy and on the time-dependent behavior of the polymer; this will be the

subject of future work.

APPENDIX A

# The finite element modelling of a thermorheologically simple material

## A.1 Introduction

The following is a brief description of how a nonlinearly viscoelastic model of material behavior can be implemented into a finite element code. The code used was FEAP (Finite Element Analysis Program), originally developed at UC Berkeley and later expanded at Brown University. The relevant feature of the code is its extreme flexibility, stemming from the computation of the different variables at the element level. The code was originally capable of nonlinear elastic/plastic analyses; the nonlinear viscoelastic model was implemented as explained in the following pages. Since the following description is necessarily brief, the reader is referred to specialized textbooks for more detailed explanations of the algorithm. In particular, the notation used by Zienkiewicz (1977) will be used, since a first version of the program is included in his book. Also, it has to be noticed that this model is strictly a small deformation analysis; no distinction between current and reference configuration is ever made and, furthermore, only two parameters (bulk and shear moduli) are used to describe the material response.

## A.2 Finite element theory

The theory of finite elements states that, for a single element, the following equation must hold

$$\int_{V_e} [B]^T \{\sigma\} dV + \{f\} = \{0\} \ , \tag{A.2.1}$$

where $[B]$ is the matrix relating the strains to the nodal displacements, *i.e.*,

$$\{\epsilon\} = [B]\{U\} \ , \tag{A.2.2}$$

where $\{U\}$ is the vector of nodal displacements. The vectors $\{\sigma\}$ ,$\{\epsilon\}$ and $\{f\}$ are defined according to the convention adopted in reference 1 as

$$\{\epsilon\} = \begin{pmatrix} \epsilon_{xx} \\ \epsilon_{yy} \\ \epsilon_{zz} \\ \gamma_{xy} \\ \gamma_{yz} \\ \gamma_{zx} \end{pmatrix} \qquad \{\sigma\} = \begin{pmatrix} \sigma_{xx} \\ \sigma_{yy} \\ \sigma_{zz} \\ \sigma_{xy} \\ \sigma_{yz} \\ \sigma_{zx} \end{pmatrix} \qquad \{f\} = \int_{V_e} [N]^T \{b\} dV \ , \tag{A.2.3}$$

where $[N]$ is the matrix relating the displacements in the interior of the element to those at the nodes (*i.e.*, the matrix of shape functions) and $\{b\}$ is the body force vector field

$$\{u\} = \begin{pmatrix} u_x \\ u_y \\ u_z \end{pmatrix} = [N]\{U\} \qquad \{b\} = \begin{pmatrix} b_x \\ b_y \\ b_z \end{pmatrix} \ . \tag{A.2.4}$$

Equation A.2.1 is derived from virtual work principles, so it is valid for any class of material behavior. In the case of a linearly elastic solid, the stress and strain vectors are related through a material dependent matrix $[D]$, such that

$$\{\sigma\} = [D]\{\epsilon\} \ . \tag{A.2.5}$$

Eq. A.2.1 with Eq. A.2.5 leads to the linear equation

$$[K]\{U\} + \{f\} = \{0\} \ , \tag{A.2.6}$$

where $[K]$ is the stiffness matrix, defined as

$$[K] = \int_{V_e} [B]^T [D][B] dV \quad . \tag{A.2.7}$$

In the case of a thermorheologically simple material, the stress has a functional dependence on the strain history that can be schematically represented as

$$\{\sigma(t)\} = \Phi_{\xi=0}^{\xi=\xi(t)} [\{\epsilon(\xi)\}, \xi] \quad , \tag{A.2.8}$$

where $\xi$, a parameter of the strain history, is called the *internal time* of the material, defined as

$$\xi(t) = \int_0^t \frac{dt'}{a(t')} \quad , \tag{A.2.9}$$

$a(t)$ being the shift factor at time $t$. In general, $a(t)$ depends on several factors, including dilatation, solvent concentration and temperature. For such a material the equilibrium equation for the finite element reads

$$\int_{V_e} [B]^T \Phi_{\xi=0}^{\xi=\xi(t)} [\{\epsilon(\xi)\}, \xi] dV + \{f(t)\} = \{0\} \quad . \tag{A.2.10}$$

## A.3 Constitutive model

In the case of small deformations of an isotropic solid, the mechanical response can be completely described through two material functions, namely the shear modulus $G(t)$ and the bulk modulus $K(t)$. The time dependent behavior of these two quantities can be characterized by a Prony-Dirichlet series of the form

$$G(t) = G_\infty + \sum_{k=1}^{M} G_i exp(\frac{-t}{\lambda_k}) \tag{A.3.1}$$

$$K(t) = K_\infty + \sum_{k=1}^{N} K_i exp(\frac{-t}{\gamma_k}) \quad . \tag{A.3.2}$$

A typical functional relation between stresses and strains is written as

$$\sigma_{xx}(t) = \int_0^{\xi(t)} [\frac{4}{3}G(\xi - \xi') + K(\xi - \xi')]\frac{\partial \epsilon_{xx}(\xi')}{\partial \xi'} d\xi' +$$

$$+\frac{1}{3}\int_0^{\xi=\xi(t)} [3K(\xi - \xi') - 2G(\xi - \xi')][\frac{\partial \epsilon_{xx}(\xi')}{\partial \xi'} + \frac{\partial \epsilon_{xx}(\xi')}{\partial \xi'}]d\xi' \qquad \text{(A.3.3)}$$

and similarly for the other components of the stress tensor.

A concise representation of the functional relation A.2.8 can be written in the form

$$\{\sigma(t)\} = [\Psi]\{\epsilon(s)\} \quad , \qquad \text{(A.3.4)}$$

where $[\Psi]$ is a convolution operator, defined as

$$[\Psi] = \begin{pmatrix} A_1* & A_2* & A_2* & 0 & 0 & 0 \\ A_2* & A_1* & A_2* & 0 & 0 & 0 \\ A_2* & A_2* & A_1* & 0 & 0 & 0 \\ 0 & 0 & 0 & A_3* & 0 & 0 \\ 0 & 0 & 0 & 0 & A_3* & 0 \\ 0 & 0 & 0 & 0 & 0 & A_3* \end{pmatrix} \quad , \qquad \text{(A.3.5)}$$

in which

$$A_1* = \int_0^{\xi(t)} [\frac{4}{3}G(\xi - \xi') + K(\xi - \xi')]\frac{\partial}{\partial \xi'} d\xi'$$

$$A_2* = \int_0^{\xi(t)} \frac{1}{3}[3K(\xi - \xi') - 2G(\xi - \xi')]\frac{\partial}{\partial \xi'} d\xi'$$

$$A_3* = \int_0^{\xi(t)} G(\xi - \xi')\frac{\partial}{\partial \xi'} d\xi' \quad . \qquad \text{(A.3.6)}$$

Denoting the generic element of $[\Psi]$ as $\Psi_{ij} * (\bullet)$, the $*$ denoting the convolution on the argument $(\bullet)$, Eq. A.2.10 can now be rewritten, in component form, as

$$\int_{V_e} B_{ki}\Psi_{kl} * (B_{lj}U_i(\xi))dV + f_i = 0 \quad . \qquad \text{(A.3.7)}$$

The operator $[\Psi]$ is linear in internal time, *i.e.*, all the nonlinearities collapse onto Eq. A.2.9, expressing the relation between internal and experimental time. Furthermore, the matrix $[B]$ is determined once and for all, in the hypothesis of small deformations, by the shape functions chosen for the finite element. That implies that $[B]$ does not have any time dependence and that it can be pulled out of the convolution integral. Thus, Eq. A.3.7 can be rewritten as

$$\int_{V_e} B_{ki} B_{lj} \Psi_{kl} * (U_j(\xi)) dV + f_i = 0 \ . \tag{A.3.8}$$

Note also that $[\Psi]$ remains within the integrand of the volume integral since it is a function of the local internal time, which ultimately depends on the local histories of dilatation, solvent concentration and so on.

The volume integral of Eq. A.3.8 can be evaluated using numerical integration at a certain number of quadrature points, *i.e.*,

$$\int_{V_e} B_{ki} B_{lj} \Psi_{kl} * (U_i(\xi)) dV = \sum_{q=1}^{Q} w_q B_{ki} B_{lj} \Psi_{kl} * (U_i(\xi)) \ , \tag{A.3.9}$$

where the $w_q's$ are the integration weights at the Q quadrature points. At each quadrature point a convolution needs to be performed, which fact greatly increases the computation time.

## A.4 Time integration

The time dependence of Eq. A.3.8 involves convolutions in internal time on the nodal displacements and the time dependent components of the functional $[\Psi]$. To achieve a numerical solution, one needs to discretize the time domain, and consequently the internal time, since the two are related by Eq. A.2.9. Consider therefore a set of instants in time $t_0, t_1, t_2, .....t_N$, with $t_i < t_j$ for $i < j$. Assume that the values of the nodal displacements, dilatation, etc., are known up to $t = t_{\tau-1}$. The values of the internal time $\xi_0, \xi_1, \xi_2, ..., \xi_{\tau-1}$ are therefore also known, since the two sets are related through Eq. A.2.9, and the values of the shift factor are obtainable, when all the relevant quantities are known. One would like to find the nodal displacements after the next time step, *i.e.*, $U_j(t_\tau) = U_j(\xi_\tau)$. Since an iterative search of the solution is required, let it be assumed initially that the value of the internal time $\xi(t_\tau) = \xi_\tau$ is known, and, to simplify the notation, denote by $U_j(\rho)$ the values $U_j(\xi_\rho)$, with $\rho = 0, ...., \tau.$; also denote by $\Psi_{ij}$ (without the $*$) the kernel appearing in the operator $\Psi_{ij}*$, *i.e.*,

$$\Psi_{11}(\xi) = \frac{4}{3}\, G(\xi) + K(\xi) \tag{A.4.1}$$

and similarly for the other components. This kernel will admit, from the representation for the bulk and shear moduli, a Prony series expansion, *i.e.*,

$$\Psi_{ij}(\xi) = \sum_{p=0}^{M+N} \Psi_{ij}^{(p)} exp(\frac{-\xi}{\lambda_p}) \ , \tag{A.4.2}$$

where $\lambda_0$ can be chosen to be infinitely large in order to retain a constant term in the summation to represent the possible asymptotic behavior. With these premises, Eq. A.3.8 can now be rewritten as

$$\int_{V_e} B_{ki} B_{lj} \int_0^{\xi=\xi(t)} \sum_{p=0}^{M+N} \Psi_{kl}^{(p)} exp(\frac{-(\xi(t)-\xi')}{\lambda_p}) \frac{\partial U_j(\xi')}{\partial \xi'} d\xi' dV + f_i = 0 \ . \tag{A.4.3}$$

By using Eq. A.3.9 and subdividing the convolution integral in $\tau$ subintervals going from $\xi_\rho$ to $\xi_{\rho+1}$, one can then write

$$\sum_{q=1}^{Q} w_q B_{ki} B_{lj} \sum_{\rho=0}^{\tau-1} \sum_{p=0}^{M+N} \Psi_{kl}^{(p)} \int_{\xi_\rho}^{\xi_{\rho+1}} exp(\frac{-(\xi_\tau - \xi')}{\lambda_p}) \frac{\partial U_j(\xi')}{\partial \xi'} d\xi' + f_i = 0 \ , \qquad (A.4.4)$$

where $\xi_\tau = \xi(t)$. If one approximates the displacement history during any time step with a linear law, *i.e.*,

$$\frac{\partial U_j(\xi')}{\partial \xi'} = \text{constant} = U_j'(\rho) = \frac{U_j(t_{\rho+1}) - U_j(t_\rho)}{\xi(t_{\rho+1}) - \xi(t_\rho)} =$$

$$= \frac{U_{\rho+1}^j - U_\rho^j}{\xi_{\rho+1} - \xi_\rho} \qquad (A.4.5)$$

on the interval $(\xi_\rho, \xi_{\rho+1})$, then the above integral can be performed exactly in internal time $\xi'$, yielding

$$\sum_{q=1}^{Q} w_q B_{ki} B_{lj} \sum_{\rho=0}^{\tau-1} \sum_{p=0}^{M+N} \Psi_{kl}^{(p)} \lambda_p \frac{U_{\rho+1}^j - U_\rho^j}{\xi_{\rho+1} - \xi_\rho} \cdot$$

$$\cdot [exp(\frac{-(\xi_\tau - \xi_{\rho+1})}{\lambda_p}) - exp(\frac{-(\xi_\tau - \xi_\rho)}{\lambda_p})] + f_i = 0 \ . \qquad (A.4.6)$$

If one isolates the term containing the unknowns, *i.e.*, the vector of displacements $U_\tau^j$, then the above is rewritten as

$$\sum_{q=1}^{Q} w_q B_{ki} B_{lj} \sum_{p=0}^{M+N} \Psi_{kl}^{(p)} \lambda_p \frac{U_\tau^j - U_{\tau-1}^j}{\xi_\tau - \xi_{\tau-1}} [1. - exp(\frac{-(\xi_\tau - \xi_{\tau-1})}{\lambda_p})] =$$

$$= -f_i - \sum_{q=1}^{Q} w_q B_{ki} B_{lj} \sum_{\rho=0}^{\tau-2} \sum_{p=0}^{M+N} \Psi_{kl}^{(p)} \lambda_p \frac{U_{\rho+1}^j - U_\rho^j}{\xi_{\rho+1} - \xi_\rho} \cdot$$

$$\cdot [exp(\frac{-(\xi_\tau - \xi_{\rho+1})}{\lambda_p}) - exp(\frac{-(\xi_\tau - \xi_\rho)}{\lambda_p})] \ . \qquad (A.4.7)$$

The equilibrium equation can be concisely rewritten in the form

$$[K]\Delta\{U\} = -f_i - f_i^* \ , \qquad (A.4.8)$$

where $\Delta\{U\}$ is the current displacement increment,

$$[K] = \sum_{q=1}^{Q} w_q B_{ki} B_{lj} \sum_{p=0}^{M+N} \Psi_{kl}^{(p)} \lambda_p \frac{1}{\xi_\tau - \xi_{\tau-1}} [1. - exp(\frac{-(\xi_\tau - \xi_{\tau-1})}{\lambda_p})] \qquad (A.4.9)$$

is the "incremental" stiffness matrix, $f_i$ is the usual body force vector and $f_i^*$ is the additional nodal load vector arising from the effect of the previous history on the viscoelastic behavior of the material

$$f_i^* = \sum_{q=1}^{Q} w_q B_{ki} B_{lj} \sum_{\rho=0}^{\tau-2} \sum_{p=0}^{M+N} \Psi_{kl}^{(p)} \lambda_p \frac{U_{\rho+1}^j - U_\rho^j}{\xi_{\rho+1} - \xi_\rho} \cdot$$

$$\cdot [exp(\frac{-(\xi_\tau - \xi_{\rho+1})}{\lambda_p}) - exp(\frac{-(\xi_\tau - \xi_\rho)}{\lambda_p})] \ . \qquad (A.4.10)$$

Consider now the contribution of one quadrature point and a single Prony element of the constitutive operator to the load vector

$$f_{i,pq}^*(\tau) = B_{ki} B_{lj} \sum_{\rho=0}^{\tau-2} \Psi_{kl}^{(p)} \lambda_p \frac{U_{\rho+1}^j - U_\rho^j}{\xi_{\rho+1} - \xi_\rho} \cdot$$

$$\cdot [exp(\frac{-(\xi_\tau - \xi_{\rho+1})}{\lambda_p}) - exp(\frac{-(\xi_\tau - \xi_\rho)}{\lambda_p})] \ . \qquad (A.4.11)$$

Notice that there are two variations in the above expression from one time step to the next, *i.e.*,

- the number of terms in the summation;
- the value of the internal time, $\xi_\tau$ (which appears in both exponentials contained in each member of the summation).

Eventually, one can prove that

$$f_{i,pq}^*(\tau + 1) = f_{i,pq}^*(\tau) * exp(-\frac{\xi_\tau - \xi_{\tau-1}}{\lambda_p}) +$$

$$+ B_{ki} B_{lj} \Psi_{kl}^{(p)} \lambda_p \frac{U_\tau^j - U_{\tau-1}^j}{\xi_\tau - \xi_{\tau-1}} [1.0 - exp(\frac{-(\xi_\tau - \xi_{\tau-1})}{\lambda_p})] \ . \qquad (A.4.12)$$

Therefore, it is only necessary to save each component $f_{i,pq}$, one for each Prony element and for each quadrature point, instead of the whole displacement history, thus greatly improving the efficiency of the algorithm.

The above holds if the current internal time at each quadrature point is known, which is not true in general since the same depends also on the current values of the strains, temperature and possibly solvent concentration. In particular, the nonlinearly viscoelastic model presented in this work assumes that the free volume changes are, above the glass transition, a constant fraction of the volumetric changes, which are computed from the current nodal displacements, which in turn depend on the current and past free volume content through a Doolittle-type dependence. At each time step, iteration of the solution is therefore necessary until convergence is achieved.

APPENDIX B

# Numerical conversion of viscoelastic functions

## B.1 Preface

Viscoelastic functions represent the time-dependent response of a polymeric material to a change in applied stress or deformation. Such functions, like the shear creep compliance or the corresponding relaxation modulus, often exhibit time-dependent behavior over several decades of time, with the initial and asymptotic response that can differ in orders of magnitude. The computation of the modulus from creep data or vice versa has been investigated in the past, mainly because of its ill-posedness and high vulnerability to problems of numerical stability and convergence. One of the most cited works on this subject in the context of viscoelasticity is the study by Hopkins and Hamming (1957), who defined an algorithm that still is among the most accurate ones for the handling of the stability issues.

As an example, consider the case of the shear modulus and corresponding compliance. According to the linear theory of viscoelasticity, the shear stress and the shear strain in a viscoelastic solid are related through the convolution integral

$$\tau_{xy}(t) = \int_{0-}^{t} \mu(t-\eta) 2 \frac{\partial \epsilon_{xy}(\eta)}{\partial \eta} d\eta \quad , \tag{B.1.1}$$

where $\mu(t)$ is the time dependent shear modulus of the material. Conversely, one can write an equation for the dependence of the strain on the stress history, namely

$$2\epsilon_{xy}(t) = \int_{0-}^{t} J(t-\eta) \frac{\partial \tau_{xy}(\eta)}{\partial \eta} d\eta \quad , \tag{B.1.2}$$

$J(t)$ being the time-dependent shear compliance.

The two functions $J(t)$ and $\mu(t)$ cannot therefore be independent but are related through a convolution equation. If one takes the Laplace transform of Eq. B.1.2 and B.1.1, with zero initial conditions one obtains

$$2\bar{\epsilon}_{xy}(s) = s\bar{J}(s)\bar{\tau}_{xy}(s) \tag{B.1.3}$$

$$\bar{\tau}_{xy}(s) = 2s\bar{\mu}(s)\bar{\epsilon}_{xy}(s) \ , \tag{B.1.4}$$

where $\bar{\epsilon}_{xy}(s)$, $\bar{\tau}_{xy}(s)$, $\bar{\mu}(s)$ and $\bar{J}(s)$ are the Laplace transforms of the shear strain, shear stress, shear modulus and shear compliance. The two equations combined yield

$$s\bar{\tau}_{xy}(s)\bar{\epsilon}_{xy}(s) = 1 \ , \tag{B.1.5}$$

which, upon application of the inverse Laplace transformation, can be written as

$$\int_0^t J(t-\eta)\mu(\eta)d\eta = t \ , \tag{B.1.6a}$$

or, equivalently,

$$\int_0^t \mu(t-\eta)J(\eta)d\eta = t \ . \tag{B.1.6b}$$

Eq. B.1.6 shows that, aside from stability issues of the numerical inversion procedure, it is possible to find the inverse of a viscoelastic function.

## B.2 The Hopkins-Hamming algorithm

The integral of Eq. B.1.6 is performed by discretizing the interval $(0,t)$ into subintervals $t_i, t_{i+1}$, with $i = 0, 1, ....n$. Furthermore, since $J(t)$ or $\mu(t)$ can be the input function, it is better to write the integral in a more general form, *i.e.*,

$$\int_0^t \phi(t-\eta)\psi(\eta)d\eta = t \quad , \tag{B.2.1}$$

where the function $\psi(t)$ is assumed to be known at the points $t_0, t_1, ...t_n$, and $\phi(t)$ is the function that has to be generated. The function $\psi$ can be either a modulus or a compliance depending on the available experimental data; the dual nature of Eq. B.1.6a and B.1.6b allows the application of the forthcoming algorithm to both cases.

If one denotes by $f(t)$ the quantity

$$f(t) = \int_0^t \psi(\eta)d\eta \tag{B.2.2}$$

and discretizes the integral of B.2.1 in the form

$$t_{n+1} = \int_0^{t_{n+1}} \phi(\eta)\psi(t_{n+1}-\eta)d\eta =$$

$$= \sum_{i=0}^{n} \int_{t_i}^{t_{i+1}} \phi(\eta)\psi(t_{n+1}-\eta)d\eta \quad , \tag{B.2.3}$$

then all the individual integrals in the summation can be approximated by

$$\int_{t_i}^{t_{i+1}} \phi(\eta)\psi(t_{n+1}-\eta)d\eta = \phi(t_{i+1/2}) \int_{t_i}^{t_{i+1}} f\prime(t_{n+1}-\eta)d\eta =$$

$$= -\phi(t_{i+1/2})[f(t_{n+1}-t_{i+1}) - f(t_{n+1}-t_i)] \quad , \tag{B.2.4}$$

where $t_{i+1/2}$ is the average $\frac{1}{2}(t_i + t_{i+1})$. Solving for $\phi(t_{n+1/2})$, one obtains

$$\phi(t_{n+1/2}) = \frac{t_{n+1} - \sum_{i=0}^{n-1} \phi(t_{i+1/2})[f(t_{n+1}-t_i) - f(t_{n+1}-t_{i+1})]}{f(t_{n+1}-t_n)} \quad , \tag{B.2.5}$$

where

$$\phi_{1/2} = \frac{t_1}{f(t_1)} \quad , \tag{B.2.6}$$

under the provision that such ratio is defined, which occurs whenever $\psi(0)$ is nonzero. The difference $f(t_{n+1} - t_i) - f(t_{n+1} - t_{i+1})$ can be written as

$$f(t_{n+1} - t_i) - f(t_{n+1} - t_{i+1}) = \int_{t_{n+1}-t_{i+1}}^{t_{n+1}-t_i} \psi(\eta) d\eta \quad . \tag{B.2.7}$$

If the points $t_i$ are generally distributed, one or both of the values $(t_{n+1} - t_{i+1})$ or $(t_{n+1} - t_i)$ may be less than or equal to $t_0$, the first point at which $\psi(t)$ is known from experimental data. Therefore, it is necessary to interpolate the function $\psi(t)$ between $t = 0$ and $t = t_0$. Two different choices seem reasonable: to define the value of $\psi(t)$ at $t = 0$ to be equal to the value $\psi(t_0)$, or to compute $\psi(0)$ using a linear interpolation of the function between $t_0$ and $t_1$, *i.e.*,

$$\psi(0) = \psi(t_0) - \frac{t_0}{t_1 - t_0} \frac{\psi(t_1) - \psi(t_0)}{t_1 - t_0} \quad . \tag{B.2.8}$$

The linear interpolation approach was found to be very sensitive to numerical noise in the inversion procedure. If the cycle of inversion is repeated several times †, linear interpolation tends to create a divergence of the numerical solution from the correct‡ one near time $t = 0$. The choice $\psi(0) = \psi(t_0)$ gives a better stability than the linear interpolation approach.

Another problem one has to confront for the inversion of viscoelastic functions is the presence of an experimental error. This is particularly true when one has to compute a compliance from experimental data for the modulus; for a viscoelastic

---

† *i.e.*, computing the compliance from the modulus, recomputing the modulus from the inverted compliance and repeating this procedure starting with the newly computed modulus.

‡ At time $t = 0$ there is a correct solution, which can be computed from $\phi(0) \frac{\partial \psi}{\partial t}_{t=0} = 1$.

material, the long time shear modulus is considerably smaller than the initial response, sometimes differing by a few orders of magnitude. Therefore, even a very small absolute error in the determination of the long time behavior of the modulus can be a large percent error, the presence of which is then reflected in the curve for the compliance obtained through the numerical inversion. To overcome this problem, it was found useful to smooth the experimental data before performing the numerical inversion. This smoothing was achieved by running a five-point window through the set of experimental points, using a least-square method to adapt a third degree polynomial to the values of these points, and computing, from the interpolating function, a new value for the midpoint. The process can be repeated a few times, and also the degree of the polynomial can be lowered, to increase the damping of the irregularities where the curve has a low grade of smoothness. The curve so obtained can be indistiguishable from the experimental one within plotting accuracy, but the outcome of the inversion procedure can be notably improved.

## B.3 Conversion of viscoelastic functions

The behavior of an isotropic viscoelastic solid can be described in different ways using different choices for the pair of material parameters that are needed. One can use Young's modulus and shear modulus, bulk and shear, or Poisson's ratio with either bulk or Young's modulus. Obviously, the material parameters cannot be independent and are related through integral equations that are the viscoelastic analogs of the linearly elastic laws. A typical example is the relation that gives Young's modulus $E(t)$ in terms of bulk and shear moduli, $K(t)$ and $\mu(t)$, which, in one of its forms, reads

$$\int_0^t E(t-\tau)[3K(\tau)+\mu(\tau)]d\tau = \int_0^t 9K(t-\tau)\frac{d\mu(\tau)}{d\tau}d\tau \quad . \tag{B.3.1}$$

The above expression can be cast in other equivalent forms, all of them resulting from the manipulation of the relation that connects the Laplace transforms of the moduli, *i.e.*,

$$E(s)[3K(s) + \mu(s)] = 9K(s)\mu(s)s \quad . \tag{B.3.2}$$

It has to be noted that Eq. B.3.1 is formally equivalent to the convolution equation that relates a modulus to the corresponding compliance, with the only difference that the known function inside the integral is a combination of other viscoelastic moduli, and that the known side of the equation is itself a convolution in time of bulk and shear moduli. The Hopkins-Hamming algorithm, with very few modifications, can therefore be used to compute the time-dependent Young's modulus. The largest change in the numerical procedure is the replacement of the vector of $t_i$'s with the values of the bulk-shear convolution, which needs to be computed at several instants in time.

## B.4 Application to experimental data

McKinney and Belcher (1963) experimentally determined the complex bulk compliance of PVAc under sinusoidal excitation. From those data, the bulk modulus can be extracted using a numerical procedure. If one denotes by $M(t)$ the bulk compliance, $M'(\omega)$ the storage compliance, *i.e.*, the compliance in phase with the load under sinusoidal excitation, and by $M_g$ the glassy (short term) compliance, then the two quantities $M(t)$ and $M'(\omega)$ are related through the following expression*

$$M(t) = M_g + \frac{2}{\pi}\int_0^\infty \frac{M' - M_g}{\omega} sin(\omega t) d\omega \quad . \tag{B.4.1}$$

---

* *cfr.* Ferry, "Viscoelastic Properties of Polymers", Third Edition, p. 70.

The inversion task can be performed quite easily if one expresses the storage compliance in form of a Prony series in $\omega$-space, *i.e.*,

$$M'(\omega) = M_g + \sum_i^N M_i exp(\frac{-\omega}{\omega_i}) \ , \tag{B.4.2}$$

which can be easily done using an algorithm developed by Emri (1985). The above integral can then be solved in close form for each contributing exponential.

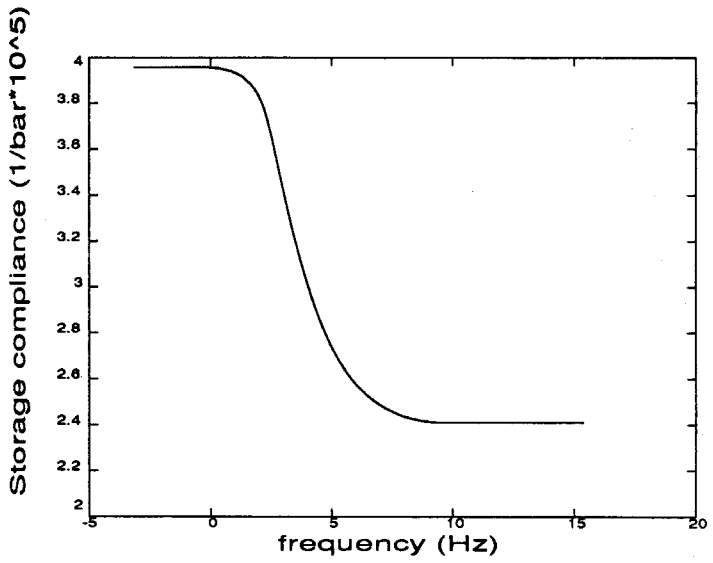


FIGURE B.1 Experimental bulk storage compliance ($\text{bar}^{-1} \times 10^5$) referenced to 50 C (McKinney and Belcher, 1963).

The experimental bulk storage compliance is shown in Fig. B.1, with the frequency scale referenced to a temperature of 50 C. The storage compliance was approximated in terms of a Prony series, and from there the bulk compliance was obtained. This compliance, shown in Fig. B.2, was then inverted, and the result of the inversion is shown in Fig. B.3. The time scale of the bulk modulus is now referenced to 40 C, using time-temperature shift data by Heymans, found by experimental measurements of the shear compliance, shown in Fig. B.4. The inverted shear modulus is also shown in Fig. B.5.

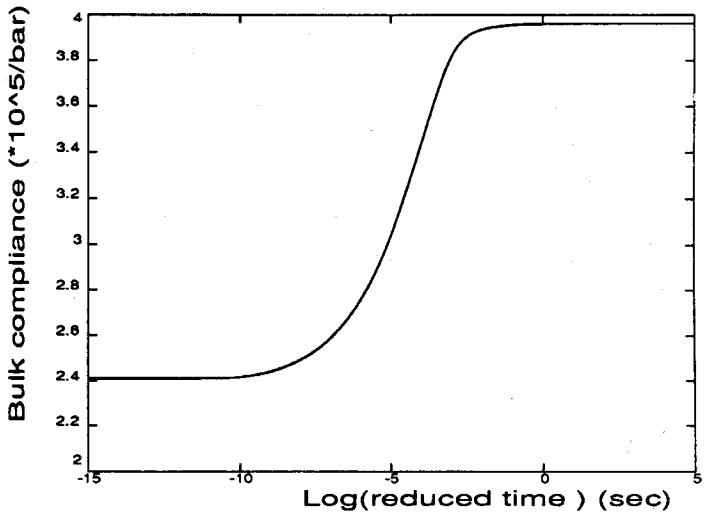


FIGURE B.2 Computed bulk compliance ($\text{bar}^{-1} \times 10^5$) referenced to 40 C upon time shifting based on experimental data by Heymans (1983).

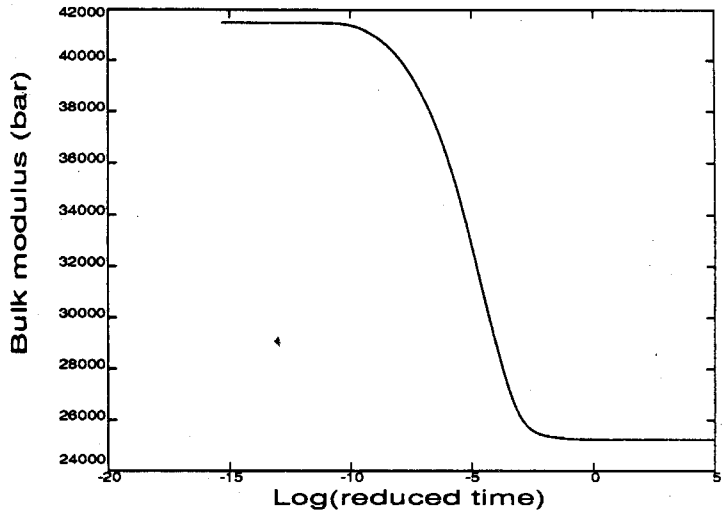


FIGURE B.3 Inverted bulk modulus (bar) referenced to 40 C.

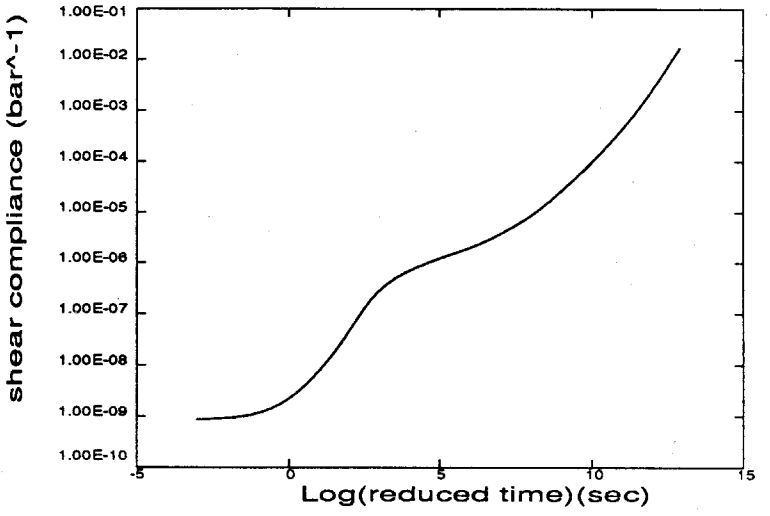


FIGURE B.4 Experimental shear compliance ($bar^{-1}$) at 40 C (Heymans, 1983).

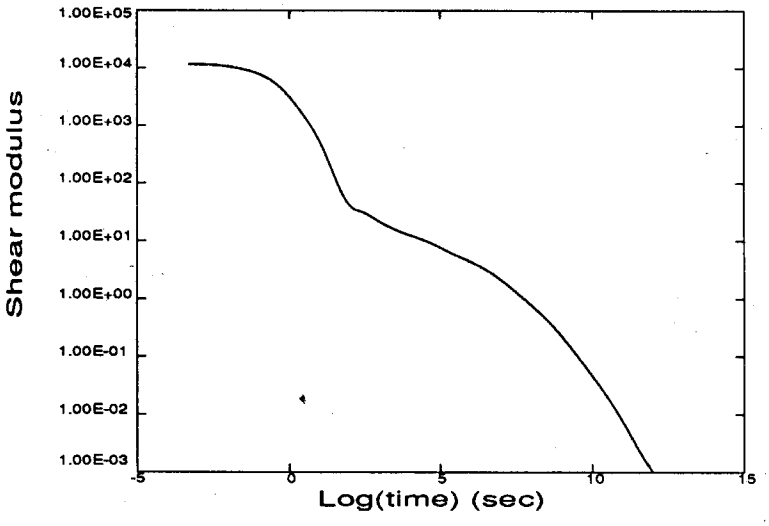


FIGURE B.5 Inverted shear modulus (bar) referenced to 40 C.

APPENDIX C

# Stochastic Integration

A brief, and therefore incomplete, introduction to stochastic integration will be presented in this appendix; for a more detailed exposure, the reader can refer to specialized textbooks, such as Gardiner's (1985).

A continuous Markov process is a process influenced by one or more stochastic (random) variables, with the following features:

- the conditional probability that a process is in a certain state $S$ at time $t$, given that the same process was in states $S_1, S_2, S_3, .....S_N$ at instants $t_1, t_2, ....., t_N$, where $t \geq t_1 \geq t_2 \geq ..... \geq t_N$, depends only on the most recent state $S_1$, *i.e.*, the process has no memory beyond the most recent event. If one denotes such conditional probability as $p(S,t|(S_1,t_1),(S_2,t_2),...,(S_N,t_N))$, then one has

$$p(S,t|(S_1,t_1),(S_2,t_2),...,(S_N,t_N)) = p(S,t|S_1,t_1) \ ; \qquad \text{(C.1)}$$

- if $p(S,t+\Delta t|Z,t)$ is the conditional probability that the process is in the state $S$ at time $t+\Delta t$, given the fact that the same process was in state $Z$ at time $t$ ($\Delta t > 0$), then for every $\epsilon > 0$,

$$\lim_{\Delta t \to 0} \frac{1}{\Delta t} \int_{|S-Z|>\epsilon} p(S,t+\Delta t|Z,t) dS \ = \ 0 \ . \qquad \text{(C.2)}$$

Thus, the probability of the process being in a state $S$ different from $Z$ at time $t + \Delta t$ tends to zero *faster* than $\Delta t$, as $\Delta t \to 0$.

Under appropriate conditions, a continuous Markov process can be described by a differential equation known as the Fokker-Planck equation. These conditions require the finiteness of the expected increment and variance of the stochastic process. If one restricts attention to processes that can be described by one single variable, *e.g.*, $x$, these conditions read

$$\lim_{\Delta t \to 0} \frac{1}{\Delta t} \int_{|x-z|<\epsilon} (x - z)\, p(x, t + \Delta t | z, t)\, dx \;=\; A(z,t) + O(\epsilon) \qquad \text{(C.3)}$$

and

$$\lim_{\Delta t \to 0} \frac{1}{\Delta t} \int_{|x-z|<\epsilon} (x - z)^2\, p(x, t + \Delta t | z, t)\, dx \;=\; B(z,t) + O(\epsilon) \;, \qquad \text{(C.4)}$$

where $A(z,t)$ and $B(z,t)$ are finite functions of position and time. If the above conditions are met, then the Markov process can be described by a differential equation, known as the forward Fokker-Planck equation, which describes the changes in the probability distribution $p(x,t)$, *i.e.*, the function giving the probability of the process being in the state $x$ at time $t$. Such an equation, for a process characterized by a single variable, can be written as

$$\frac{\partial p(x,t)}{\partial t} \;=\; -\frac{\partial A(x,t)p(x,t)}{\partial x} + \frac{\partial^2 B(x,t)p(x,t)}{\partial t^2} \;. \qquad \text{(C.5)}$$

The proof of such a connection is omitted here; any specialized textbook can be consulted for the demonstration of Eq. C.5.

A particular kind of random process is stochastic white noise, of which the variations have a null expected value and variance proportional to time, *i.e.*,

$$E(d\underline{b}) \;=\; 0 \;, \qquad \text{(C.6)}$$

and

$$E([d\underline{b}]^2) \;=\; dt \;\;, \tag{C.7}$$

where $E(\underline{x})$ is used to denote the expected value of the random variable $\underline{x}$. The following stochastic integral will now be considered

$$H \;=\; \int_{t=\alpha}^{t=\beta} g(\underline{b}(t))d\underline{b}(t) \;\;. \tag{C.8}$$

This integral is different from the known Riemann and Lebesgue integrals in the fact that the integration variable, $\underline{b}(t)$, is continuous but does not have a continuous derivative anywhere. There are two interpretations to this stochastic integral, and they are known as the Stratonovich ($S$) and the Itô ($I$) interpretations. They are given as follows:

$$I \;=\; \int g(\underline{b}(t))d\underline{b}(t) \;=\; \lim_{\Delta t\to 0}\sum_{\nu=0}^{\nu=N} g(\underline{b}(t_\nu)) \;\;, \tag{C.9}$$

and

$$S \;=\; \int g(\underline{b}(t))d\underline{b}(t) \;=\; \lim_{\Delta t\to 0}\sum_{\nu=0}^{\nu=N} \frac{1}{2}[g(\underline{b}(t_\nu)+g(\underline{b}(t_{\nu+1})]\Big[\underline{b}(t_{\nu+1})-\underline{b}(t_\nu)\Big] \;\;, \tag{C.10}$$

where

$$\Delta t \;=\; \max_{\nu=1,2,\ldots.} (t_{\nu+1}-t_\nu) \;\;, \tag{C.11}$$

and

$$t_0 \;=\alpha \quad t_N \;=\; \beta \;\;. \tag{C.12}$$

One can reduce these stochastic integrals to standard integrals. $G(t)$ will here denote the indefinite integral of $g(t)$, *i.e.*,

$$G(t) \;=\; \int g(t)dt \;\;. \tag{C.13}$$

A (nontrivial) theorem of stochastic analysis proves that the Stratonovich and Itô integrals can be rewritten in terms of nonrandom, classical variables as

$$I = \int g(\underline{b}(t))d\underline{b}(t) = [G(\underline{b}(t_\beta)) - G(\underline{b}(t_\alpha))] - \frac{1}{2}\int_\alpha^\beta g'(\underline{b}(t))dt \ , \qquad \text{(C.14)}$$

and

$$S = \int g(\underline{b}(t))d\underline{b}(t) = G(\underline{b}(t_\beta)) - G(\underline{b}(t_\alpha)) \ , \qquad \text{(C.15)}$$

where $g'(t)$ is the derivative of the function $g(t)$. The lengthy proof of this theorem will be omitted here.

Attention is next devoted to the differences of these two kinds of integrals on the integration of stochastic differential equations. Consider a stochastic differential equation of the form

$$dx = A(x,t)dt + B(x,t)d\underline{b}(t) \ . \qquad \text{(C.16)}$$

The stochastic differential equation C.16 can be transformed into an ordinary differential equation by evaluating its expected value, *i.e.*, by considering $E(\Delta x)$. The two interpretations of the stochastic equation, due to Itô and Stratonovich, attribute different features to the random process $x(t)$. The Itô interpretation assumes that $dx(t)$ and $d\underline{b}(t)$ are independent; in this case the random process is denoted as nonanticipating. The Stratonovich integral states instead that the increments $dx(t)$ and $d\underline{b}(t)$ are dependent (anticipating process). In order to see that, one should consider the Stratonovich differential intepretation of the stochastic equation, which can be written as

$$dx = A(x,t)dt + \frac{1}{2}[B(x+dx,t+dt) + B(x,t)]d\underline{b}(t) \ . \qquad \text{(C.17)}$$

Expanding $B(x)$ in a Taylor series, assuming $B(x+dx,t+dt|x,t) = B(x+dx,t|x,t) + o(dt)$ and neglecting all second or larger powers of $dT$, one has

$$dx \simeq A(x,t)dt + [B(x,t) + \frac{1}{2}\frac{dB(x,t)}{dx}dx]d\underline{b}(t) \ . \qquad \text{(C.18)}$$

Collecting the terms multiplying $dx$, one obtains

$$dx = \frac{A(x,t)dt + B(x,t)d\underline{b}(t)}{1 - \frac{1}{2}\frac{dB(x,t)}{dx}d\underline{b}(t)} \quad . \tag{C.19}$$

If one expands the denominator in a geometric series for small values of the quantity $\frac{1}{2}\frac{dB(x,t)}{dx}d\underline{b}(t)$, one can write

$$dx = \left[A(x,t)dt + B(x,t)d\underline{b}(t)\right]\left[1 - \frac{1}{2}\frac{dB(x,t)}{dx}d\underline{b}(t) + o(d\underline{b})\right] \approx$$

$$\approx \left[A(x,t)dt + B(x,t)d\underline{b}(t)\right]\left[1 - \frac{1}{2}\frac{dB(x,t)}{dx}d\underline{b}(t)\right] \quad . \tag{C.20}$$

Furthermore, if one takes the expected value of Eq. C.20, recalling that $E(d\underline{b}(t)) = 0$, $E(d\underline{b}(t))^2 = \Delta t$, and discarding terms of higher order in $\Delta t$, one obtains

$$E(\Delta x) = A(x,t)\Delta t + B(x,t)E(\Delta\underline{b}(t)) + \frac{1}{2}B(xt)\frac{dB(x,t)}{dx}E(d\underline{b}(t))^2 =$$

$$= \left[A(x,t) + \frac{1}{2}B(x,t)\frac{dB(x,t)}{dx}\right]\Delta t \quad . \tag{C.21}$$

Analogously, the Itô interpretation of the stochastic equation yields

$$E(\Delta x) = A(x,t)\Delta t \quad . \tag{C.22}$$

Eq. C.21 and C.22 represent two ordinary differential equations in the variable $x$, which can be solved by standard methods.

The application of the theory of stochastic integration to the time-dependent free volume changes will now be shown in reference to the case when the parameter $A$, representing the amplitude of the random thermal vibrations, is pressure or temperature dependent. Recall the governing equation for the free volume changes, written as

$$df_i = \frac{1}{\tau_i}(f_{i,\infty} - f_i)e^{-B(1/f - 1/f_0)}dt + \sqrt{\frac{A}{\tau_i}}f_i d\underline{b} \quad . \tag{C.23}$$

If one takes the expected value of this expression according to the Stratonovich integration rule, in the case when the parameter $A$ is a constant, one obtains (*cf.* sect. 1.1.3)

$$E(\Delta f_i) = \left[\frac{1}{\tau_i}(f_{i,\infty} - f_i)e^{-B(1/f-1/f_0)} + \frac{A}{2\tau_i}f_i\right]\Delta t \,. \qquad \text{(C.24)}$$

Conversely, if one assumes an effect of temperature and pressure on $A$, *i.e.*, $A = A(p,T)$, then one also has to differentiate $A$ with respect to $f$, *i.e.*,

$$\frac{dA}{df} = \frac{\partial A}{\partial T}\frac{\partial T}{\partial f} + \frac{\partial A}{\partial p}\frac{\partial p}{\partial f} \,, \qquad \text{(C.25)}$$

where the derivative represents the effect which the free volume *fluctuations* have on the value of $A$. In sect. 1.1.3 such an effect was assumed to be null, *i.e.*, $\frac{dA}{df} = 0$; if one relaxes that restriction, Eq. C.24 becomes

$$E(\Delta f_i) = \left[\frac{1}{\tau_i}(f_{i,\infty} - f_i)e^{-B(1/f-1/f_0)} + \frac{A}{2\tau_i}f_i + \frac{f_i^2}{4\tau_i}\left(\frac{\partial A}{\partial T}\frac{\partial T}{\partial f} + \frac{\partial A}{\partial p}\frac{\partial p}{\partial f}\right)\right]\Delta t \,. \qquad \text{(C.26)}$$

For a material with time-dependent properties, the values of $\frac{\partial T}{\partial f}$ and $\frac{\partial p}{\partial f}$ need to be expressed in terms of rate equations involving the appropriate material parameters. If one ignores all time dependence associated with such derivatives and takes their instantaneous values, then

$$\frac{\partial T}{\partial f} = \frac{1}{\frac{\partial f}{\partial T}} = \frac{1}{\frac{\partial f}{\partial \hat{p}}\frac{\partial \hat{p}}{\partial T}} = \frac{K_0}{\delta \cdot K_\infty \alpha_l} \,, \qquad \text{(C.27)}$$

where $K_0 = K_\infty + \sum_i K_i$ is the instantaneous ($t = 0^+$) value of the bulk modulus, and

$$\frac{\partial p}{\partial f} = \frac{\partial p}{\partial \epsilon_{kk}}\frac{\partial \epsilon_{kk}}{\partial f} = \frac{K_0}{\delta} \,. \qquad \text{(C.28)}$$

$K_\infty$ represents the asymptotic value of the bulk modulus in the rubbery state, $\delta$ is the ratio $\Delta V_{free}/\Delta V_{total}$ and $\alpha_l$ is the rubbery coefficient of thermal expansion. Eq. C.26 then reads

$$E(\Delta f_i) = \left[\frac{1}{\tau_i}(f_{i,\infty} - f_i)e^{-B(1/f-1/f_0)} + \frac{A}{2\tau_i}f_i +\right.$$

$$+\frac{f_i^2}{4\tau_i}\Big(\frac{K_0}{\delta K_\infty \alpha_l}\frac{\partial A}{\partial T}+\frac{K_0}{\delta}\frac{\partial A}{\partial p}\Big)\Big]\Delta t\,. \qquad \text{(C.29)}$$

# References

**Adam, G., Gibbs, J. H., (1965)**, "On the Temperature Dependence of Cooperative Relaxation Properties in Glass-Forming Liquids," *Journal of Chemical Physics*, Vol. 43, 1, pp. 139-146.

**Christensen, R. M., Naghdi, P.M., (1967)**, " Linear Non-isothermal Viscoelastic Solids," *Acta Mechanica*, Vol. I, pp. 1-12.

**Cizmecioglu, M., Fedors, R. F., Hong, S. D., Moacanin, J., (1981)**, "Effect of Physical Aging on Stress Relaxation of Poly(methyl Methacrylate)," *Polymer Engineering and Science*, Vol. 21, No. 14, pp. 940-942.

**Cohen, M. H., Grest, G. S., (1979)**, "Liquid-glass Transition, a Free-volume Approach," *Physical Review B*, Vol. 20, 3, pp. 1077-1098.

**Cohen, M. H., Turnbull, D., (1959)**, "Molecular Transport in Liquids and Glasses," *Journal of Chemical Physics*, Vol. 31, pp.1164-1169.

**Coleman, B. D., (1964)**, "Thermodynamics of Materials with Memory," *Archive for Rational Mechanics and Analysis*, Vol. 17, pp. 1-46.

**Curro, J. G., Lagasse, R. R., Simha, R., (1981)**, "Use of a Theoretical Equation of State to Interpret Time-dependent Free Volume in Polymer Glasses," *Journal of Applied Physics*, Vol. 52, No. 10, pp. 5892-5897.

**Davies, R. O., Jones, G. O., (1953)**, "The Irreversible Approach to Equilibrium in Glasses," *Proceedings of the Royal Society of London*, Vol. 217A, pp.

26-42.

**Day, W. A., (1972)**, "*The Thermodynamics of Simple Materials with Fading Memory*," Springer-Verlag.

**Day, W. A., (1985)**, "*Heat Conduction within Linear Thermoelasticity*," Springer-Verlag.

**Di Marzio, E. A., Gibbs, J. H., (1958)**, "Chain Stiffness and the Lattice Theory of Polymer Phases," *Journal of Chemical Physics*, Vol. 28, 5, pp. 807-813.

**Domb, C., Green, M. S., Eds., (1972)**, "Phase Transitions and Critical Phenomena," Vol. II, Academic Press.

**Doolittle, A. K., (1951)**, "Studies in Newtonian Flow. I. The Dependence of the Viscosity of Liquids on Temperature," *Journal of Applied Physics*, Vol.22, 8, pp. 1031-1035.

**Doolittle, A. K., (1951)**, "Studies in Newtonian Flow. II. The Dependence of the Viscosity of Liquids on Free-Space," *Journal of Applied Physics*, Vol.22, 12, pp. 1471-1475.

**Emri, I., Knauss, W. G., (1985)**, "Analytical Description of the Relaxation Functions by Prony-Dirichlet Series," GALCIT SM Report 85-31, California Institute of Technology.

**Eyring, H., Hirschfelder, J., (1937)**, "The Theory of the Liquid State," *Journal of Physical Chemistry*, Vol. 41, pp. 249-257.

**Ferry, J. D., Stratton, R.A., (1960)**, "The Free Volume Interpretation of the Dependence of Viscosities and Viscoelastic Relaxation Times on Concentration, Pressure and Tensile Strain," *Kolloid-Zeitschrift*, Vol. 171, pp. 107-111.

**Fox, T. G., Flory, P. J., (1950)**, "Second-Order Transition Temperatures and Related Properties of Polystyrene. I. Influence of Molecular Weight," *Journal of Applied Physics*, Vol. 21, pp. 581-591.

**Gardiner, C. W., (1985)** , "*Handbook of Stochastic Methods*," (Second Ed.), Springer-Verlag.

**Gibbs, J. H., DiMarzio, E. A., (1958)**, "Nature of the Glass Transition and the Glassy State," *Journal of Chemical Physics*, Vol. 28, 3, pp. 373-383.

**Grest, G. S., Cohen, M. H., (1981)**, " Liquids, Glasses and the Glass Transition: a Free-volume Approach," *Advances in Chemical Physics*, Vol. 48, pp. 455-525.

**Heymans, L., (1983)**, "An Engineering Analysis of Polymer Film Adhesion to Rigid Substrates," Ph.D. Thesis, California Institute of Technology.

**Hopkins, I. L., Hamming, R. W., (1957)**, "On Creep and Relaxation," *Journal of Applied Physics*, Vol. 28, No. 8, pp. 906-909.

**Hutchinson, J. M., Aklonis, J. J., Kovacs, A.J., (1975)**, " A New Phenomenological Approach to Volume Recovery in Glasses," *Polymer Preprints*, Vol. 16, 2, pp. 94-99.

**Hutchinson, J. M., Kovacs, A. J., (1976)**, " A Simple Phenomenological Approach to the Thermal Behavior of Glasses During Uniform Heating or Cooling," *Journal of Polymer Science*, Polymer Physics Edition, Vol.14, pp. 1575-1590.

**Knauss, W. G., Emri, I. J., (1981)**, " Non-linear Viscoelasticity Based on Free Volume Considerations," *Journal of Computers and Structures*, Vol. 13, pp. 123-128.

**Kovacs, A. J., (1958)**, "La Contraction Isotherme du Volume des Polyméres Amorphes," *Journal of Polymer Science*, Vol. 30, pp. 131-147.

**Kovacs, A.J., (1963)**, "Transition Vitrense dans les polyméres Amorphes," *Fortschr. Hochpolym.- Forsch.*, Bd. 3, pp. 394-507.

**Leaderman, H., (1943)**, "Elastic and Creep Properties of Filamentous Materials and Other High Polymers," The Textile Foundation, Washington.

**Matheson, R. R., (1987)**, " Significance of Entropic Factors in Mechanical Deformation of Polymeric Glasses," *Macromolecules*, Vol. 20, pp. 1847-1851.

**Matheson, R. R., (1987)**, " Measurements of Entropic Factors in the Mechanical Deformation of Polycarbonate and Natural Rubber ," *Macromolecules*, Vol. 20, pp. 1851-1855.

**Matheson, R. R., (1987)**, "Analysis of Some Equations of State in Relation to Microscopic Interpretation of Mechanically Significant Entropy for Polymeric Glasses and Melts," *Journal of Physical Chemistry*, Vol. 91, pp. 6062-6066.

**McKinney, J. E., Goldstein, M., (1974)**, "PVT Relationships for Liquid and Glassy Poly(vinyl acetate)," *Journal of Research of the National Bureau of Standards*, Vol. 78A, pp. 331-353.

**McKinney, J. E., Belcher, H. V., (1963)**, "Dynamic Compressibility of Poly(vinyl acetate)and Its Relation to Free Volume," *Journal of Research of the National Bureau of Standards*, Vol. 67 A, pp. 43-53.

**McKinney, J. E., Simha, R., (1974)**, "Configurational Thermodynamic Properties of Polymer Liquids and Glasses. Poly(vinyl acetate). I.," *Macromolecules*, Vol. 7, 6, pp. 894-901.

**McKinney, J. E., Simha, R., (1976)**, "Configurational Thermodynamic Properties of Polymer Liquids and Glasses. Poly(vinyl acetate). II.," *Macromolecules*, Vol. 9, 3, pp. 430-441.

**Morland, L. W., Lee, E. H., (1960)**, "Stress Analysis for Linearly Viscoelastic Materials with Temperature Variations," *Transactions of the Society of Rheology*, Vol. 4, pp. 233-263.

**Moynihan, C.T., Easteal, A. J., Wilder, J., (1974)**, "Dependence of the Glass Transition Temperature on Heating and Cooling Rate," *Journal of Physical Chemistry*, Vol. 78, 26, pp. 2673-2677.

**Muki, R., Sternberg, E., (1961)**, "On Transient Thermal Stresses in Viscoelastic Materials with Temperature Dependent Properties," *Journal of Applied Mechanics*, Vol. 28, pp. 193-207.

**Nanda, V. S., Simha, R., (1964)**, "Equation of State of Polymer Liquids and Glasses at Elevated Pressures," *Journal of Chemical Physics*, Vol. 41, 12, pp. 3870-3878.

**Oden, J.T., Armstrong, W.H., (1971)**, "Analysis of Nonlinear, Dynamic Coupled Thermoviscoelasticity Problems by the Finite Element Method," *Computer and Structures*, Vol. 1, pp.603-621.

**Peng, S. T. J., Landel, R. F., Moacanin, J., Simha, R., Papazoglou, E., (1987)**, "Cell Model and Elastic Moduli of Disordered Solids: Low Temperature Limit," *Journal of Rheology*, Vol. 31, No. 2, pp. 125-133.

**Richtmeyer, R. D., Morton, W., (1967)**, "*Difference Methods for Initial Value Problems*," 2nd. Edn., Wiley-Interscience.

**Rusch, K. C., (1968)**, "Time-Temperature Superposition and Relaxational Behavior of Polymeric Glasses," *Journal of Macromolecular Science-Physics*, Vol. B2(2), pp. 179-204.

**Sandberg, O.B., Andersson, P., Bäckström, G., (1977)**, " Heat Capacity and Thermal Conductivity from Pulsed Wire Probe Measurements under Pressure," *Journal of Physics E*, Scientific Instruments, Vol. 10, pp.474-477.

**Sandberg, O., Bäckström, G., (1980)**, " Thermal Conductivity and Heat Capacity of Liquid and Glassy Poly(vinyl acetate) under pressure," *Journal of Polymer Science*, Polymer Physics Edition, Vol. 18, pp. 2123-2133.

**Sharonov, Y. U., Vol'kenshtein, M. V., (1964)**, "Calorimetric Investigation of Softening and Annealing of Polymer Glasses," in *'The Structure of Glasses,'* Vol. 6, Consultants Bureau, New York, N.Y., pp. 62-66.

**Shay, R. M., Caruthers, J. M., (1986)**, " A New Nonlinear Viscoelastic Constitutive Equation for Predicting Yield in Amorphous Solid Polymers," *Journal of the Society of Rheology*, Vol. 30, pp. 781-827.

**Simha, R., Somcynsky, T., (1969)**, "On the Statistical Thermodynamics of Spherical and Chain Molecule Fluids," *Macromolecules*, Vol.2, 4, pp. 342-350.

**Struik, L. C. E., (1978)**, "Physical Aging in Amorphous Polymers and Other Materials," Elsevier Scientific Publishing Company.

**Taylor, R. L., Pister, K. L., Goudreau, G. L., (1970)**, "Thermomechanical Analysis of Viscoelastic Solids," *International Journal for Numerical Methods in Engineering*, Vol. 2, pp. 45-59.

**Tobolsky, A. V., Eyring, H., (1943)**, "Mechanical Properties of Polymeric Materials," *Journal of Chemical Physics*, Vol. 11, pp.125-134.

**Turnbull, D., Cohen, M. H., (1961)**, "Free Volume Model of the Amorphous Phase: Glass Transition," *Journal of Chemical Physics*, Vol. 34, pp. 120-125.

**Turnbull, D., Cohen, M. H.,(1970)**, "On The Free Volume Model of the Glass Transition," *Journal of Chemical Physics*, Vol.52, pp. 3038-3041.

**Williams, M. L., Landel, R. F., Ferry, J. D., (1955)**, "The Temperature Dependence of Relaxation Mechanisms in Amorphous Polymers and Other Glass-forming Liquids," *Journal of the American Chemical Society*, Vol. 77, pp. 3701-?.

**Wood, L. W., Lewis, R. W., (1975)**, "A Comparison of Time Marching Schemes for the Transient Heat Conduction Equation," *International Journal for Numerical Methods in Engineering*, Vol. 9, pp. 679-689.

**Zienkiewicz, O.C., (1977)** , "*The Finite Element Method*," (Third Ed.), McGraw Hill.

CHAPTER 2

# Failure of adhesive bonds

## 2.1 Introduction

The failure of structural materials is generally a consequence of the phenomenon of plastic deformation. When plastic flow is spread over a region of very small size compared to the rest of the solid, and generation and growth of discontinuities in the material are effected, one tends to address the problem in terms of the theory of fracture and crack propagation. The constitutive behavior of the material plays a predominant role in these phenomena and, particularly in the case of polymers, the interaction between the continuum breakdown and the plastic-like deformation is one of the main factors governing the acceleration or deceleration of the failure process. Polymeric solids are affected by temperature and rate-dependent properties, often varying over a time scale of several orders of magnitude, which effect a strong dependence of the rate of fracture or crack propagation on the applied load history and its interaction with the viscoelastic response of the material.

The work presented here tries to focus attention on the phenomenon of steady crack propagation in viscoelastic materials, such as polymers with time-dependent properties. The propagation of a planar discontinuity in a polymeric solid is usually addressed in the context of two different designations, namely crack propagation and/or craze growth. A craze differs from a crack through the presence of a residual

material connectivity joining the two parts of the material on opposite sides of the discontinuity, while, in the case of a crack, the separation of the solid is complete (traction-free crack surfaces). In addition to the morphological differences, the roles played by these two phenomena also differ: when a crack propagates, the growing discontinuity ultimately leads to the failure of the structural member, whereas when multiple generation of randomly arranged crazes, occurs (a phenomenon which is denoted as "crazing"), there is an alleviation of the local stress levels and conversion of mechanical energy into plastic work, which ultimately leads to a "tougher" material behavior. Also, cracks propagating in polymers very often have craze-like cohesive zones in front of them, which illustrates again the similarity and inseparability of these two kinds of failure phenomena.

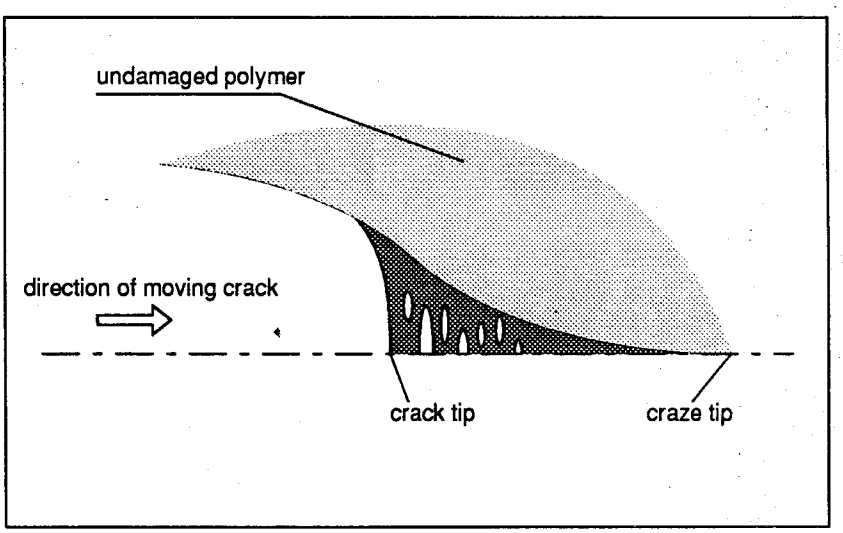


FIGURE 2.1 Schematic representation of a crack, preceded by a craze-like cohesive zone, propagating in a polymer.

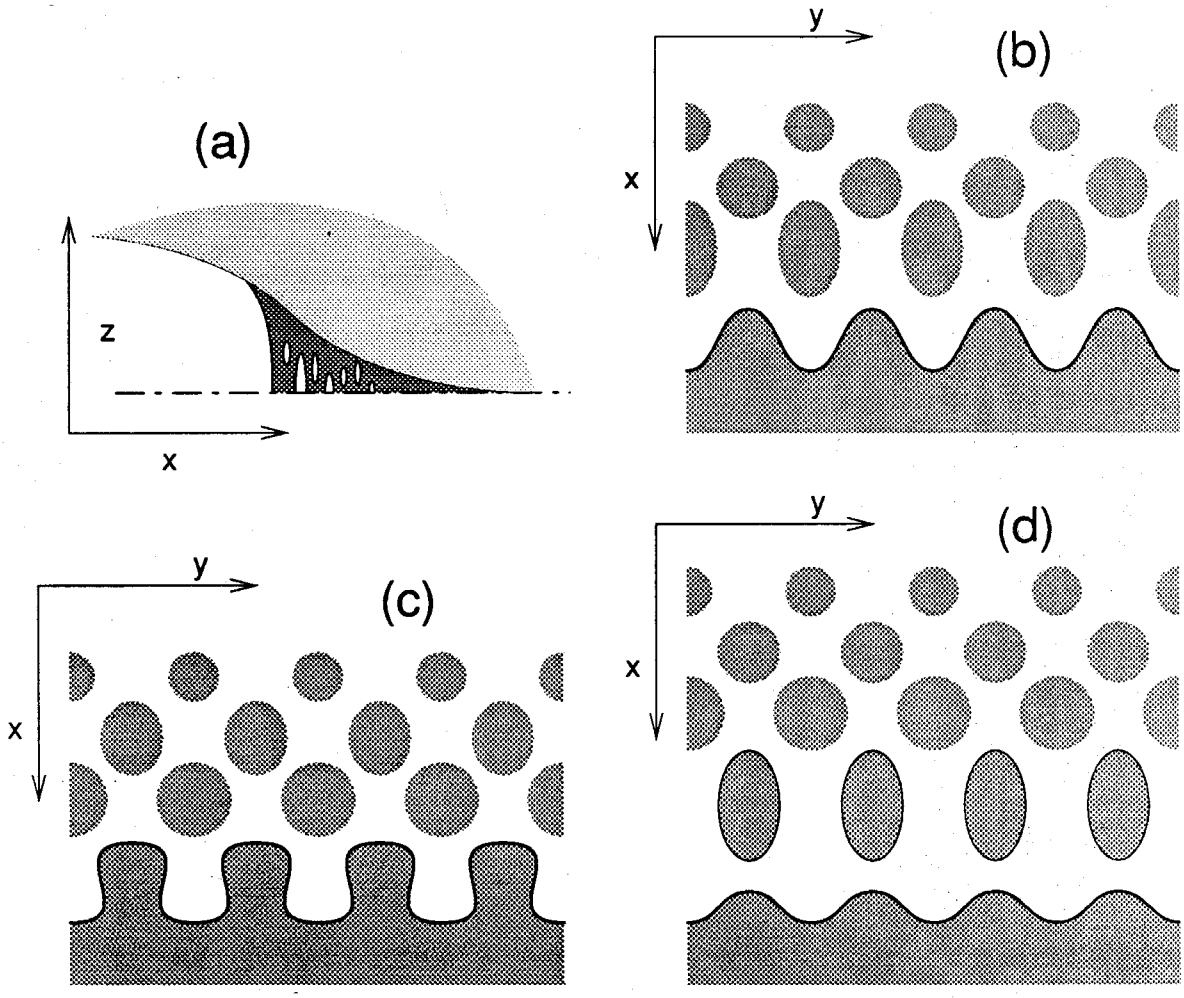


FIGURE 2.2 Schematization of the Taylor instability at the craze front. (a) craze geometry; (b) top view of the craze front; (c) instability of the craze front shown growing; (d) new fibrils created.

When a polymer fails by fracture, the departure of the material behavior from a linear continuum description is often approximated as taking place only in a narrow strip in front of the crack tip. This approximation, questionable in the case of metal plasticity * where the nonlinear material behavior governs over a spread zone around

* except in sheet geometries where plastic strain localization occurs.

the tip, is often appropriate in the case of polymeric materials, as is shown by the morphological features of crazes. A craze is a region in which the polymer departs from being a continuous solid and finds it energetically "more convenient" to break down into elongated chunks by which the polymer flows parallel to the direction of maximum tensile stress. The aspect ratio of the thin region in which this occurs, measured in terms of length over maximum thickness, can achieve values of several hundreds (Lauterwasser and Kramer, 1979). In this small volume, voids develop and elongate perpendicularly to the crack plane, forming characteristic features called fibrils, which connect the crack faces just ahead of the tip. These fibrils dissipate energy, absorb plastic work and are responsible for the toughness of polymers in fracture.

It has been suggested (Argon and Salama, 1977) that the onset of failure in the craze zone is the consequence of an instability similar to the Taylor meniscus instability, in which the wavefront of the damage zone develops a series of protruding "fingers". This situation is depicted in Fig. 2.2b, where a cross section of the craze front in the craze plane is shown; Figs. 2.2c and 2.2d show the elongation and successive separation of these fingers as isolated chunks of polymer. Experimental investigations relying on transmission electron microscopy (Lauterwasser and Kramer, 1979) show that there are two principal mechanisms of fibril elongation, *i.e.,* fibril creep and drawing of virgin polymeric material from the craze faces. Under the particular conditions examined when the latter mechanism was found to be predominant, the strains achieved in the fibrils were measured to be of the order of several hundred per cent. These observations cast serious doubts on the effectiveness of linear constitutive theories for the description of the material behavior in the craze volume, since these theories rely on small strain assumptions. A nonlinear theory of viscoelastic behavior, as the one used in this work, seems therefore to hold

more promise for the analysis of the mechanical response of polymers at the tip of a crack and for the prediction of its influence on the rate of crack propagation.

It is conceivable that the morphology of the material at the crack tip strictly resembles that typical of a craze. In fact, past studies on the subject have often assumed the presence of a thin cohesive zone at the crack tip, a zone which governs the propagation of the crack in response to the applied loads. Investigating the mechanics of cracks in elastic bodies, Barenblatt (1962) and Dugdale (1960) were able to relate the amplitude of the far-field loading to the value of the uniformly distributed stresses in the cohesive zone. Similarly, the model of Verheulpen-Heymans and Bauwens (1976) assumes a time-independent stress distribution featuring two neighboring intervals of constant cohesive stress, of which the one carrying the larger loads was closer to the crack tip. An attempt to include a constitutive model based on molecular concepts for the degradation of the material is contained in the work by Goodier and Kanninen (1966), which evaluated the cohesive forces using nonlinear atomic separation laws. A common denominator of these studies is the absence of time-dependence in the failure process, which was first introduced by Williams (1963), by assuming a model of discontinuous crack growth governed by a finite strain criterion, and by Mueller and Knauss (1971), who took into account the effect of the viscoelastically unloading tractions at the crack tip in the discrete jump propagation. Later, Knauss (1974) developed a model of continuous crack growth in which the time-dependent behavior of the material surrounding the failure zone could be taken into account, but the distribution of loads in the decohesion zone was still considered to be time-independent.

The study presented here has the objective of studying the consequences of a rate-dependent nonlinear viscoelastic behavior in the propagation of a crack in a

polymer, assuming the existence of a craze-like cohesive zone in front of the crack tip. The topology of deformation is assumed to be similar to that presented in Fig. 2.2. The volume of polymer entering the cohesive zone is confined to within a thin strip in front of the propagating crack. Two softening mechanisms, namely void growth and free-volume induced softening, are considered to be affecting the nonlinearly viscoelastic behavior of the polymer in the failure zone. The undamaged material surrounding the propagating crack will be characterized by a linear (possibly viscoelastic) response.

This investigation can also be easily related to the failure of adhesive bonds, where the decohesion in the polymeric adhesive is responsible for the separation of generally much stiffer adherends (*cfr.* Fig. 2.3); this alternate view is possible since the effects of the nonlinear material behavior in the failure zone and the linear response of the surrounding volume are taken into account separately, allowing the study of cases where the two sets of constitutive properties are completely different. The adhesion problem will be considered in this work, with the additional advantage of the related terminology creating a clear distinction between the material which becomes part of the failure zone (adhesive) and the surrounding, undamaged solid (adherends). The beginning of the cohesive zone will be designated as "craze tip" and the end of it as "crack tip" (see Fig. 2.1).

The method of solution follows the approach presented by Knauss (1974) in which the time-dependent compliance of the polymer surrounding the propagating crack is taken into account by using a complex potential solution and a time convolution to compute the crack opening displacement. The dependence of the far-field loading parameter, the stress intensity factor at failure, on the values of crack speed is inferred from the imposition of a bounded strain at the craze tip. The onset

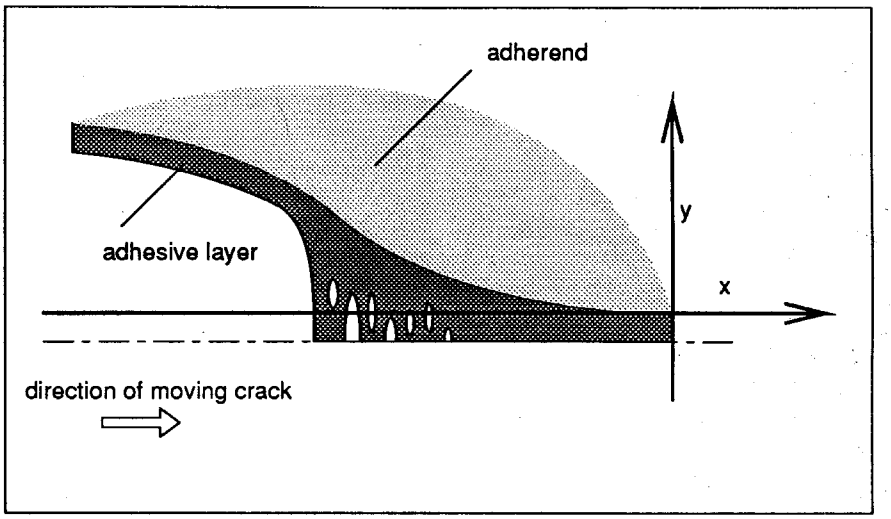


FIGURE 2.3 Schematic representation of a crack propagating through an adhesive layer.

of void growth depends on a critical value of strain, $\epsilon_{crit}$, measured at the craze tip and normal to the plane of propagation; the void growth itself is considered to be time-independent and affected by local strain values only. The length of the cohesive zone and the initial cohesive stress are also part of the solution, which is presented for two values of the critical strain $\epsilon_{crit}$, namely .3 and 1 per cent.

## 2.2 Schematization of the problem

The mathematical formulation of the problem, shown schematically in Fig. 2.1, considers the adhesive layer (or, in the case of a crack propagating in a polymer, the strip of material which enters the cohesive zone) as a thin layer, having a small thickness compared to the other length scale, *e.g.*, the extent of the cohesive zone. The problem can then be separated into two parts, namely the linear deformation of the adherends due to the effect of the cohesive stresses and the nonlinear mechanical response of the adhesive layer to the opening of the crack faces and the consequent straining.

The first part of the problem can be reduced to that of a linearly elastic or viscoelastic half-space, representing one of the adherends, on which mixed boundary conditions are specified in terms of tractions $T(x)$ and displacements $v(x)$ on the undeformed configuration, *i.e.*, on the straight line delimiting the half-space. The original problem is shown in Fig. 2.3 and its schematization in Fig. 2.4.

In front of the craze tip, the crack-normal displacement of the adherends is taken to be null. The tractions due to the nonlinear adhesive act on the crack faces between the craze and crack tips while the crack faces are load-free behind the crack tip.

The second part of the problem, sketched in Fig. 2.5, concerns the constitutive response of the adhesive in reaction to a given strain history. Since the crack is considered to be propagating at constant speed in the adhesive, a reference system moving with the crack is appropriate. In such a reference system, centered at the onset of void growth (craze tip), the strip material passes into nonlinear material behavior at the position $x = 0$ on the crack axis; ahead of this point it obeys a

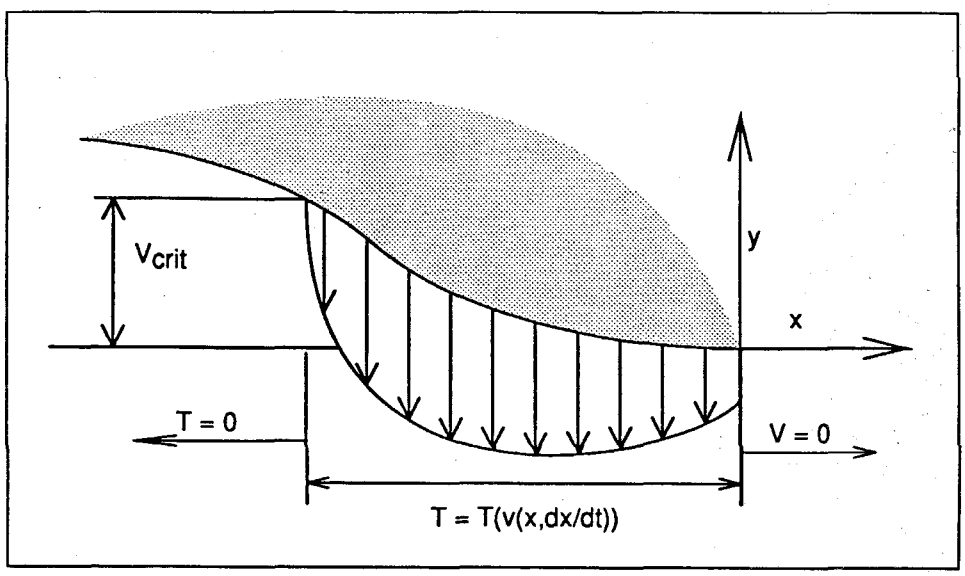


FIGURE 2.4 Schematization of the linear problem for the adherend deformation.

linearly viscoelastic law. The cohesive zone, the presence of which allows to satisfy the finiteness condition at the crack tip (Barenblatt, 1962), is characterized by the nonlinear constitutive response of the adhesive.

## 2.3 The constitutive response of the adhesive

The two relevant features affecting the material behavior in the failure zone are the generation and growth of voids, plus the effects of the high strains on the viscoelastic behavior of the undamaged material; both of these aspects need to be taken into consideration. These two features are not independent of each other, since nonlinearly viscoelastic theories of polymeric behavior (Knauss and Emri, 1981; Shay and Caruthers, 1986) show that the mechanical history affects

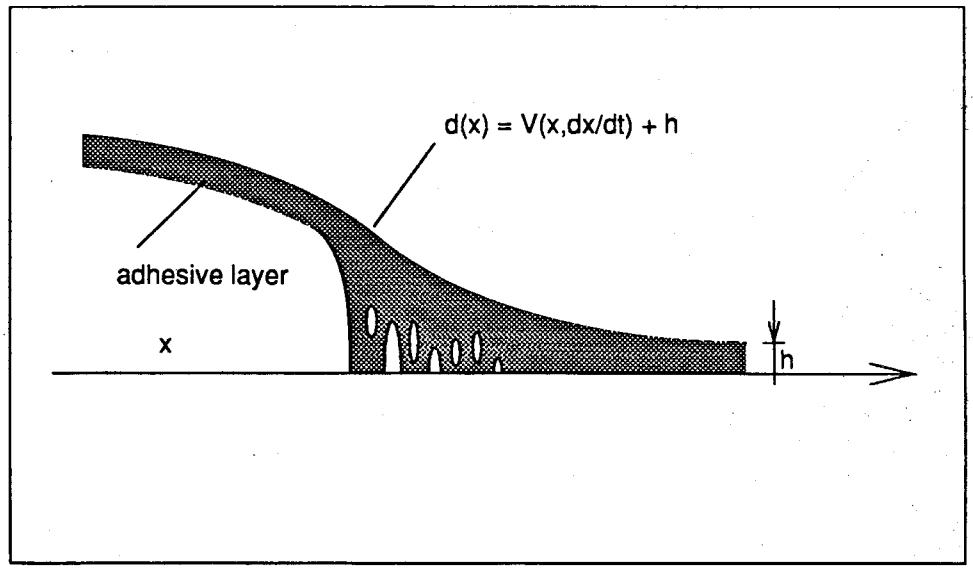


FIGURE 2.5 Nonlinear viscoelastic behavior of the adhesive layer in response to the displacement $V = V(x, \dot{c})$ of the adherends (the half-thickness of the adhesive in the undeformed configuration is denoted by h).

the relaxation behavior through a dilatation-induced time shift. The capability of the polymer to flow consequently affects the phenomenon of void growth at the tip of the failure zone. Since a consistent theory of large strain viscoelastic behavior, including the induced anisotropy in the material response due to large molecule orientation, is still in the making, one has to make simplifications in the mechanical problem. For approximation purposes, it will be assumed here that void growth and free volume induced softening of the polymer are two independent phenomena; the first one will be assumed to depend on the current strain level only and not on the past history or on other parameters such as the current free volume, while the second one, the nonlinear viscoelastic behavior of the undamaged material, will be taken to depend only on the strain history but be independent of the volume of the

voids in the failure zone. Consequently, the cumulative damage due to these two factors can be assumed to be additive, *i.e.,* the effective reduction in stress levels is taken to be that due to free-volume induced softening, times a factor that takes into account the volume of voids currently present in the material and which depends solely on the current value of the strain.

An experimental attempt to investigate the degradation of the material response due to void growth was carried out in our laboratories by M. Parvin (Knauss and Parvin, 1989), using an interferometric technique to infer the stresses in an adhesive layer sandwiched between two stiff adherends which are pulled apart. One of the quantities that is difficult to determine in these experiments is the local thickness of the adhesive layer, which in turn determines the local strains from the local displacements. It was therefore decided to allow for a scaling of the effect of void growth, relying on a parametric curve fitted to Parvin's data, the parameter being the maximum value of the strain at failure, $\epsilon_{max}$. In the presented computations, the value of $\epsilon_{max}$ was set to six percent.

The free-volume induced softening is taken into account by formulating the cohesive response of the adhesive in terms of the nonlinear theory of viscoelasticity of Knauss and Emri (1981). In this description, the time dependence of the rheological response in the viscoelastic adhesive is modified through a time-multiplying factor $a_t$, which depends on the value of mechanical dilatation through the Doolittle equation

$$Log(a_t) = \frac{B}{2.303}\left(\frac{1}{f} - \frac{1}{f_0}\right) , \tag{2.3.1}$$

where $f$ is the fractional free volume and $f_0$ is the free volume at reference conditions. The time shift factor modifies the experimental time scale to produce an internal time scale for the polymer, which is the one ultimately governing the vis-

coelastic response. In the presence of mechanical dilatation, one assumes that such dilatation contributes to an increase in free volume according to

$$f = f_0 + \delta\, \epsilon_{kk} \tag{2.3.2}$$

$\epsilon_{kk}$ being the dilatational strain and $\delta$ the ratio between free volume and total volume changes, which ranges between 0 and 1. For the model case considered, values of .015 for $f_0$ and .997 for $B$ were used. The value of $\delta$ was set to unity. The reason for this choice of parameters is that they affect the non-linear viscoelastic behavior of the material moduli, shown in Figs. 2.6 and 2.7, giving rise to softening behavior, as shown in Fig. 2.8, where the predicted tensile stress for a uniaxial tension test is shown for the linear and nonlinear viscoelastic theory.

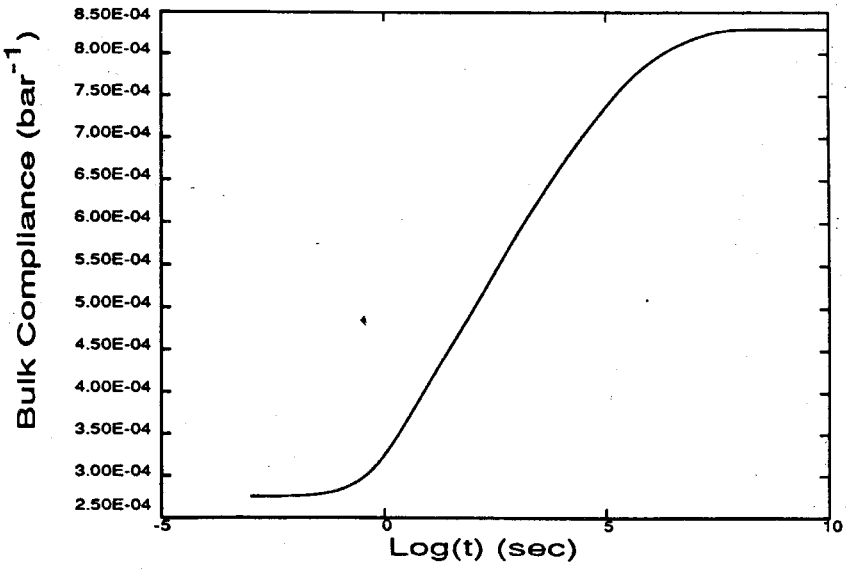


FIGURE 2.6 Bulk Compliance

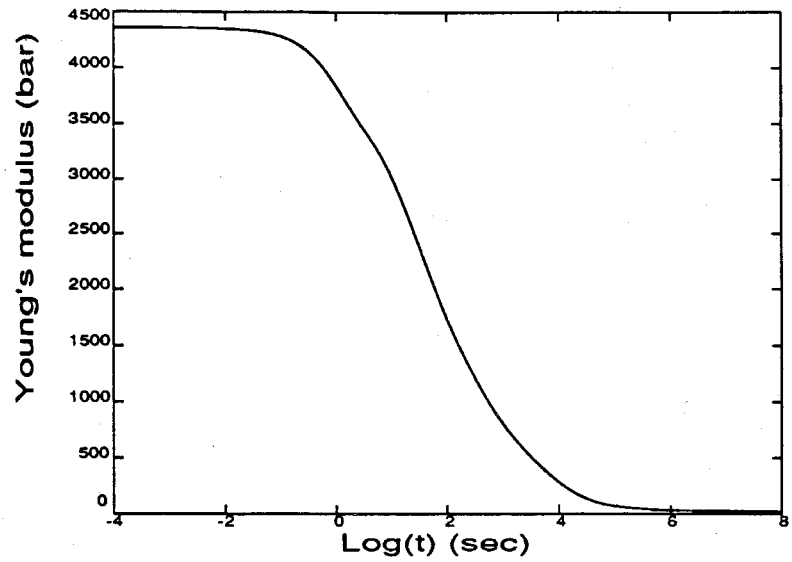


FIGURE 2.7 Young's modulus

In the failure zone, as shown in Fig. 2.2, the adhesive is modelled as undergoing a uniaxial extension; this deformation is intended to represent the strain history of the fibrils, which are strained perpendicularly to the plane of the crack and with no restraint to lateral contraction. Since the crack is assumed to be propagating steadily, the convolution integrals necessary to compute the viscoelastic response of the solid can be written in terms of line integrals, where the path of integration follows a material particle from the moment it enters the failure zone. In a reference system moving with the crack, with the craze tip located at $x = 0$ and the cohesive zone located on the negative $x$ axis, the following equations represent the constitutive behavior of the adhesive:

$$\sigma_{yy}(x) = \Psi\left(\frac{\epsilon_{yy}}{\epsilon_{max}}\right)\left[\sigma_0 + \int_0^{\xi(x)} E\Big(\xi(x) - \xi(x')\Big)\frac{\partial \epsilon_{yy}}{\partial x'}dx'\right] , \tag{2.3.3}$$

$$\epsilon_{kk}(x) = \epsilon_0 + \int_0^{\xi(x)} M\Big(\xi(x) - \xi(x')\Big)\frac{\partial \sigma_{yy}}{\partial x'}dx' , \tag{2.3.4}$$

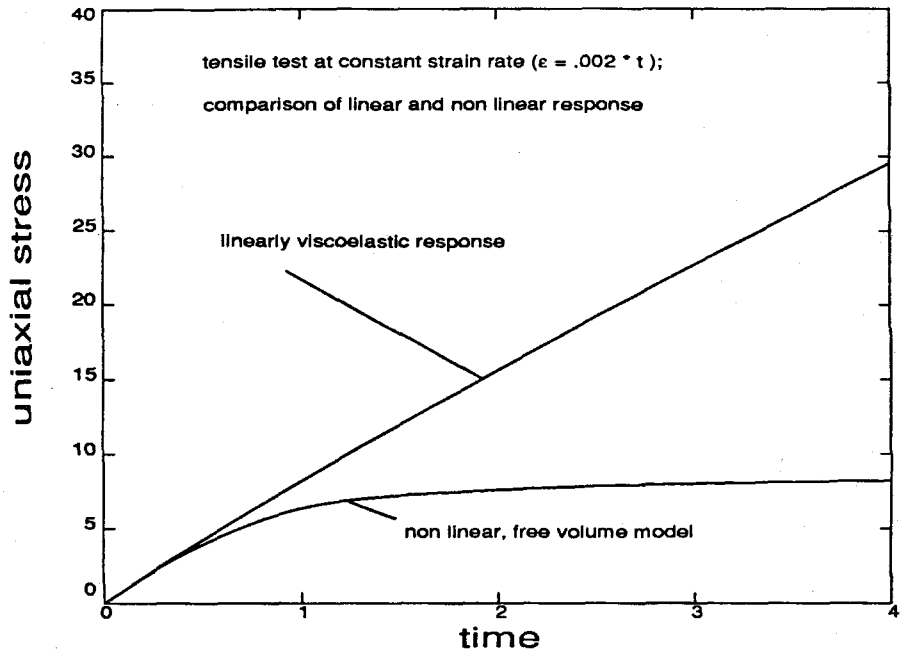


FIGURE 2.8 Comparison of linearly and non linearly viscoelastic response for a uniaxial tension test.

where $\xi$ is the internal time of the material particle, referenced to the arrival at the craze tip, *i.e.*,

$$\xi(x) = \int_0^t \frac{d\tau}{a_t(\tau)} = \int_0^x \frac{dx}{\dot{c}\, a_t(f_0, f(\epsilon_{kk}(x)))} \quad . \tag{2.3.5}$$

$\dot{c}$ represents the velocity of the propagating crack, $E(t)$ the time-dependent Young's modulus, $M(t)$ the bulk compliance and $\epsilon_0$ and $\sigma_0$ are the stress and strain at the beginning of the cohesive zone (*i.e.*, at $x = 0$ in a reference system moving with the crack). It has to be noted that Eq. 2.3.3 implies a uniaxial stretch of the fibrils in the failure zone, as is suggested from experimental evidence. The value for $\epsilon_0$, which represents the initial strain at the tip of the craze, is that which delimits the boundary between linear and nonlinear viscoelastic behavior.

The material properties at each point of the cohesive zone depend on the local

value of free volume, through Eq. 2.3.2, which is a function through 2.3.4 of the local dilatation, which in turn requires the local properties in order to be computed. A careful integration procedure is therefore required in order to accurately capture the nonlinear material response. The set of constitutive equations was integrated using a Runge-Kutta scheme which computed the time shift as a combination of the time shifts at the two extremes and at the midpoint of the current interval along the craze. The stability of the resulting solution, with respect to variations in the opening profile due to successive iterations, was excellent; convergence was also checked by changing the mesh size, which typically consisted of 300 points along the failure zone.

In the above integrals, the mechanical history before a material point reaches the failure zone is partly ignored; the effect of the previous history on the material condition in the failure zone is approximated by the constants $\sigma_0$ and $\epsilon_0$, rather than having a linearly viscoelastic dependence on the strain and stress history in front of the running crack. A justification for this approximation can be found in the highlighting of the time-dependent behavior in the failure zone by nonlinear viscoelasticity of the adhesive and also in the high stress gradients which are generated by the void-growth function. The effect of $\epsilon_0$ on the dilatation-induced time shift was not taken into account, and it was assumed that the material entered the decohesion zone with a content of free volume equal to the reference value, $f_0$. The value of $\sigma_0$ was prescribed according to a criterion discussed below.

The multiplicative factor $\Psi$ present in Eq. 2.3.3 represents the effect of void growth on the material response. $\Psi(\frac{\epsilon_{yy}}{\epsilon_{max}})$ is a decreasing function of $\epsilon_{yy}$, and varying between unity and zero; the uniaxial strain in the adhesive layer $\epsilon_{yy}$ is scaled by the maximum extension attainable before failure, $\epsilon_{max}$. As stressed before,

this function is assumed to be time and rate-independent. The chosen form for the function was computed from Parvin's experimental data (Knauss and Parvin, 1989), and it is shown in Fig. 2.9. The parameter $\epsilon_{max}$ was set to six per cent in the following calculations.

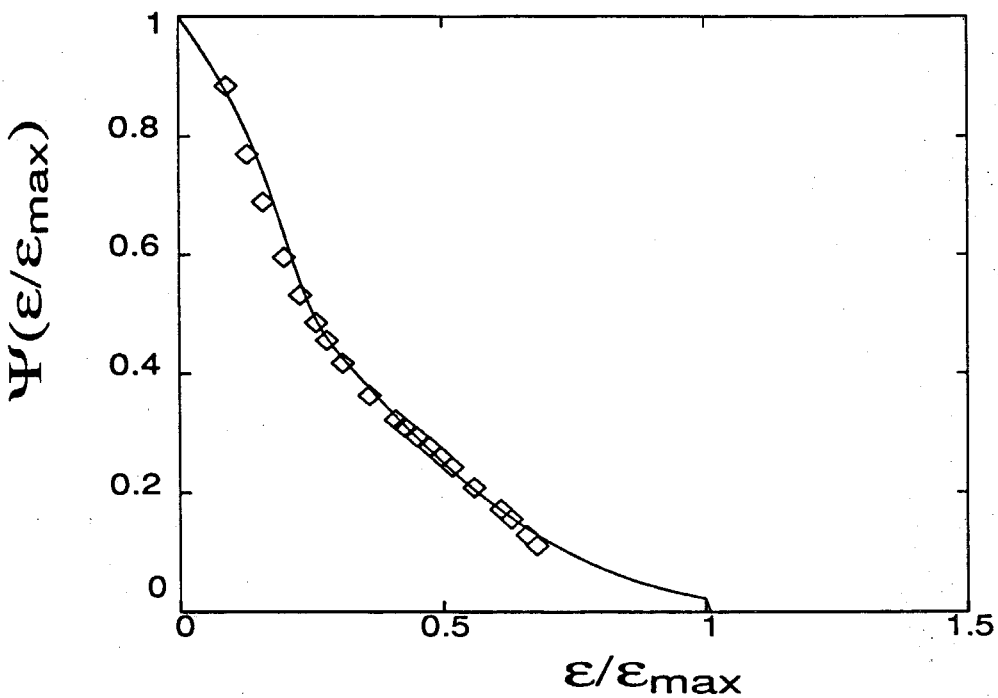


FIGURE 2.9 Function expressing the cumulative damage due to void growth.

It has to be remarked here that the chosen fit to the experimental curve of the function $\Psi(\frac{\epsilon_{yy}}{\epsilon_{max}})$ had an unexpected feature. When multiplied by a linear function of $\epsilon_{yy}$, it gave rise to a small oscillation of the resulting curve around its maximum, as it will be shown in the plots of the load distribution on the crack faces. This circumstance arises for sufficiently high crack speeds to cancel the nonlinear viscoelastic softening in the cohesive zone, so that the material response is there governed only by the void growth and by a time-independent, linearly elastic re-

sponse which gives a direct proportionality between loads and displacements. While this feature appears to result no adverse effects to the conclusions of this investigation, the appearance of a "hat" around the maximum in the load distribution on the crack faces signalled the lack of free-volume induced softening from the craze tip up to the location of maximum load, providing additional information for the evaluation of the results.

Once the crack opening displacement was found in the iterative solution scheme, the strain in the adhesive could be computed by dividing it by the original thickness of the layer, which therefore becomes the main characteristic length scale of the problem. The point at which the critical strain was achieved determined the extent of the cohesive zone along the crack faces, which was therefore part of the problem solution and not given *a priori*. A "polite" guess for the cohesive zone length needs to be known before initiating the numerical search for the solution, so that most of the points of the discretized crack faces are load-carrying and contributing to the solution. The points of zero cohesive load have no effect on the stress intensity factor and the displacement profile, and therefore the effective mesh size is given only by the total number of load-carrying points along the discretized cohesive zone. As a consequence, it was necessary to re-mesh the cohesive zone periodically; the load distribution at the new discretized points was found by linear interpolation over the old mesh. In the preliminary calculations, it was found that an adhesive thickness of .0007 was effecting a craze length not too dissimilar from the dimension of the initially discretized domain, therefore this value was chosen and set as a reference quantity.

## 2.4 The deformation of the adherends

The stress and strain fields in the adherends are obtained using a fundamental solution developed by Knauss (1974), on the basis of complex potentials†. The theory of complex potentials‡ maps the two-dimensional elasticity problem, in the $(x, y)$ plane, into a problem on a complex plane, where the position vector is defined as

$$z = x + i\,y \ , \tag{2.4.1}$$

and where the stress and displacement fields are related to the values and derivative of functions of the complex variable $z$. Consider a crack propagating at constant speed in a linear material, subject to a given load distribution on the crack faces in proximity of the crack tip. The properties of the linear material in which the crack propagates can be specified arbitrarily as time dependent, thus accounting for the influence of the viscoelastic compliance of the adherends on crack propagation. The limit case, in which the mechanical properties of the adherends and the linearized adhesive are taken to be the same, mimics rather well the propagation of a crack, preceded by a craze.

In a reference system moving with the crack, the crack tip is chosen as the origin and the $x$ axis was aligned with the direction of the propagating crack. The relations between the coordinates $(x, y)$ in the moving system and the ones $(X, Y)$ of a reference system not moving with respect to the material points can be easily written as

$$x = X - \dot{c}t \tag{2.4.2a}$$

† For a thorough exposition of the method of complex potentials in linear elasticity, *cfr.* Mushkelishvily, 1963.

‡ Sometimes incorrectly referred to as the method of analytic functions, a rather misleading designation since these functions are not at all analytic, except for very special cases.

$$y = Y \ . \tag{2.4.2b}$$

Within the approximation that the craze opening in the failure zone is very small compared to the length of the latter, one can impose boundary conditions and compute the solution in the undeformed configuration, *i.e.*, in this special case on the crack faces on the $y = 0$ axis. The vertical displacement component $v(x)$ on the crack faces is consequently expressed as

$$v(x,0) = v(0,0) + \int_0^x \frac{\partial v(\eta,0)}{\partial \eta} d\eta \ . \tag{2.4.3}$$

If one takes the craze tip as the origin, then $v(0,0) = 0$. Denoting by $J(t)$ the shear creep compliance of the adherends, the theory of complex potentials states that one can express the crack opening displacement in terms of a complex potential $\phi(z)$ as

$$v(x,0) = \lim_{y \to 0+} \frac{\kappa+1}{2} Im\left[\int_0^{t(x)} J(t-\xi)\frac{\partial \phi(\zeta)}{\partial \xi} d\xi\right] \ , \tag{2.4.4}$$

where $Im$ denotes the imaginary part of the integral, $t$ is the time elapsed for a material particle from the moment it leaves the propagating craze tip to the moment it reaches the point $z = x + iy$ on the crack faces, and $\xi$ is the time elapsed while the material particle goes from the craze tip to the point $z = \zeta + iy$, *i.e.*, (*cfr.* Eq. 2.4.2)

$$t(x) = \frac{x}{\dot{c}} \ . \tag{2.4.5}$$

The parameter $\kappa$ is a factor depending on whether one considers a plane stress or plane strain case, in particular

$$\kappa = 3 - 4\nu \text{ for plane strain,} \tag{2.4.6a}$$

$$\kappa = \frac{3-\nu}{1+\nu} \text{ for generalized plane stress.} \tag{2.4.6b}$$

$\nu$ being the Poisson's ratio of the material. The above equations for $\kappa$ are valid when $\nu$ is time-independent. When $\nu$ is a time operator, then the above equations 2.4.6a and 2.4.6b can be reformulated in accordance with the laws of linearly viscoelastic analysis, *e.g.*, in the case of plane strain,

$$v(x,0) = 2\ Im\left[\int_0^{t(x)} J(t-\xi)\frac{\partial\phi(\zeta)}{\partial\xi}d\xi\right] - 2\ Im\left[\int_0^{t(x)} J(t-\xi)\frac{\partial\Phi(\zeta)}{\partial\xi}d\xi\right] \ , \quad (2.4.7)$$

where

$$\Phi(\zeta) \ = \ \lim_{y\to 0+}\int_{-\infty}^{\zeta} \nu(\tau(\zeta)-\tau(\xi))\frac{\partial\phi(\xi)}{\partial\xi}d\xi \ , \quad (2.4.8)$$

and

$$\tau(\zeta)-\tau(\xi) \ = \ -\frac{\zeta-\xi}{\dot{c}} \ , \quad (2.4.9)$$

and the path of integration in Eq. 2.4.8 follows a material particle as it approaches the crack tip located at $x = 0$ from $x = +\infty$. Behind the craze tip, *i.e.*, for $x < 0$, one has to consider a limit process since the cohesive zone coincides with a branch cut of the complex potential $\phi(z)$. In the presented calculations, $\nu$ was approximated by a constant, with simplifications for the algorithm, and the crack was considered to be propagating under plane strain conditions.

The particular case considered was that of a crack, preceded by a craze, propagating in a polymer, therefore the shear creep compliance of Eq. 2.4.4 was taken to be the same as the shear compliance of the linearized adhesive, and such a compliance in shown in Fig. 2.10. Obviously, the three curves for the viscoelastic response of the material are not independent of each other; thus the shear compliance curve was obtained from the time-dependent Young's and bulk moduli through a conversion procedure outlined in Appendix A. The glassy value of Poisson's ratio for the adhesive was used to determine a value for $\kappa$, which was then kept constant as explained above.

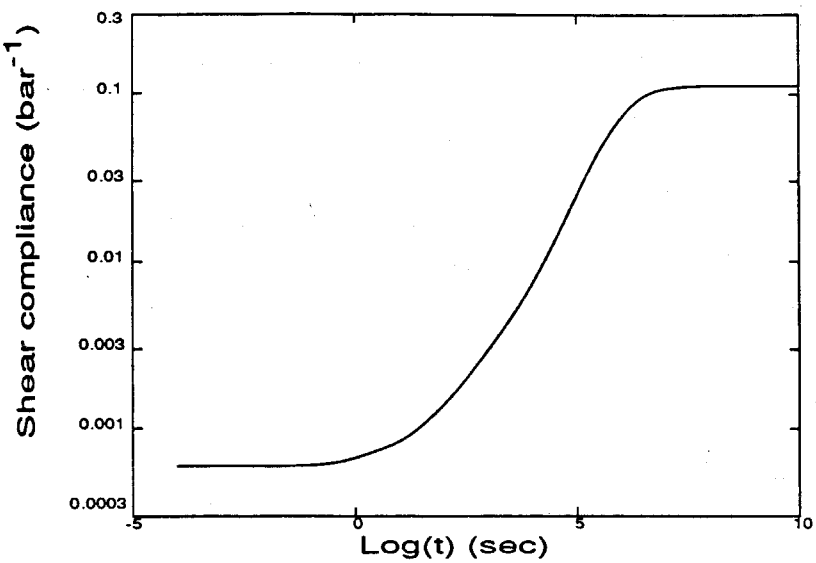


FIGURE 2.10 Shear compliance.

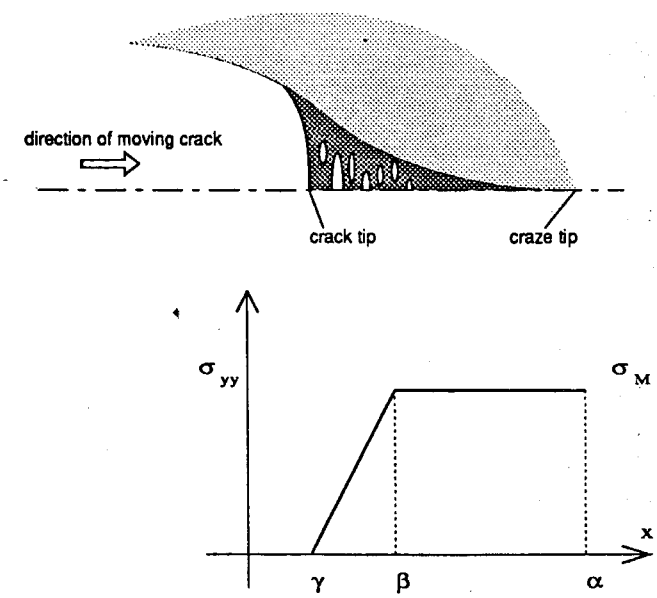


FIGURE 2.11 Trapezoidal distribution of tractions.

For the case of a semi-infinite crack in an infinite medium, with the craze tip located at $x = 0$ and the crack tip (*i.e.*, the end of the cohesive zone) located at $x = c$, the theory of complex potentials asserts that the derivative of the potential function $\phi(z)$ needs to satisfy the following boundary condition on the crack faces, in order for the solution to render bounded stresses anywhere

$$\phi'(z) = \frac{1}{2\pi\sqrt{z-\alpha}} \int_0^c \frac{\sigma_{yy}(\tau)\sqrt{\tau-\alpha}}{\tau - z} d\tau \quad , \tag{2.4.10}$$

where the distribution of $\sigma_{yy}$ is given by Eqs. 2.3.3, 2.3.4, 2.3.5, and the domain of integration extends over all the cohesive zone, from the craze tip to the crack tip. In addition to the particular solution, there is always a homogeneous solution, corresponding to zero loads on the crack faces, given by

$$\phi_f(z) = \frac{K}{\sqrt{2\pi}}\sqrt{z-\alpha} \quad , \tag{2.4.11}$$

in which the stress intensity factor $K$ is the "far field loading parameter". Thus, the effective complex potential is the sum of the homogeneous and particular solutions,

$$\phi(z) = \phi_c(z) + \phi_f(z) \quad , \tag{2.4.12}$$

where $\phi_c(z)$ satisfies Eq. 2.4.10. For the case of a trapezoidal loading extending from $x = \gamma$ to the crack tip located at $x = \alpha$ and with $\sigma_M$ being the maximum value of the stress, as shown in Fig. 2.11, the function $\phi_c(z)$ can be computed (Knauss, 1974), with its imaginary part given by*

$$Im(\phi_c(z)) = \left\{ (-z^2 + (\alpha+\beta)z - \alpha\beta) 3log\left(\frac{\sqrt{\alpha-z}+\sqrt{\alpha-\beta}}{\sqrt{\alpha-z}-\sqrt{\alpha-\beta}}\right) + \right.$$

$$\left. + (z^2 - (\alpha+\gamma)z + \alpha\gamma) 3log\left(\frac{\sqrt{\alpha-z}+\sqrt{\alpha-\gamma}}{\sqrt{\alpha-z}-\sqrt{\alpha-\beta}}\right) + \right.$$

* In the following expressions, all the functions as logarithms and square roots are intended to be real functions, since the expressions in which they appear follow from the separation between real and imaginary parts of the complex potential $\phi(z)$.

$$-\sqrt{\alpha-z}\left[\sqrt{\alpha-\beta}(6z-4\beta-2\alpha)+\sqrt{\alpha-\gamma}(2\alpha-6z+4\gamma)\right]\Big\}\bullet$$

$$\bullet\frac{\sigma_M}{\pi(\alpha-z)(6\beta-6\gamma)} \text{ for } z=x+iy, x<\alpha, y\to 0^+ \text{ and } \gamma<\alpha\ . \qquad (2.4.13)$$

If one imposes the vanishing of the singular term in $\phi(z)$, one obtains the condition

$$K=2\sqrt{2\pi}\lim_{z\to\alpha}\sqrt{z-\alpha}\phi_c'(z)\ . \qquad (2.4.14)$$

By substituting Eq. 2.4.13 into the above condition, one finds

$$K=\left\{\sqrt{\alpha-\beta}(4\alpha-4\beta)-\sqrt{\alpha-\gamma}\,(4\alpha-4\gamma)\right\}\bullet$$

$$\bullet\frac{\sigma_M}{6(\beta-\gamma)\sqrt{2\pi}}\ . \qquad (2.4.15)$$

For later use it is necessary to compute the (initial) strain at the crack tip in the adherends, which, after having taken into account branch cuts and rotations of $\pi$ in the complex plane (cfr. Mushkelishvily, 1963), is found to be related to the real part of $\phi'(z)$ in front of the running crack through the following convolution integral

$$\epsilon_{yy}(x=0)=\epsilon_{yy}(x=+\infty)+\frac{\kappa-1}{2}Re\Big[\int_\infty^0 J(\frac{x}{\dot c})\frac{\partial\phi'(z)}{\partial x}dx\Big]\ , \qquad (2.4.16)$$

where $z=x=X-\dot ct$ and

$$Re\Big[\phi'(z)\Big]=\Big\{3[z^2-(\alpha+\beta)z+\alpha\beta]arctg\left(\frac{\sqrt{\alpha-\beta}}{\sqrt{z-\alpha}}\right)-\sqrt{(z-\alpha)(\alpha-\beta)}(3z-2\beta-\alpha)+$$

$$+[3z^2-3(\alpha+\gamma)z+3\alpha\gamma]arctg\left(\frac{\sqrt{\alpha-\gamma}}{\sqrt{z-\alpha}}\right)+\sqrt{(z-\alpha)(\alpha-\gamma)}(3z-2\gamma-\alpha)\Big\}\bullet$$

$$\bullet\frac{\sigma_M}{3\pi(z-\alpha)(\beta-\gamma)}+$$

$$+\frac{K}{\sqrt{2\pi}\sqrt{z-\alpha}}\quad for\quad z=x>0 \qquad (2.4.17)$$

There is no limit process in this case since the branch cut of the complex potential is located behind the craze tip.

## 2.5 Numerical procedure

The solution presented in the previous section assumes a trapezoidal load distribution in the cohesive zone. A more general loading on the crack faces can be represented as a superposition of trapezoidal distributions, to which Knauss's fundamental solution can be applied individually; such an approximation is sketched in Fig. 2.12. Upon discretization of the cohesive zone, the contributions of each trapezoidal load can be computed after the substitutions in the expression for the complex potential $\phi(z)$ of

$$\sigma_M = \sigma_{yy}(k-1) - \sigma_{yy}(k) \tag{2.5.1}$$

$$\alpha_k = \text{constant} = 0 \tag{2.5.2}$$

$$\gamma_k = x(k) \tag{2.5.3}$$

$$\beta_k = x(k-1) \ , \tag{2.5.4}$$

where $x(k)$ and $x(k-1)$ are the coordinates of the discretization points along the cohesive zone. The choice for the parameter $\alpha_k$ is a consequence of the craze tip being located at $x = 0$ in the system of reference moving with the propagating crack. The total stress and strain fields are then obtained as the sum of each of these individual contributions.

Once the crack opening displacement is obtained through this procedure, the time history of straining in the adhesive is known and can be employed to obtain a more accurate cohesive load distribution on the boundary of the adherends, which in turn is used to yield a new crack opening profile. The whole process is iterated until convergence is achieved. This method, known as Picard iteration, does not

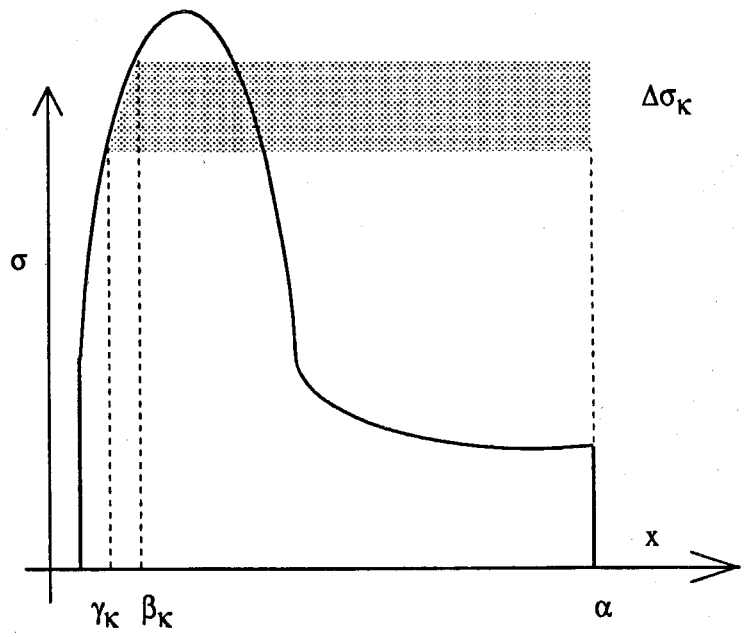


FIGURE 2.12 Representation of a general loading distribution as a superposition of trapezoidal loads.

guarantee convergence under all possible conditions**; one modification that overcomes the problem is to take, at every new iteration, not the newly computed crack opening displacement as that used to compute the nonlinear viscoelastic response of the adhesive, but the sum of the old one and a fraction of the difference between the two; if one denotes by $v(x)^{(n)}$ and $v(x)^{(n+1)}$ the displacement profiles at the n-th and (n+1)-st iterations, then the actual diplacement profile $\hat{v}(x)$ used to compute the new stresses in the cohesive zone is given by

$$\hat{v}(x)^{(n+1)} = v(x)^{(n)} + \beta[v(x)^{(n+1)} - v(x)^{(n)}] \ , \qquad (2.5.5)$$

The minimum value of the relaxation parameter $\beta$ that ensured stability of the iterations was found to depend on the shape of the loading distribution in the

** see, for example, Ungsuwarunsgri and Knauss, 1988.

cohesive zone; a typical value of 20 percent sometimes had to be scaled down to five percent under unfavorable conditions, as in the case of sharp peaks in the cohesive load distribution away from the crack tip. This procedure takes care of the instabilities inherent in the iterative process, but nonetheless many iterations have to be performed, since the same procedure also slows down the convergence rate. The convergence was checked on the value of the stress intensity factor, which was found to be the quantity most sensitive to variations in the displacement profile. Typically, convergence of the solution was considered to be achieved when the adjusted difference in stress intensity factors between an iteration and the next, *i.e.*,

$$\frac{\Delta K}{\beta} = \frac{K^{(n+1)} - K^{(n)}}{\beta} \tag{2.5.6}$$

was found to be of the order of one or two percent. In rare occasions (indicated by the occasional glitches in the plots showing the results) such a tolerance was not achieved because of the extremely "unstable" nature of the solution.

A favorable aspect of the computation of the crack opening displacement from the loads on the crack faces is its linearity; as long as the point at which the critical opening displacement $\epsilon_{max}$ is achieved lies in the discretized craze domain, the effects of the load distribution on the stress intensity factor and crack opening profile can be cast, through Eqs. 2.4.13 and 2.4.15, in a matrix form. The governing matrix is a function of geometry and does not depend on the loads, so it needs to be recomputed only when re-meshing was necessary due to the extension of the cohesive zone past the current position of the last point.

The initial stress in the cohesive zone, $\sigma_0$, is an essential parameter of the problem, since it contributes significantly to the loads on the crack faces. This value of stress can be set constant or can be determined through some failure criterion

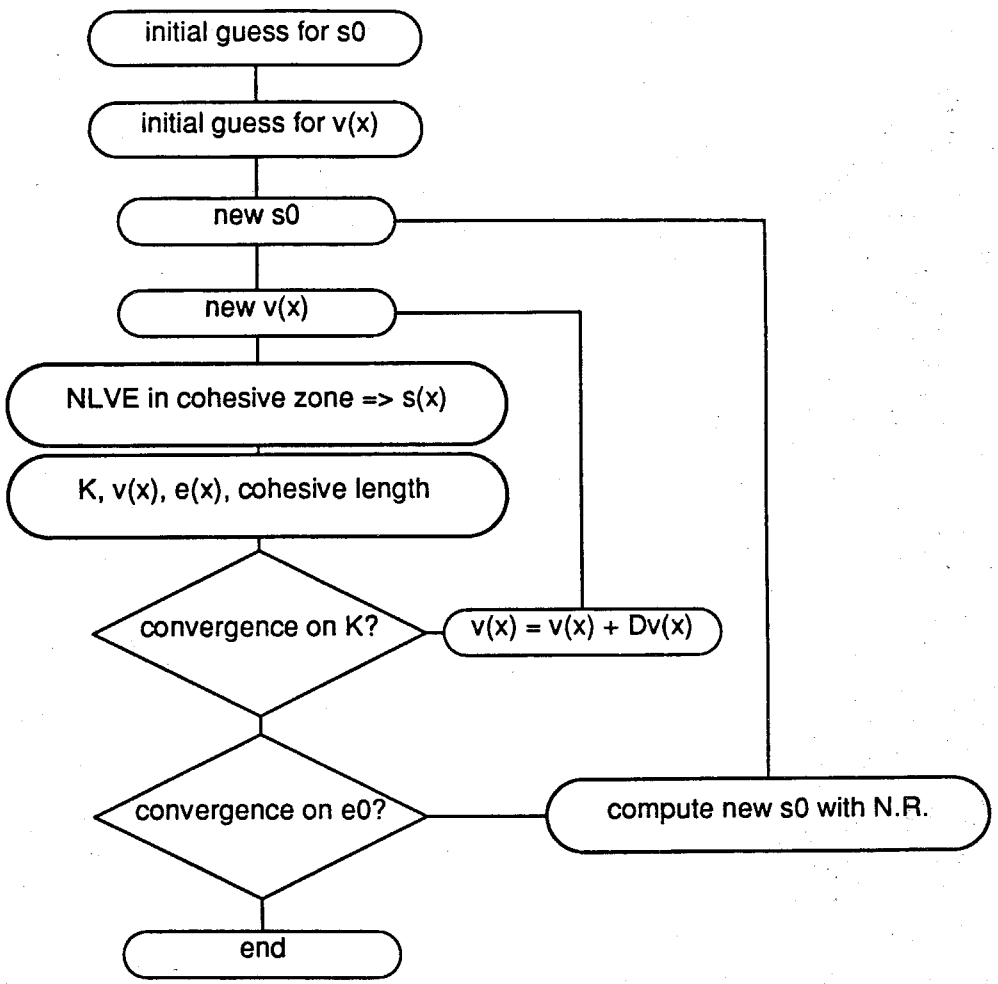


FIGURE 2.13 Iteration scheme. N.R. = Newton-Raphson; s0 = $\sigma_0$; e0 = $\epsilon_0$.

predicting the onset and growth of voids in the adhesive. If one limits attention to the case of the crack running in a polymer then, since there are no discontinuities in the material properties between the inner and outer domain, the strain characterizing the outer domain at the craze tip, computed using Eq. 2.4.16 and 2.4.17, is also the same strain affecting the layer of polymer which enters the degradation zone. This situation allows one to investigate the consequences of assuming that

a critical strain characterizes the onset of void generation: here the onset of void growth was related to a particular value of strain, independent of crack speed.

For this reason, an outer loop of iterations needed to be performed on the correct value of the initial cohesive stress $\sigma_0$, which was otherwise completely arbitrary, so that the assumed critical value of the strain is achieved at the crack tip. These calculations were performed using a modified Newton-Raphson's method which yielded more accurate values of initial stress at every iteration. A sketch of the algorithm is shown in Fig. 2.13.

## 2.6 Results and discussion

In the following pages, the crack speed will be considered as a given parameter and the corresponding stress intensity factor and load distribution on the crack faces will be determined. Alternately the stress intensity factor can be considered the input parameter of the problem, and the crack velocity that can sustain such a stress intensity in a steady fashion would be the output of the numerical solution. The choice of considering instead the crack velocity as the given parameter comes purely from the structure of the algorithm seeking the numerical solution.

The crack speed was normalized by a reference crack speed defined by the thickness of the adhesive layer and a characteristic relaxation time. The latter was determined as the average relaxation time

$$\tau = \frac{\sum_{i=1}^{N} J_i \tau_i}{\sum_{k=1}^{N} J_k} \quad , \tag{2.6.1}$$

where the $J_i$'s represent the discrete relaxation spectrum of the shear compliance, and the $\tau_i$'s are the corresponding retardation times. This characteristic time $\tau$ was

approximately $2.3\times10^6$ seconds. Analogously, the stress intensity factor was normalized by invoking as the reference stress the glassy value of the Young's modulus of the adhesive (4300 bar), and the adhesive thickness (.0007 m).

One of the quantities of interest is the energy $\Gamma$ dissipated in the cohesive zone per unit crack advance,

$$\Gamma = \int_{cohesive\ zone} \sigma(x) d\epsilon(x) \ ; \tag{2.6.2}$$

here the path of integration follows the strain history of a material particle as it progresses through the craze. The cohesive fracture energy was also normalized by the glassy value of Young's modulus.

Two values of the critical strain parameter $\epsilon_{crit}$ were considered, .3 and 1 percent. Thus, the onset of void growth was taken to depend on the critical value of the $\epsilon_{yy}$ strain, which was computed through Eq. 2.4.16. Figs. 2.14 through 2.19 show the evolution of the load distribution on the crack faces as a function of crack speed. Some relevant features can be pointed out. At high speeds, the progressive hardening of the material response in the cohesive zone results in a tendency to move the high stress gradients away from the craze tip. This progressive hardening can be seen (*cf.* Fig. 2.16) in the formation of the "hat" at the top of the cohesive zone distribution, which indicates that the material behavior in that area is exclusively influenced by the features of the void growth function, and the nonlinearly viscoelastic softening is removed by virtue of the very high the strain rates. When this phenomenon happens, no further changes in stress intensity factor or stress distribution occur by increasing the crack velocity, since then all the time dependence of the problem is absent. This regime is perfectly representable by a Dugdale/Barenblatt model in which one assigns a rate independent $(\sigma, v)$ relation to

the material behavior in the cohesive zone. Since the $(\sigma, v)$ relation has to represent the effect of void growth only, it necessarily coincides with the function $\Psi(\epsilon)$.

As the speed decreases, the size of the cohesive zone also reduces, and the maximum value of the stresses also decreases. This trend continues until the crack speed becomes so small that the outer linear material has time to relax while it runs along the crack faces, and this interaction between the nonlinearly viscoelastic softening of the fibrils and the creep of the linear material surrounding the craze effects an increase of the cohesive zone size, as shown in Fig. 2.15. The initial stress at the crack tip also exhibits a large decrease. As the crack slows down further, again all the time dependence disappears, since now the adherends behave as elastic materials having the rubbery values of the moduli, and this enforces a strong reduction in the cohesive zone size.

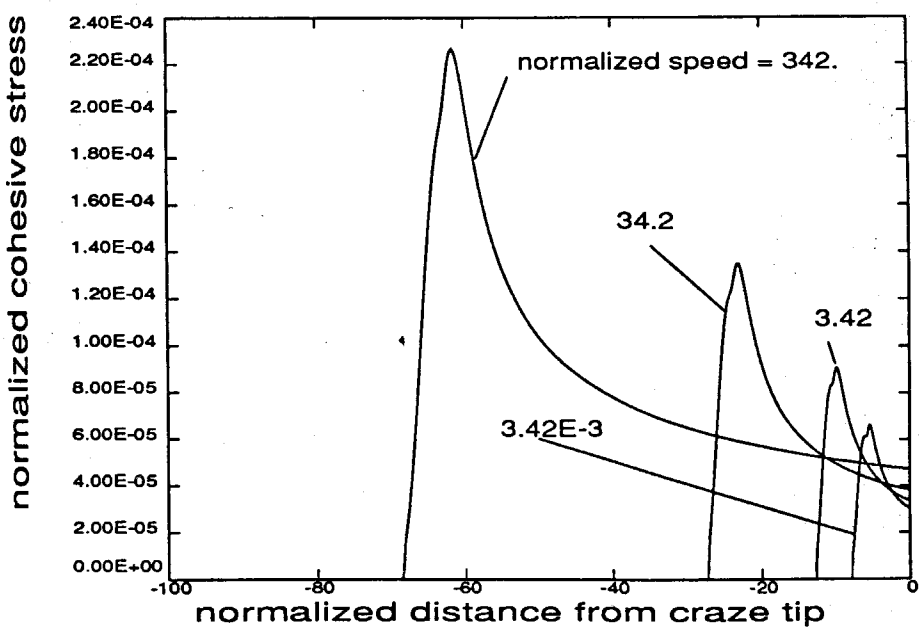


FIGURE 2.14 Load distribution on the crack faces for different values of crack speed, for a critical strain of .3 percent.

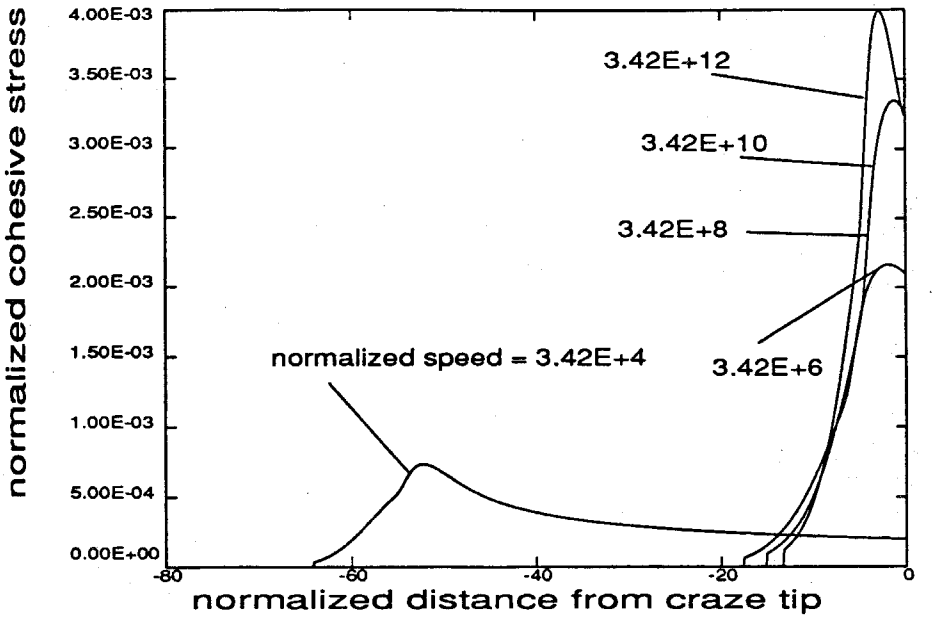


FIGURE 2.15 Load distribution on the crack faces for different values of crack speed, for a critical strain of .3 percent.

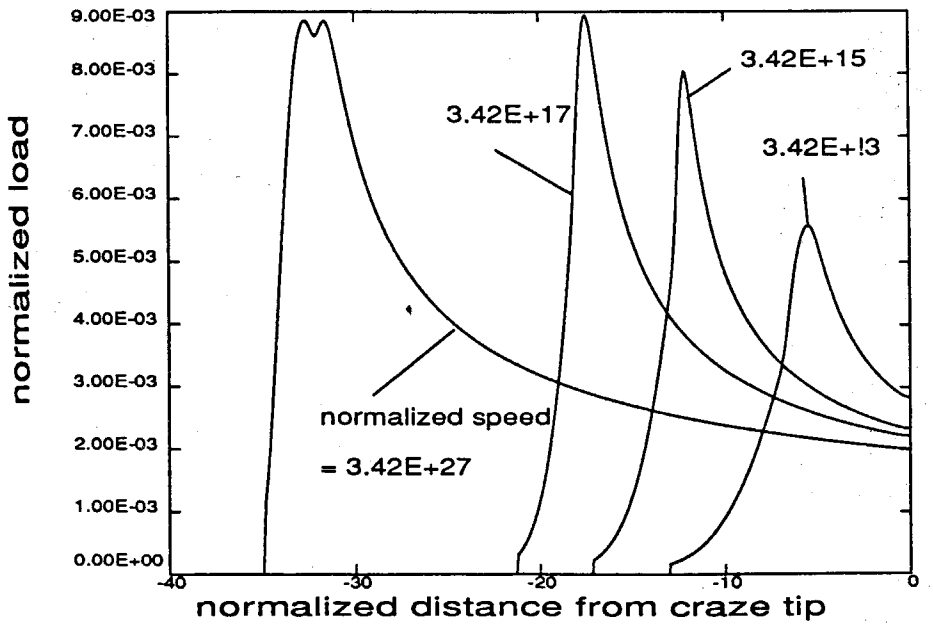


FIGURE 2.16 Load distribution on the crack faces for different values of crack speed, for a critical strain of .3 percent.

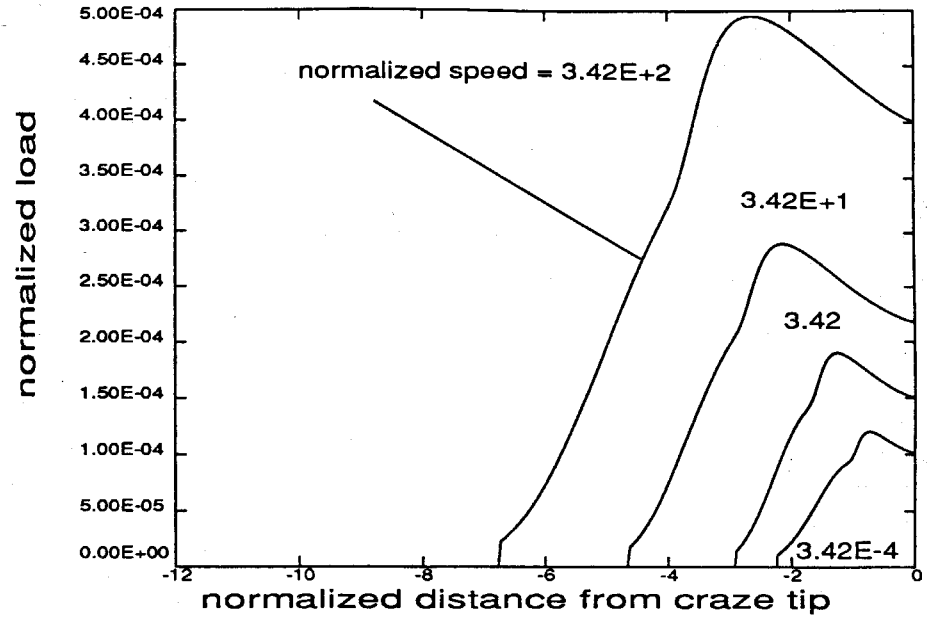


FIGURE 2.17 Load distribution on the crack faces for different values of crack speed, for a critical strain of 1. percent.

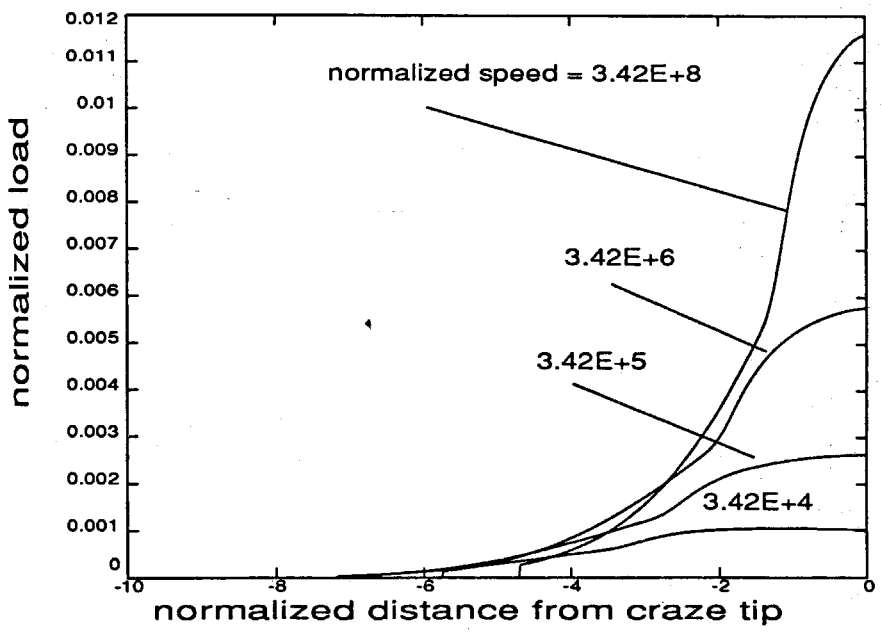


FIGURE 2.18 Load distribution on the crack faces for different values of crack speed, for a critical strain of 1. percent.

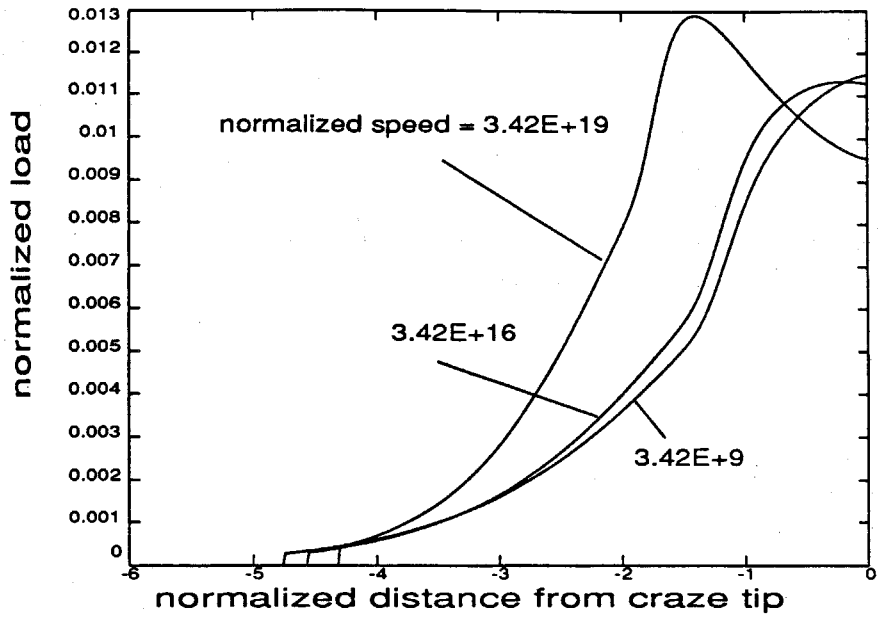


FIGURE 2.19 Load distribution on the crack faces for different values of crack speed, for a critical strain of 1. percent.

Similar conclusions can be drawn from the inspection of the dependence of the stress intensity factor, cohesive zone size and initial stress on the values of crack speed, as presented in Figs. 2.20 through 2.23. It should be recalled that a normalized crack speed equal to unity implies that the crack covers a distance equal to the thickness of the adhesive in the same time as the average retardation time. Since the normalized size of the cohesive zone ranges from a few units to almost seventy as in the case of the .3 per cent critical strain, the time needed for a material particle to pass along the cohesive zone varies from two or three times to more than sixty times the characteristic retardation time. Since the shear compliance, shown in Fig. 2.10, shows time dependence for more than six orders of magnitude below the average retardation time ($\sim 2 \times 10^6$ seconds), one concludes that the effect of the viscoelastic compliance of the adherends is felt in a range of normalized crack speed between one (the time of passage through the cohesive zone

is of the order of the reference time) and $10^7$ (the time of passage is so short that the adherends behave in a glassy manner). This explanation accounts for the rise in stress intensity factor, fracture energy and the changes in cohesive zone size in this velocity range (*cfr.* Figs. 2.20, 2.21, 2.22, 2.23). For a crack speed below this range, the adherends can be characterized essentially as elastic media of rubbery shear compliance. In between these two extreme ranges, the material passing through the cohesive zone experiences a constitutive response of the adherends which evolves from rubbery to glassy behavior, causing changes in the stress intensity factor and cohesive zone size as portrayed in Figs. 2.20 through 2.23. For much higher values of crack speed, the progressive hardening of the response in the cohesive zone starts playing a predominant role, and an increase in stress intensity factor and cohesive fracture energy is observed.

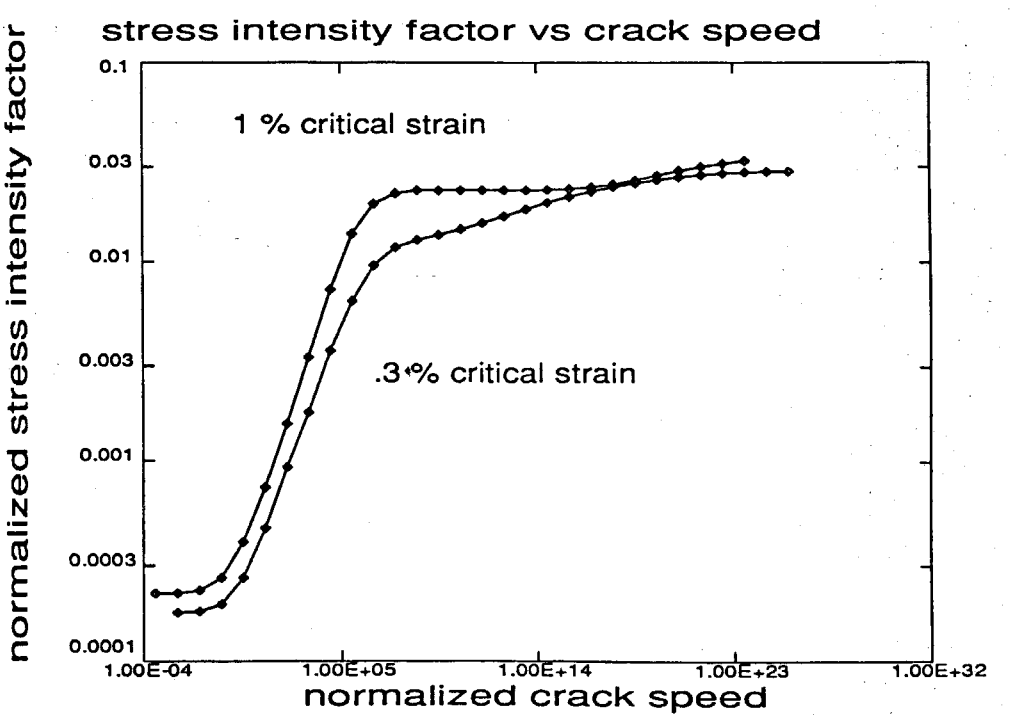


FIGURE 2.20 Stress intensity factor as a function of crack velocity.

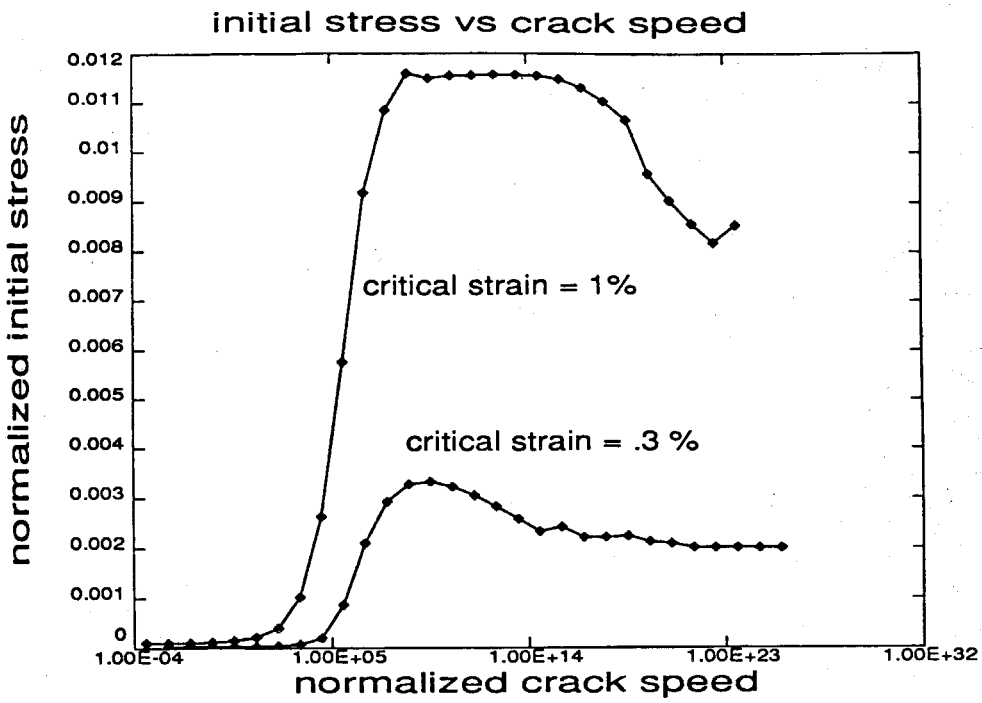


FIGURE 2.21 Initial stress in the cohesive zone as a function of crack velocity.

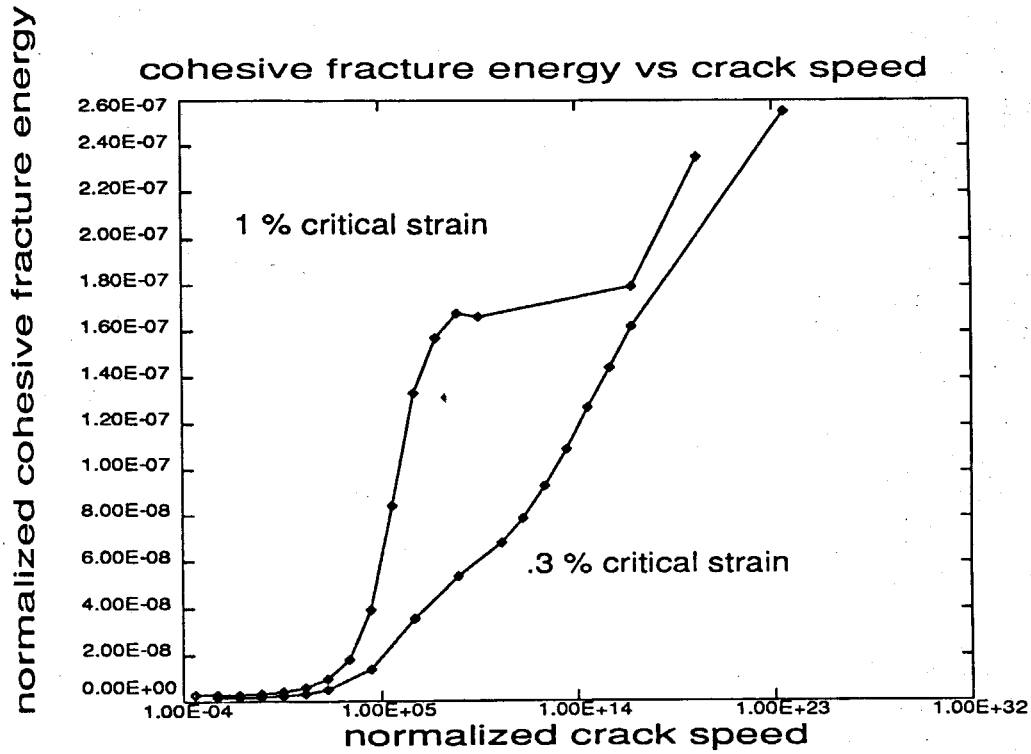


FIGURE 2.22 Cohesive fracture energy as a function of crack velocity.

The behavior of the fracture energy as a function of crack speed exhibits an interesting feature. Fig. 2.22 shows a sharp change from a strong dependence on crack velocity to a regime in which the fracture energy is rather insensitive to crack speed. This transition occurs at a normalized speed of about $1. \times 10^8$ for a value of critical strain of 1 percent. Although the analysis presented here is strictly a steady state analysis, this latter transition might be indicative of a regime of crack speed which could favor unstable crack growth in polymers, which is often detected in experiments (*e.g.*, Washabaugh, 1990). For a qualitative argument one would consider the energy dissipated in the cohesive zone as the relevant mechanism of energy dissipation, *i.e.*, without taking into account the strain energy which is lost in the adherends or in the undamaged adhesive. Within this approximation and that of applying the results of a steady state analysis to transient behavior, one can appreciate that an oscillation in crack speed around the transition velocity implies a decrease in the energy dissipated in the cohesive zone. If $\dot{c}_{crit}$ is the transition velocity and $\Delta\dot{c}$ is the variation, assuming that the crack spends equal periods of time propagating at $\dot{c} = \dot{c}_{crit} - \Delta\dot{c}$ and at $\dot{c} = \dot{c}_{crit} + \Delta\dot{c}$, then the average energy expenditure is given by the intersection of the line connecting the points on the energy vs. speed curve at $\dot{c} = \dot{c}_{crit} - \Delta\dot{c}$ and $\dot{c} = \dot{c}_{crit} + \Delta\dot{c}$ with the vertical line $\dot{c} = \dot{c}_{crit}$. If the curve has a negative second derivative, this average energy is lower; in the case of a sharp "corner", as the one shown in Fig. 2.22 for the critical strain of 1 percent, the decrease in the dissipated energy is furthermore emphasized, and this can indicate the presence of a mechanism which favors unstable crack growth.

It is of interest to qualitatively compare these predictions with the results of simpler treatments. In particular, if one assumes a constant load distribution on the crack faces, similar to that shown in Fig. 2.11 but without the triangular part, then the predictions of simpler fracture criteria can be considered. Here $\alpha_0$ will be used

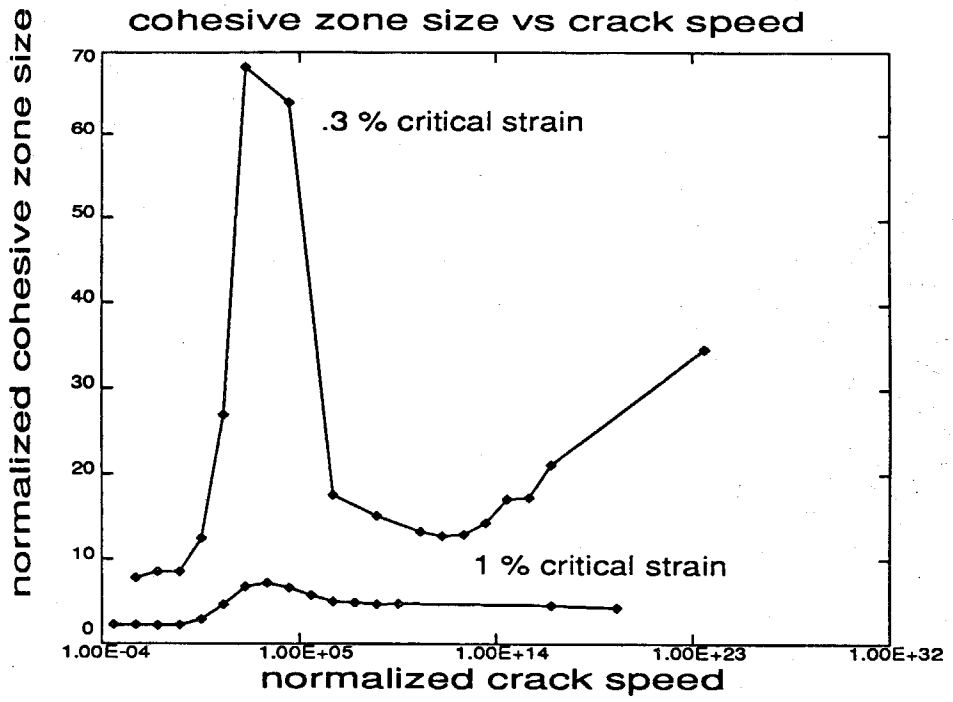


FIGURE 2.23 Cohesive zone size as a function of crack velocity.

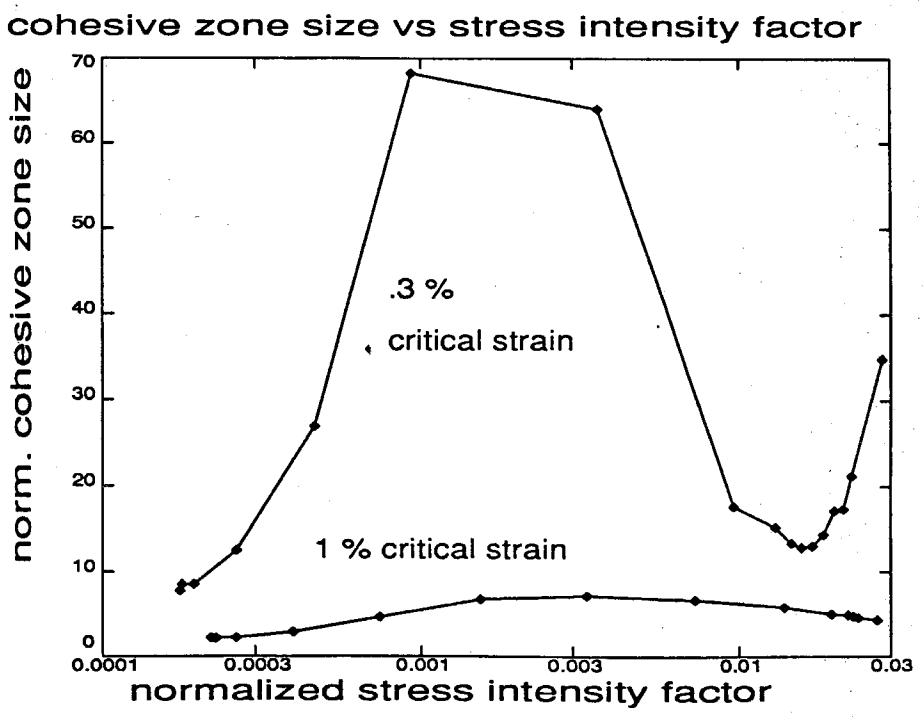


FIGURE 2.24 Cohesive zone size vs. stress intensity factor.

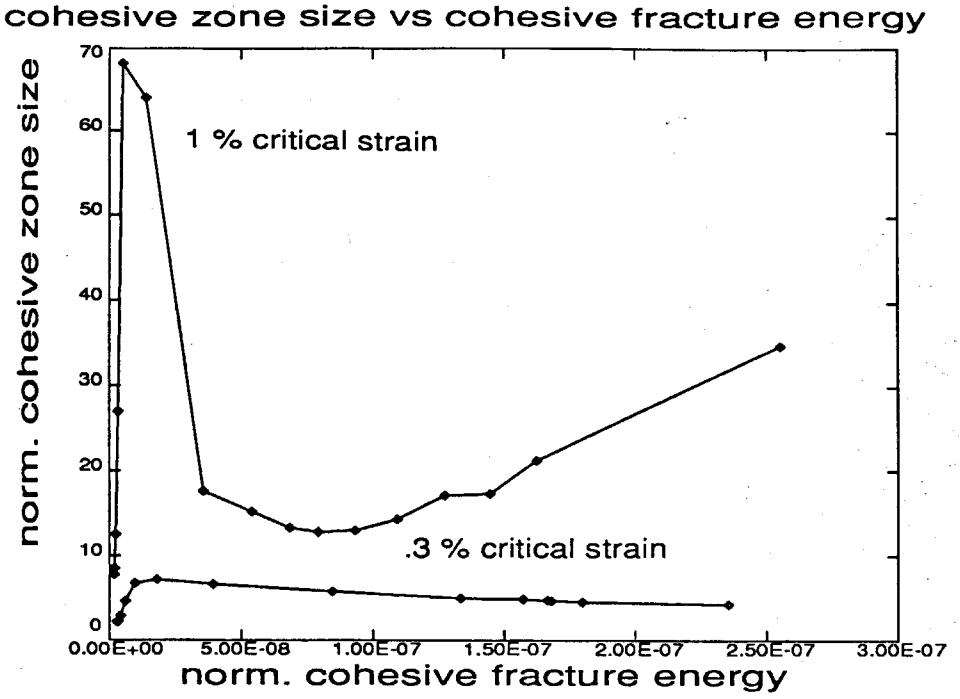


FIGURE 2.25 Cohesive zone size vs. cohesive fracture energy.

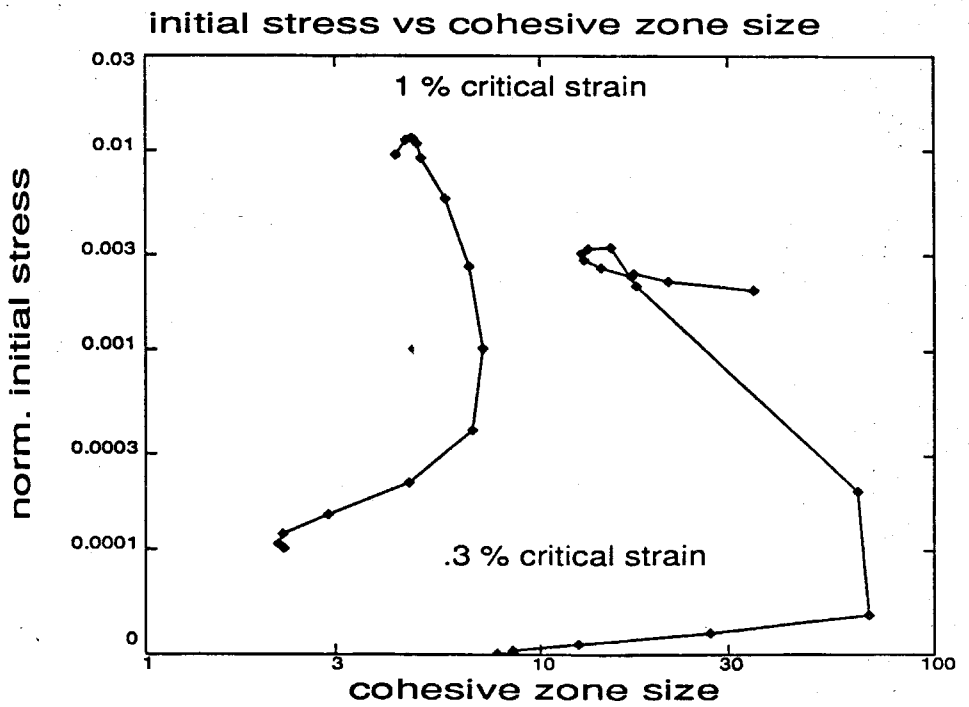


FIGURE 2.26 Initial stress in cohesive zone vs. zone size.

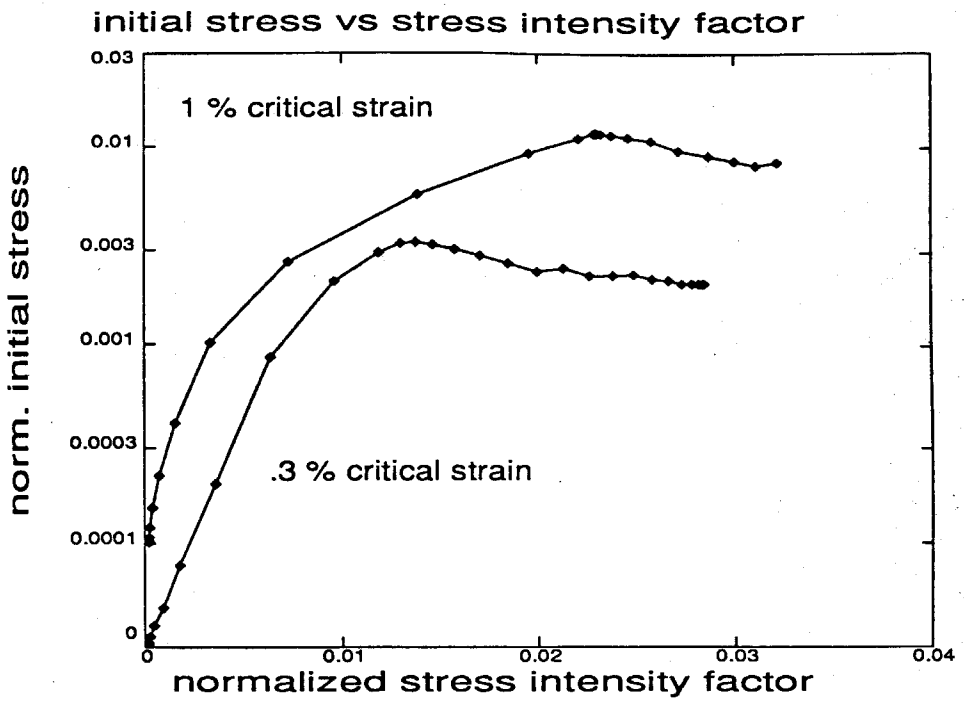


FIGURE 2.27 Initial stress in the cohesive zone vs. stress intensity factor.

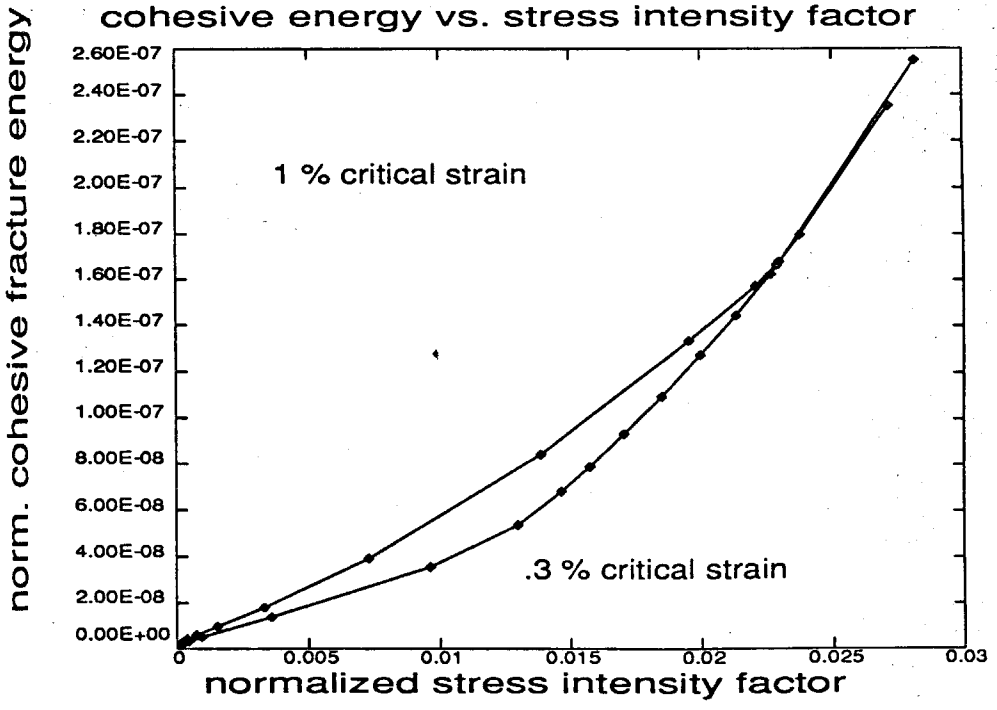


FIGURE 2.28 Cohesive fracture energy vs. stress intensity factor.

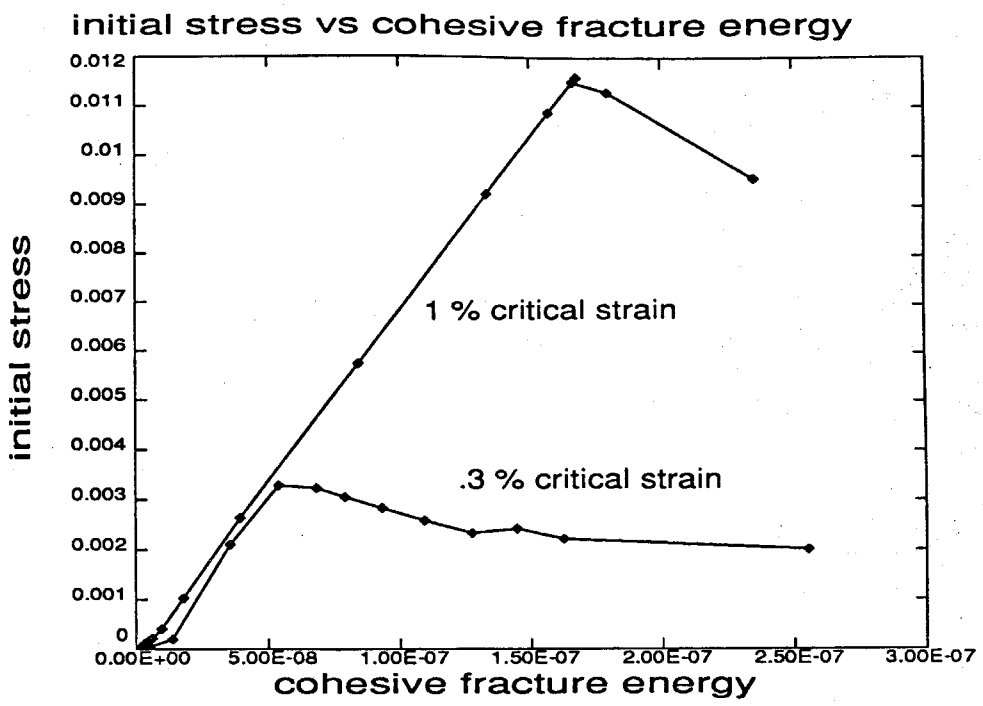


FIGURE 2.29 Initial stress in the cohesive zone vs. cohesive fracture energy.

to denote the extension of the cohesive zone, $\sigma_0$ the value of the cohesive stress, and $\dot{c}$ the velocity of propagation. The crack opening displacement (COD) criterion, which assumes that the crack propagates once a critical opening displacement is reached at the trailing boundary of the cohesive zone, demands (Knauss, 1974)

- for a constant† length of the cohesive zone $\alpha_0$ and a variable cohesive stress

$$K\ J(\frac{\alpha_0}{\dot{c}}) = \text{constant}\ ; \tag{2.6.3}$$

- for a constant cohesive stress $\sigma_0$ and a variable extension of the cohesive zone

$$K^2\ J(\frac{C_0 K^2}{\dot{c}}) = \text{constant}\ , \tag{2.6.4}$$

† The word constant is used to mean not a function of crack speed.

where $C_0$ is a material parameter depending on the cohesive stress $\sigma_0$ and the asymptotic Young's modulus of the material $E_\infty$. Similarly, the energy criterion requires (Knauss, 1974)

- for a constant length of the cohesive zone $\alpha_0$ and a variable cohesive stress

$$K^2 \; J(\frac{\alpha_0}{\dot{c}}) = \text{constant} \;\; ; \tag{2.6.5}$$

- for a constant cohesive stress $\sigma_0$ and a variable extent of the cohesive zone

$$K^2 \; J(\frac{C_0 K^2}{\dot{c}}) = \text{constant} \;\; . \tag{2.6.6}$$

The comparison between the presented model, which assumes a value of critical strain at the craze tip, and the four criteria listed above is presented in Fig. 2.30, where the values of $\alpha_0$ and $C_0$ have been adjusted so that the four curves coincide for low values of the crack speed.

The predictions of the current model fall in between the two predictions of the crack opening displacement criterion and also follow closely the curves for the energy criterion.

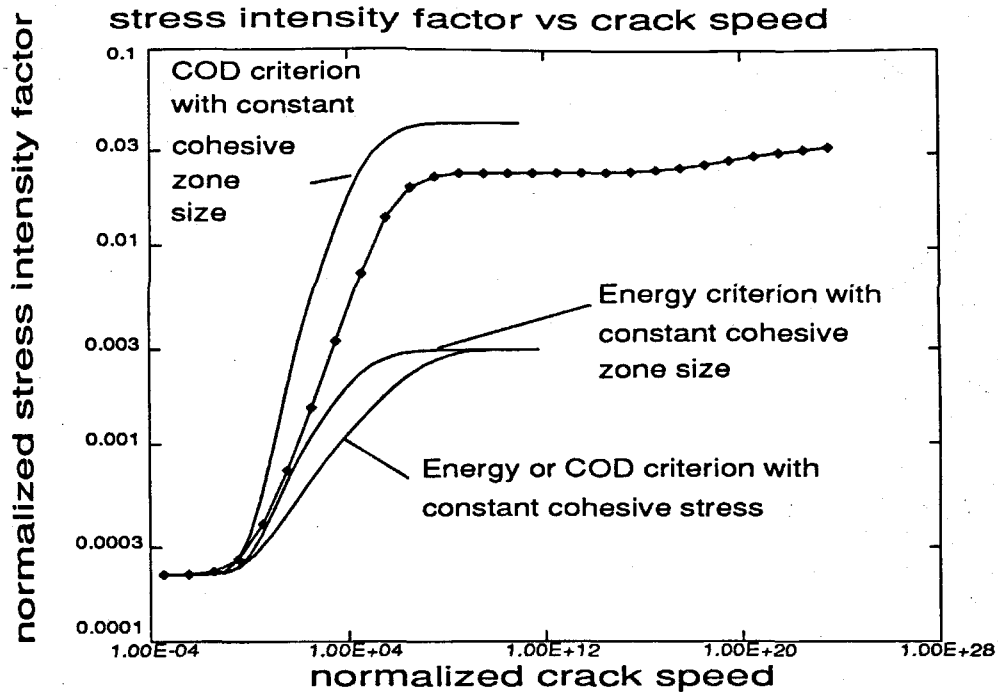


FIGURE 2.30 Comparison between the current model and the predictions of classical theories (critical strain $\epsilon_{crit} = 1$ percent ).

## 2.7 Conclusions

The consequences of rate dependent material properties on the propagation of a crack in an adhesive layer have been investigated. Two relevant features of this problem have been shown in the analysis, namely the interaction between the compliance of the adherends and the time history of loading in the adhesive near the tip of the propagating crack and the hardening in the decohesion zone which occurs as the crack speed increases. The constitutive properties of the adhesive in the decohesion zone have been taken to be affected by free volume induced softening and void growth, assumed to be independent of each other. The fracture criterion which has been used in the analysis assumes a critical strain determining the onset of void growth. Two values of the critical strain have been considered, but its possible rate dependence has not been investigated, and this could be done in the

future. It has been shown that there can be regimes of crack speed which might favor unstable crack growth and, in order to investigate this feature, the current steady-state analysis would need to be reformulated to accommodate a fully time-dependent problem with appropriate initial conditions.

# References

**Argon, A. S., Salama, M. M., (1977)**, "Growth of Crazes in Glassy Polymers," *Philosophical Magazine*, Vol. 36, No. 5, pp. 1217-1234.

**Barenblatt, G.I. (1962)**, "The Mathematical Theory of Equilibrium Cracks in Brittle Fracture," *Advances in Applied Mechanics*, Vol. 7, pp. 59-129.

**Dugdale, D. S., (1960)**, "Yielding of Steel Sheets Containing Slits," *Journal of Mechanics and Physics of Solids*, Vol. 8, pp. 100-104.

**Goodier, J. N., Kanninen, M., (1966)**, "Crack Propagation in a Continuum Model with Nonlinear Atomic Separation Laws," Technical Report No. 165, Division of Engineering Mechanics, Stanford University, 1966.

**Knauss, W. G., (1974)**, "On the Steady Propagation of a Crack in a Viscoelastic Sheet: Experiment and Analysis," *Deformation and Fracture of High Polymers*, H.Henning Kausch Ed., Plenum Press, pp. 501-541.

**Knauss, W. G., Emri, I., (1981)**, "Non Linear Viscoelasticity Based on Free Volume Considerations," *Computers and Structures*, Vol. 13, pp. 123-128.

**Knauss, W. G., Parvin, M., (1987)**, "Damage Induced Constitutive Response of a Thermoplastic Related to Composites and Adhesive Bonding," GALCIT SM 87-15a, to appear in the *International Journal of Fracture.*

**Lauterwasser, B. D., Kramer, E.J., (1979)**, "Microscopic Mechanisms

and Mechanics of Craze Growth and Fracture," *Philosophical Magazine A*, Vol. 39, No. 4, pp. 469-495.

**Mueller, H. K., Knauss, W. G., (1971)**, "Crack Propagation in a Linearly Viscoelastic Strip," *Journal of Applied Mechanics*, Vol. 38, Series E, pp. 483-488.

**Muskhelishvili, N.I. (1963)**, "Some Basic Problems of the Mathematical Theory of Elasticity," P. Noordhof Ltd., Groningen, The Netherlands.

**Shay, R. M., Caruthers, J. M., (1986)**, " A New Nonlinear Viscoelastic Constitutive Equation for Predicting Yield in Amorphous Solid Polymers," *Journal of the Society of Rheology*, Vol. 30, pp. 781-827.

**Verheulpen-Heymans, N., Bauwens, J. C., (1976)**, "Effect of Stress and Temperature on Dry Craze Growth Kinetics during Low-Stress Creep of Polycarbonate"," *Journal of Material Science*, Vol. 11, pp. 1-16.

**Washabaugh, P., (1990)**, Doctoral Dissertation (to be submitted), Graduate Aeronautical Laboratories, California Institute of Technology.

**Williams, M. L., (1963)**, "The Fracture of Viscoelastic Material," in *"Fracture of Solids,"* (Drucker and Gilman Eds.) p. 157, Interscience Publ.

**Ungsuwarunsgri, T., Knauss, W. G., (1988)**, "A Nonlinear Analysis of an Equilibrium Craze," *Journal of Applied Mechanics*, Vol. 55, pp. 44-58